# Structural diversity of frameshifting signals : reprogramming the programmed

Yu, C.H.

# Structural Diversity of Frameshifting Signals

Reprogramming the Programmed

**PROEFSCHRIFT**

ter verkrijging van de graad van Doctor aan de Universiteit Leiden,

op gezag van de Rector Magnificus prof. mr. P.F. van der Heijden,

volgens besluit van het College voor Promoties

te verdedigen op donderdag 22 december 2011

te klokke 16.15 uur

door

**Chien-Hung Yu**

geboren te Nantou, Taiwan, in 1980

**Promotiecommissie**

**Promotor**

Prof. dr. M.H.M. Noteborn

**Co-promotor**

Dr. R.C.L. Olsthoorn

**Overige leden**

Prof. dr. B. Berkhout (Universiteit van Amsterdam)

Prof. dr. C.W.A. Pleij

Prof. dr. J. Brouwer

Prof. dr. J.P. Abrahams

Dr. A.P. Gultyaev

The front cover depicts the idea of the publication by J.-D. Wen *et al.* (J.-D., Wen *et al.*, 2008, *Nature*, **452**, 598-603) who used optical tweezers to monitor the translation of a single mRNA by an *E.coli* ribosome. It is astonishing that translation is not a continuous process but one of successive translocation and pause cycles. Understanding the details of the mechanism of translation in combination with atomic level structure of ribosomes may solve the thirty years old mystery of frameshifting. (Graphic by Laura Lancaster and Courtney Hodges, Berkeley Lab)

# Contents

# Chapter I

## General introduction and outline

Translation is the process by which the genetic code is decoded by ribosomes and information (genes) is converted into functional products (proteins). In most cases, decoding follows the rule to decipher codon triplets one by one, however, alternative ways of decoding can expand the repertoire of gene expression. The term "recoding" initially proposed by R.F. Gesteland et al. in 1988 revealed the diversity of re-programmed genetic decoding utilized by organisms. Although the outcome of recoding events are diverse, the common feature in these processes is the requirement of cis-acting or recoding signals, including specific sequence motifs and RNA secondary structure elements embedded within mRNAs, to initiate non-linear translation. Most of these recoding events especially those focusing on −1 programmed ribosomal frameshifting (−1 PRF) are reviewed in Chapter 2.

It has long been believed that a given stem-loop structure cannot induce efficient -1 PRF although several hairpin-induced -1 PRF events have been reported in eubacteria and eukaryotic viruses. One of the reasons to assume that hairpins are not capable of stimulating -1 PRF is that the derivative stem-loop structure of the *Infectious bronchitis virus* (IBV) frameshifting pseudoknot cannot promote significant -1 PRF. We argued this dogma by demonstrating that the stem-loop derivative of the *Simian retrovirus type-1* (SRV-1) gag-pro frameshifting pseudoknot is very competent in inducing -1 PRF and as well as other artificial stem-loop structures. These results are presented in Chapter 3 of this thesis.

Antisense oligonucleotides (AONs) can form duplexes with mRNA, can mimic the stem region of a hairpin and induce substantial levels of frameshifting. Since a lot of modifications either on riboses or internucleotide linkages have been created to increase duplex stability or resistance to nuclease degradation, it is of interest and practical importance to know whether these nucleotide analogs can be used to promote -1 PRF *in vitro* and to shed light on the therapeutic potential in treating frameshifting diseases by AONs. In Chapter 4, we demonstrate that locked nucleic acid (LNA) is a promising modification for AONs to induce -1 PRF *in vitro*.

Although a simple hairpin can induce efficient -1 PRF, a pseudoknot is still considered to be a superior frameshifter because of its elevated stability contributed by tertiary interactions between loops and stems. Therefore, in Chapter 5 we decribe the design of AONs that simulate pseudoknot structures with the goal to enhance induced -1 PRF by AONs. Based on known tertiary interactions of the SRV-1 frameshifting pseudoknot, we rebuilt efficient pseudoknot-mimicking AONs. Furthermore, the correlation between stem length and the requirement of tertiary interactions for a frameshifting pseudoknot were also addressed.

A recently discovered riboswitch that regulates biosynthesis of nucleoside queuosine from GTP in bacteria drew our attention because of its high similarity to a

frameshifting pseudoknot in its ligand-bound state. Using our frameshift reporter assay, we identified queusoine riboswitches as efficient ligand-responsive frameshifters. By computer-assisted molecular dynamic (MD) simulation, we further characterized an unidentified residue playing an important role in ligand binding thereby affecting the overall stability of riboswitches from different species. These experiments were part of a collaborative effort with the Leiden Biophyical Structural Chemistry department and are presented in Chapter 6.

Finally, the main findings, discussions, and further ideas in relation to this thesis are described in Chapter 7.

# Chapter Ⅱ

## Structural diversity of RNA structures involved in programmed ribosomal frameshifting: a literature review

## Introduction

Messenger ribonucleic acid or mRNA is defined as the medium of information flow from deoxyribonucleic acid (DNA) into proteins and needs to be decoded in a string of non-overlapping codons into amino acids by ribosomes. During this process, called translation, the reading frame of codon triplets is strictly maintained to ensure synthesis of the correct protein. However, in addition to the standard rule of decoding, several alternative ways to decipher genetic information, namely recoding (1, 2), have been documented in all kingdoms of life.

Recoding, including translational bypassing, stop codon readthrough and stop codon redefinition, and programmed ribosomal frameshifting (PRF), is used by many organisms to regulate gene expression and/or to expand their gene expression repertoire. To compete with standard decoding, specific signals, sometimes in conjunction with *trans*-acting factors, should be embedded in the mRNA to promote recoding. The recoding signals in mRNA consist of two main elements: one is the sequence where the actual recoding takes place and the other is a stimulator. The stimulator affects directly or indirectly via RNA binding proteins translating ribosomes to alter their normal decoding behavior. Examples of such sequences are the pentanucleotide motif downstream of a stop codon which enhances near-cognate transfer RNA (tRNA) to compete with release factors from yeast to mammals (3–5) or the selenocysteine insertion element (SECIS), an elaborate RNA structure that is bound by specific protein co-factors, which is required for incorporation of the 21$^{st}$ amino acid, selenocysteine, at designated UAG stop codons (6–8).

## 1. Programmed ribosomal frameshifting

Programmed ribosomal frameshifting (PRF) is one of the most studied topics of recoding. During PRF ribosomes are "programmed" to switch the original reading frame at a so-called slip site by one nucleotide into the 3'-direction, named +1 PRF, or by one or two nucleotides into the 5'-direction, named -1 or -2 PRF, respectively, at a defined ratio. The different types of PRF require distinct recoding elements.

In the case of -2 PRF, which is rarely documented, bacteria phage Mu utilizes -2 PRF at C.GG_G.GG_C.GA_ (the underscores indicate the original reading frame while the dots denotes the frame after the shift) without identified stimulatory element to synthesize proteins involved in tail assembly (9).

+1 PRF has been found in both prokaryotes and eukaryotes and is responsible for the expression of certain important physiological genes. Most cases of +1 PRF found to date rely on RNA motifs to stall ribosomes on a slippery sequence (hungry codon) and/or generate tension on mRNA [Shine-Dalgarno (SD)-like sequences] to promote frameshifting towards the 3'-end (10). The paradigm of +1 PRF in prokaryotes is the

expression of *prfB* gene, encoding release factor 2 (RF2), in *Escherichia coli* (*E. coli*). Combination of three mRNA elements is important for *prfB* frameshifting. First, the in-frame UGA stop codon of the CUU_ U.GA_C. frameshift site is in a weak context to promote translation termination. Second, a SD-like sequence in optimal spacing upstream of the slip site (11, 12) interacts with 16S ribosomal RNA (rRNA) to build up tension on the mRNA. Finally, the identity of peptidyl-tRNA is critical, which means the peptidyl-tRNA has to re-pair to the codon after the +1 shift (13). In this case the 5'-GAG-3' anticodon of the tRNA-Leu retains base pairing with the UUU codon in the +1 frame. The synthesis of RF2 demonstrates an elegant autoregulatory mechanism (14) and the relative cellular abundance of RF2 may also correlate with UGA (re)definition (15).

Two retrotransposons, Ty1 and Ty3, of yeast *Saccharomyces cerevisiae* (*S. cerevisiae*) utilize +1 PRF to express essential genes but by different mechanisms. In Ty1, a low-abundance tRNA-Arg, which is encoded by a single-copy gene and decodes the rare ("hungry") AGG codon, plays a major role in inducing +1 PRF on a CUU_A.GG_C slippery sequence (16). This mechanism strongly resembles the case of *prfB* of *E. coli* as mentioned above. Ty3 uses a different way to achieve +1 PRF. A mechanism of out-of-frame binding of aminoacyl-tRNA was proposed. The frameshifting-inducing peptidyl-tRNA and a 14 nts stimulatory sequence immediately distal to the slippery sequence are suggested to be required for efficient +1 PRF (17), although the mechanism is still controversial (18).

The intracellular polyamine negative regulator, antizyme, is synthesized through +1 PRF by P-site tRNA slippage and this kind of regulation is conserved from yeast to mammals (19). The feedback regulation of polyamine levels by antizymes through +1 PRF is reminiscent of RF2 synthesis in *E.coli*, but the underlying mechanisms are somewhat different. An UGA stop codon in the A-site of UCC_U.GA_U. slippery sequence is responsible to stall ribosomes, as well as an upstream polyamine sensing element (20) and a downstream pseudoknot structure (in mammalian antizyme 1) (21). These elements synergistically promote P-site tRNA with anticodon 5'-GGA-3' to re-pair with the near-cognate CCU codon in the +1 reading frame. Although the role of the downstream pseudoknot is considered to stall ribosomes and proved to be insensitive to polyamine levels, a –1 PRF inducing pseudoknot from *Infectious bronchitis virus* (IBV) cannot replace it (22). Since a detailed analysis of the antizyme pseudoknot structure is still lacking, the specific differences between the two types of frameshifting pseudoknots still need to be determined. Recently, expression of antizyme in *S. cerevisiae* has been found to be regulated by prion [$PSI^+$], the aggregated (amyloid) form of release factor 3 (eRF3) (23). This and a related study (24) open a new vision of epigenetic control of such delicate gene regulation.

–1 PRF was demonstrated for the first time over 25 years ago to explain the expression of the overlapping *gag-pol* genes of *Rous sarcoma virus* (RSV) (25). Since then, numerous examples of -1 PRF in overlapping open reading frames (ORF) of eukaryotic RNA viruses, DNA and RNA bacteriophages, and bacterial insertion sequences and transposons have been found (26, 27). Although most of these cases are found in viruses or virus-like elements, one endogenous bacterial gene, *dnaX* (28), and three mammalian genes (29–31) so far have been shown to be expressed through -1 PRF, implying that -1 PRF may be involved in regulation of uncovered cellular genes in humans. Through sequence comparison and genetic analysis, a canonical -1 PRF regulating motif which contains two RNA elements has been identified: a heptameric slippery sequence where frameshifting occurs with the formulation of X_XX.Y_YY.Z (32) [for example, U_UU.U_UU.A in *gag-pol* junction of *Human immunodeficiency virus type-I* (HIV-1) (33)]; and an RNA structure which can be a pseudoknot or a simple hairpin positioned 5-8 nts downstream of the slippery sequence (34). The specific formulation of the slippery sequence is chosen to facilitate tRNA re-pairing to (near-)cognate codons after the shift (32). The downstream RNA secondary structures play a critical role in pausing ribosomes at the right position i.e. the XXY codon in the P-site and YYZ codon in the A-site to induce -1 PRF (35, 36). Although pausing is necessary, a biochemical study showed that pausing is not sufficient to induce -1 PRF (37), implying that the downstream secondary structures have an active role in this process, presumably by lowering the energy barrier for tRNA-mRNA un-pairing during translocation (38, 39). In a recent study using single-molecule optical tweezers the mechanical forces exerted by a single ribosome to unfold mRNA hairpins with different GC contents have been quantified (40). These data may help to shed light on the mechanical aspects of -1 PRF.

The diversity of -1 PRF-stimulating RNA motifs is remarkable and worthy of attention. Generally a pseudoknot is believed to be an efficient -1 PRF stimulator because of the extra stabilization from loop-stem interactions or other unknown factors that stabilize the pseudoknotted conformation at equilibrium at 37 ℃ (41). Simple hairpins, however, without complicated tertiary interactions as in pseudoknots are also genuine -1 PRF stimulators. Even antisense oligonucleotides that may form hairpin or pseudoknot-like structures have been reported to induce substantial -1 PRF. These elaborate frameshifting structures will be demonstrated and discussed below.

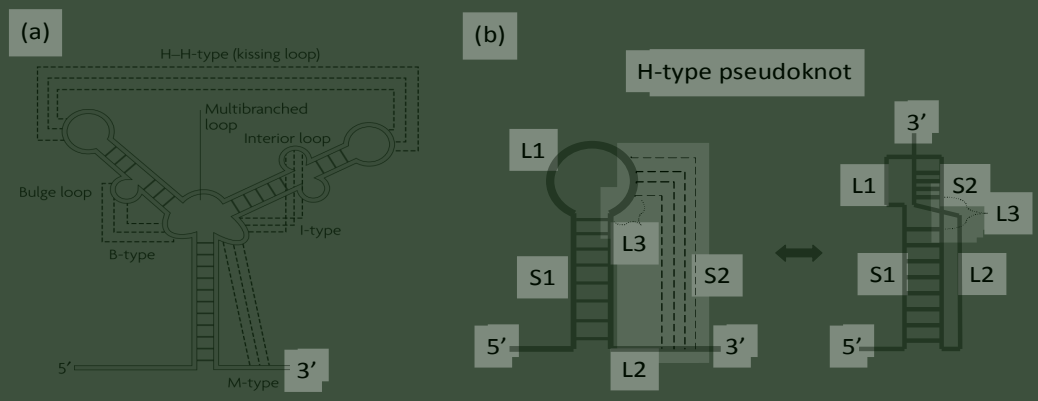


**Figure 1. Various structures of RNA pseudoknots. (a) Different types of RNA pseudoknots (except H-type) are categorized by the motif that is responsible for the formulation of the second stem with the sequences outside the major stem-loop structure. (b) The representative structure of an H-type pseudoknot. The "S" denotes the stem region and the "L" indicates loop region. (adapted from Brierley *et al.*, 2007)**

## 2. The structures of frameshifting pseudoknots

A pseudoknot, which was first discovered in Pleij's lab (42) almost 30 years ago, is defined as an RNA structure element formed upon standard base pairing of nucleotides of a loop region with residues outside the loop (43). Depending on the geometry of the loop, several types of pseudoknots, including H (hairpin), B (bulge), I (interior), or M (multibranched)-type, are recognized (Figure 1a) in various kinds of RNAs (44). The majority of pseudoknots that has been described to date are H-type pseudoknots which involve the apical loop of a hairpin; these will be referred to simply as pseudoknot in this chapter. A pseudoknot consists of two base-paired stem regions, S1 and S2, which are coaxially stacked and connected by two single-stranded loops, L1 and L2 (Figure 1b). L1 crosses the major groove of lower stem S2, while L2 crosses the minor groove of S1 (41). Some pseudoknots contain one or more unpaired nucleotides between the two stems and these nucleotides, referred to as L3, are either extruded from the junction of the two stems (45, 46) or intercalated between the two stems resulting in a specific bending (47).

Pseudoknots widely exist in RNA molecules including rRNA, mRNA, tRNA, transfer-messenger RNA (tmRNA), self-splicing RNA, and viral RNA (34, 44, 48, 49). Owing to their special 3D-structure, pseudoknots are often crucial elements in biological processes that are controlled by RNA structure. For example, riboswitches (50), telomerase (51), internal ribosome entry sites (IRES) (52–54), and several RNA-protein interactions (55) are dependent on pseudoknot formation for their function. Furthermore, pseudoknots play a key role in promoting recoding events. In this review, I will focus on the pseudoknots that induce efficient -1 PRF. The currently

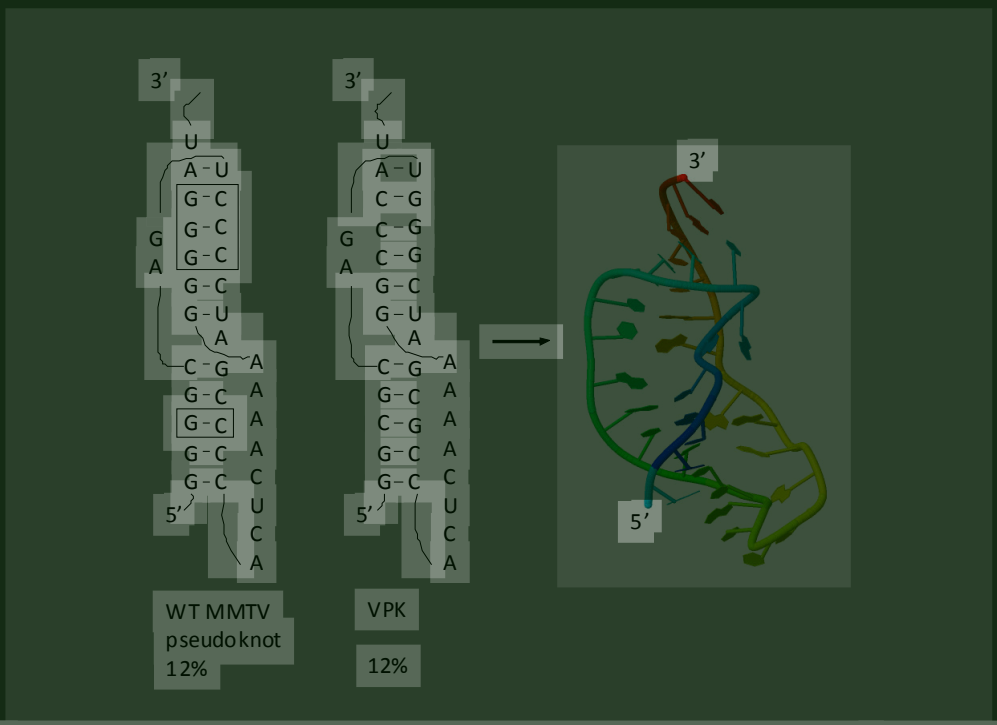


**Figure 2. Structure representation of wt MMTV frameshifting pseudoknot and its derivative VPK solved by NMR spectroscopy (PDB 1RNK). The altered base pairs are boxed and the reported frameshifting efficiencies of both constructs are indicated.**

available -1 PRF-inducing pseudoknot structures can be roughly divided into three groups. The first and second group are defined by the length of S1: (i) pseudoknots with S1 equal or smaller than 6 base pairs (bp), and (ii) those with S1 longer than 6 bp. The third group consists of pseudoknots with unusual structural features such as extra stems or loops. The differences of these signals between and within groups will be discussed in more detail below.

## 2.1 Group 1: pseudoknots with short S1

In this group there are three major types depending on certain specific structural features, and each has its representative pseudoknot: the *Mouse mammary tumor virus* (MMTV) *gag-pro* (56), the *Simian retrovirus type-1* (SRV-1) *gag-pro* (57), and plant luteoviral P1-P2 frameshifter pseudoknots (58). The MMTV *gag-pro* pseudoknot was the first -1 PRF signal whose solution structure was solved (59), and was also extensively studied by mutation analysis and structure probing (56, 60). Since then it has become a paradigm for -1 PRF stimulatory motifs. Note that the resolved structure (Figure 2) is a variant of wild-type (wt) MMTV pseudoknot called VPK with four G-C bps flipped to C-G bps while the frameshift-inducing ability remains unchanged (60). The analyzed structure reveals a 5 bp S1 crossed by L2 having 8 nts, while the 2

nts of L1 cross the deep groove of a 6 bp S2. The most interesting feature is an unpaired adenosine at the 3'-side of the helical junction of S1 and S2. This protruding nucleotide results in a pronounced bending about 60° from the vertical axis between two helices (59). Straightening of the pseudoknot by removal of the wedged adenosine decreases frameshifting efficiency dramatically (61–63). Further attempts to modify the direction of bending also resulted in inactive pseudoknots in -1 PRF. Therefore, the MMTV gag-pro represents a type of -1 PRF inducing pseudoknot that requires a specificly bent conformation as a frameshifter. Similar requirements were found for the *Feline immunodeficiency virus* (FIV) *gag-pol* (64) and the human paraneoplastic antigen *Ma3* gene frameshifter pseudoknots (29).

The representative of the second type in this group is the SRV-1 *gag-pro* pseudoknot (Figure 3). The dominant feature of this type is the coaxial stacking of S2 on top of S1. In the early studies of the SRV-1 pseudoknot, the presence of an adenosine kink at the junction of S1 and S2 was proposed, based on the observation that disruption of the putative A13-U29 (Figure 3, denoted as NMR SRV-1 pseudoknot) base pair at the junction had no effect on -1 PRF efficiency (65). However, two NMR studies have confirmed the A-U base pair by assignment of the imino proton of U29 (66, 67), which is also in agreement with the enzymatic probing results of the initial SRV-1 pseudoknot study (57). However, the solution structure did not answer the question of why A · A, A · G, or A · C mismatches at this position had no effect on frameshifting (60, 65). The confirmation of the A-U base pair at the junction further indicates that a bent conformation is dispensable for -1 PRF pseudoknots although a smaller bending allowing the single nucleotide of L1 to span S2 has been observed (67).

The identity of the single nucleotide of L1 was found to be unrelated to -1 PRF efficiency indicating this nucleotide is merely to function as a bridge between S1 and S2 and, at the same time, spans the major groove of S2 (68). However, the length and identity of L2 are highly relevant for the function of the SRV-1 pseudoknot. Although not exhaustively studied, the optimal length of L2 has been reported to be 8 to 10 nts, which is shorter than the wt L2 of 12 nts (68, 71). The sequence identity of L2 was initially thought to be less relevant since changing 10 out of 12 bases did not affect frameshifting efficiency (68). However, a recent functional study of the SRV-1 pseudoknot has shown that the identity of bases, especially those that are close to the junction, is indeed critical (69). A possible explanation for these contradictory findings is that the two nts proximal to the junction that are important for -1 PRF pseudoknot were maintained in the earlier study (68).

In addition to loops, a role for stems in -1 PRF has also been proposed for the SRV-1 pseudoknot. It was found that the calculated stability of S1 is not correlated to frameshifting efficiency but that the presence of G-C base pairs in the lower half of S1 is important; conversely, the thermodynamic stability of S2 was observed to correlate with frameshifting efficacy although no clear linear dependence was revealed. These results inspired the authors to propose that a certain threshold stability of the first few base pairs in S1 was important to stall ribosomes over the slip site, then the approaching ribosomes might be designated to alternative fates depending on the stability of S2 (68). A hybrid pseudoknot frameshifter (DH40) build up from S2 of a non-frameshifting pseudoknot from bacteriophage T2, and a coaxially stacked S1 of a frameshifting pseudoknot in the *gag-pro* junction of *Human endogenous retrovirus* (HERV)-K10 may support this idea. DH40, although preserving the structure of the T2 pseudoknot, induced identical levels of frameshifting as the wt HERV pseudoknot. NMR data showed a similar local structure at the junction of the stems in hybrid (active) and T2 pseudoknot (inactive), indicating that the relatively unstable S1 (two A-U base pairs in S1) of the T2 pseudoknot, may not exceed the threshold to fix ribosomes over the slippery sequence (70).

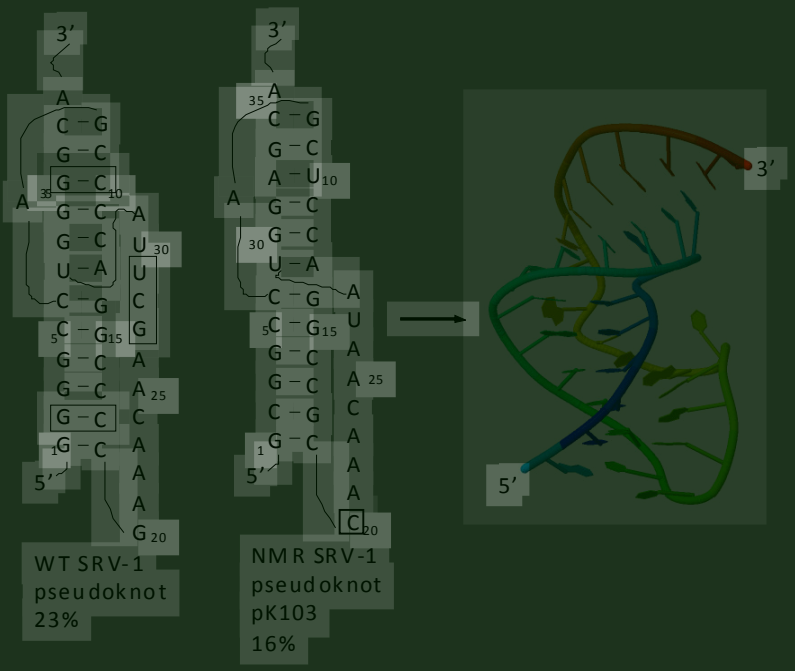


**Figure 3. Structure representation of wt SRV-1 frameshifting pseudoknot and its derivative pk103 solved by NMR spectroscopy (PDB 1E95). The differences between wt and pk103 are indicated by boxes.**

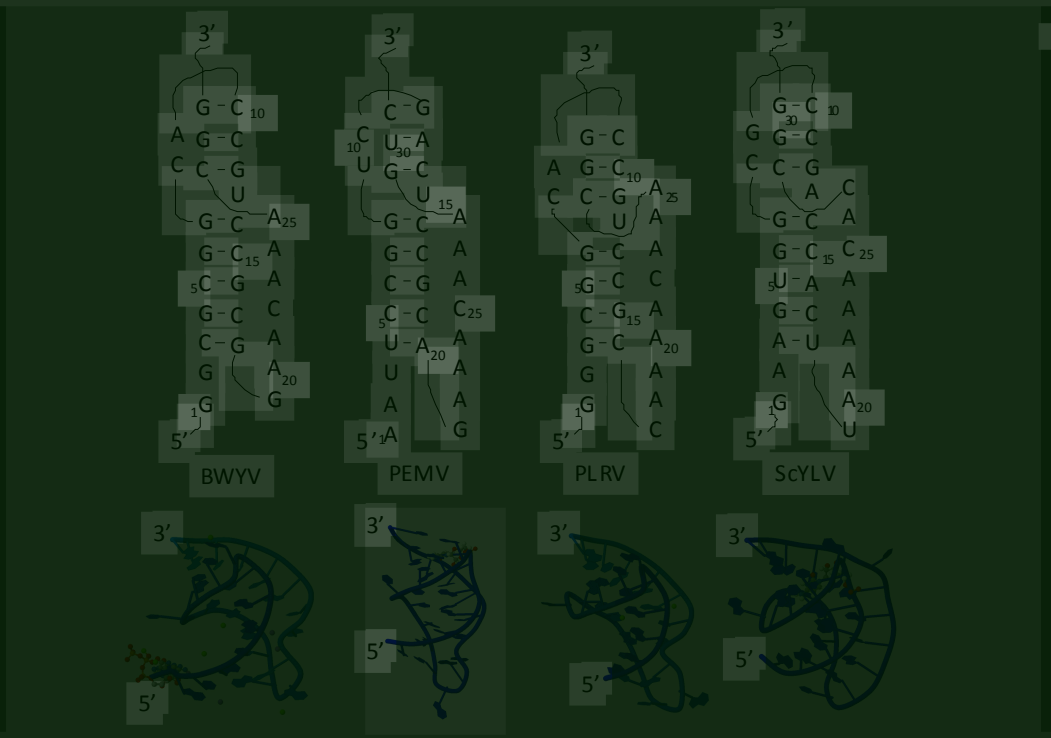


**Figure 4. Structure representation of luteoviral frameshifting pseudoknots. The solved structures are also shown. PDB codes of BWYV, PEMV, PLRV, and ScYLV are 1L2X, 2RP1, 2A43, and 1YG4, respectively.**

The third type in this group comprises the P1-P2 pseudoknots of plant luteoviruses (Figure 4). The representative pseudoknot is present at the overlapping P1-P2 genes of *Beet western yellow virus* (BWYV). This pseudoknot was initially proposed to consist of two coaxially stacked short stems (5 bps of S1 and 4 bps of S2) connected by a 2 nts L1 and a 6 nts L2 (34). In fact, after the crystal structure of the pseudoknot was obtained (71), a different picture emerged. The predicted U13-A25 base pair at the top of S2 does not exist but an unpaired U13 is present at the helical junction. Although similar to the MMTV *gag-pro* pseudoknot with non-coaxially stacking of S1 and S2, the distortion of S2, however, resulting from the short length of L1 and continuous stacking of L2 on A25 together with the bulged out U13 make the BWYV P1-P2 pseudoknot a distinct type of -1 PRF stimulating pseudoknot.

Another remarkable feature is the minor groove triplex between L2 and S1. A conserved 5'-AACAAA-3' sequence found in the 3'-end of L2 forms numerous non-canonical base-base or base-sugar hydrogen bonding interactions using their Watson-Crick edges in the minor groove of S1. This kind of S1-L2 interaction was first described for BWYV and later on shown to exist in other luteoviruses, including *Pea enation mosaic virus* (PEMV), and *Potato leaf roll virus* (PLRV) (58, 72–74) (Figure 4). It is noteworthy that the 3' adenine (the last nucleotide in L2) extensively

interacts with neighboring nucleotides through its Watson-Crick and Hoogsteen faces to stabilize the junction (74, 75). Interestingly, a highly similar L2 sequence 5'-AAACAAUA-3' is present in a non-related pseudoknot pk103, which is a modified version of wild–type SRV-1 *gag-pro* pseudoknot used for NMR studies (67). Several adenines of this L2 are involved in triplex formation with S1 like the luteovirus L2 sequences. However, a different structural detail is present: the N4 amino group of the cytidine in BWYV-type L2 forms a hydrogen bonding with the 2'OH of a G residue in S1 whereas the cytidine is bulged out from the L2 in the solution structure of pk103.

In *Sugar cane yellow leaf virus* (ScYLV) the C25 is bulged out as well (Figure 4) and the deletion mutant shows increased frameshift-indcucing activity (76). Mutational analyses have confirmed these findings from structural studies and shown the C is critical in luteoviral frameshifting pseudoknots (77), whereas the C in pk103 can be replaced by any other nucleotide without affecting or even partially increasing frameshifting efficiency (69). These results further demonstrate the diverse nature of frameshifting pseudoknots.

In addition to minor groove triples, a protonated cytidine in BWYV L1 forms a standard Hoogsteen base pair with the G-C in S2 and aligns in the major groove of S2. This major groove $C^+$ · G-C triple is conserved in all luteoviral pseudoknots, and shown to strongly enhance the pseudoknots stability (78, 79) and their frameshifting efficiency (76, 78). Although this is the only known group of natural -1 PRF stimulators showing this structural feature, the human telomerase pseudoknot hTPK-DU177 was recently found to be an efficient frameshifting stimulator whose activity is strongly correlated with the presence of major groove triples (80). These data may further improve the algorithm to propose more frameshifting related pseudoknot structures in the future.

The nature of life is the presence of exceptions. The pseudoknot in the P1-P2 junction of ScYLV, although still a luteovirus, reveals some structure variations (50, 82). For example, the 9 nts L2 of the ScYLV pseudoknot align well in the minor groove of S1 forming a triple helix and exhibit continuous base stacking, except for one cytidine which is extruded from the triplex whereas other luteoviral pseudoknots feature extruded nucleotide(s) proximal to the junction of S1 and L2 and continuous base stacking of the 3' side of L2. The most striking difference is the identity of the nucleotide of the L2 in the helical junction. In ScYLV, the N3 of cytidine (C27) at the 3'end of L2 forms a hydrogen bonding with the 2'OH of a cytidine paired with guanosine (C14-G7) while an adenosine is found at the relative position in BWYV, PLRV, and, PMEV to interact with 2'OH via N1 (48). An interesting study showed that the C27A mutant of ScYLV is almost inactive in frameshifting although both wt

and mutant pseudoknots adopt indistinguishable global structures (82), and further comparison showed that the structure of helical junction of the C27A mutant is superimposable on that of the BWYV pseudoknot. These data suggest that the "ground-state" structure does not directly correlate with frameshifting. Since the A25C mutation in the helical junction of the BWYV pseudoknot does improve frameshifting (83), it can be concluded that stability of the helical junction is disfavorable for the architecture in the C27A mutant (82). The exact details still need to be elucidated.

### 2.2 Group 2: pseudoknots with long S1

The frameshifting pseudoknots in the second group feature a longer S1 compared to those of the first group. Most notably, the sequence identity of L2 is independent of frameshifting efficiency (32), indicating that no L2-S1 triple helix is needed to stabilize these pseudoknot structures, although a recent study of mammalian coronavirus frameshifting pseudoknots demonstrated opposite results (84). Due to the absence of a three-dimensional structure either in crystal or solution, the precise role of L2 in long S1 pseudoknots is still a matter of debate.

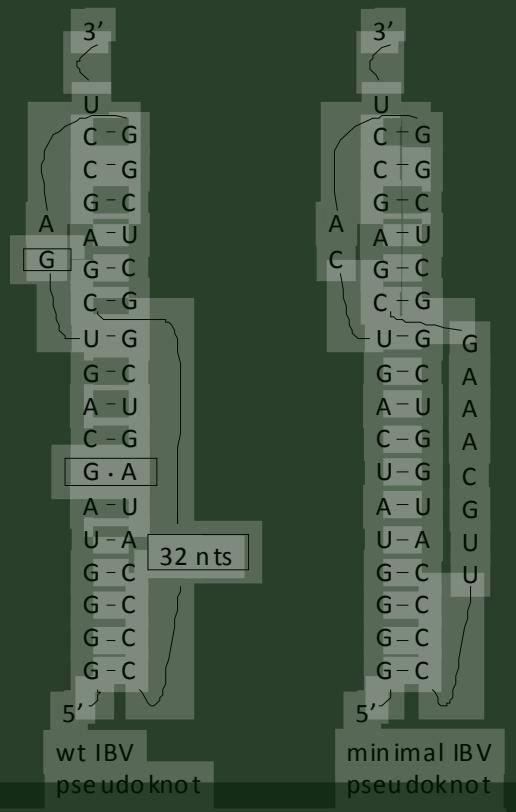


**Figure 5. Structure representation of wt IBV pseudoknot and its derived minimal IBV pseudoknot, the wt in nowadays. The differences are boxed.**

The most representative pseudoknot in this group is the frameshift-stimulatory signal present at the 1a-1b overlap of avian coronavirus IBV (85). Although discovered over 20 years ago, the three-dimensional structure is still unknown, and the detailed information of this frameshifting pseudoknot comes from mutational studies and probing analysis mainly contributed by Brierley's group (86). The topology of the wt IBV frameshifting pseudoknot is an 11 bp S1 and 6 bp S2, linked by a 2 nts L1 and an L2 of 32 nts without apparent structure (Figure 5) (85). The IBV frameshifting signal is located 6 nts downstream of a U_UU.A_AA.C slippery sequence. In vitro frameshifting assays have shown that an 8 nts loop can effectively substitute the wild type 32 nts L2. This modified pseudoknot, named minimal IBV pseudoknot is the "current" wt IBV pseudoknot (Figure 5) (87).

This functional variant with much shorter L2 may indicate that a certain length of L2 is simply needed to cross the 11 bps in S1 (88). For IBV it has been shown that the length rather than the thermodynamic stability of S1 is critical for frameshift activity (89). Removal of a single bp in S1 reduces frameshifting already 7 fold, removal of 2 bps from S1 almost abolishes its activity, even though thermodynamic stability and overall structure, as determined by probing, are similar to the wt pseudoknot. On the other hand, pseudoknots having longer S1 stems (12-14 bp) were fully functional in frameshifting (89).

The relatively weak G-U base pair at the top of S1 was examined to see if the IBV pseudoknot adopts an intercalated structure like the MMTV or luteovirus frameshifting signals. Replacing G-U with the more stable G-C or C-G base pairs promotes frameshifting efficiency at slightly higher level (87, 89). Combined with structural probing data (89) it seems unlikely that there is a kink nucleotide in the helical junction. However, an unpaired nucleotide is of great importance to a shorter S1 (6 bp) variant of the IBV pseudoknot. Similar to the MMTV pseudoknot (56, 61), an inactive IBV-like pseudoknot was converted into an efficient frameshifting stimulator, named pKA-A, when an unpaired adenosine was inserted into the helical junction, meanwhile the last nucleotide of L2 was switched from G to A (90). Inverting the fourth, C-G, and fifth, G-C, bps of pKA-A S1 decreased frameshifting about 3.5-fold, indicating there are specific S1-L2 interactions like those observed in group I introns (91) and the *turnip yellow mosaic virus* (TYMV) tRNA-like pseudoknot (92). However, the requirement for this interaction is bypassed when the length of L2 is increased to 14 nts. High-resolution structures may help to uncover the relation between L2 length and sequence identity of S1 (86).

Further studies have shown related frameshifting pseudoknots within the *1a-1b* overlapping region in other coronaviruses genomes, including murine hepatitis virus (MHV) (93), human coronavirus (HCoV)-229E (94), and the recently identified SARS-coronavirus, the causative of agent severe acute respiratory syndrome (SARS), (95). Extensive mutational studies, RNA structure probing analysis, and preliminary NMR data have shown that the frameshifting signal of SARS-CoV, located 6 nts downstream of an UUUAAAC slip site, adopts an H-type pseudoknot possessing an additional hairpin called S3 or SL1 within L2 (Figure 6) (96–99).

Similar to other frameshifting pseudoknots, disruption of base pairs in either S1 or S2 severely reduces frameshifting efficiency further confirming the pseudoknot conformation. However, disruption or deletion of S3 in the L2 region has no dramatic effect on stimulating frameshifting both *in vitro* and in cultured cells (97–99). It was, therefore, proposed that the necessity of S3 is not for efficient ribosomal frameshifting

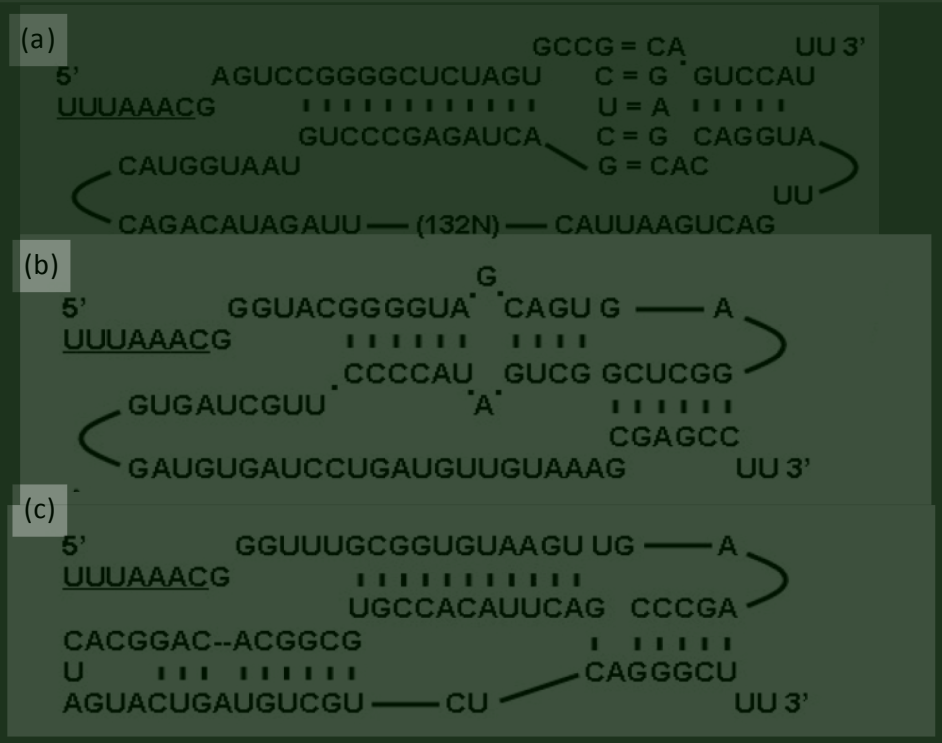


**Figure 6. Structure representation of the representative of frameshifting pseudoknots in three groups of coronavirus. (a) The frameshifting pseudoknot of HCoV-299 belonging to group 1 coronavirus. (b) The frameshifting pseudoknot of IBV belonging to group 2 coronavirus. (c) The frameshifting pseudoknot of SARS-CoV belonging to group 3 coronavirus. (taken from Plant *et al.*, 2008)**

but for global folding of the pseudoknot (97) or for functional switching between transcription and translation by RNA remodeling as proposed for another (+) strand RNA virus (98). The last assumption, although elegant and promising, seems controversial since the S3 is not conserved in all three groups of coronaviruses. In all group 2 coronaviruses, including SARS-CoV and MHV, the S3 motif resided in L2 can be identified in their frameshifting pseudoknots (Figure 6). However, in group 3 coronaviruses such as IBV the L2 seems to be a single-stranded loop. In addition, the frameshifting pseudoknot of group 1 coronaviruses, like HCoV-229E, forms a more "elaborated" structure as the S2 is formed by kissing loops connected by a long, 150 nts, L2 without apparent secondary structure (Figure 6) (94, 100).

A diversity of frameshifting stimulatory structures has recently been defined in Alphaviruses to stimulate production of transframe (TF) protein which overlaps the 6K ORF (101). One of these stimulatory structures is a pseudoknot, found in *Middelburg virus* (MIDV), featuring (Figure 7): (i) an unstable 3 bp lower S1 and high GC content 7 bp upper S1 interrupted by an A · G mismatch; (ii) a 7 bp S2; (iii) 3

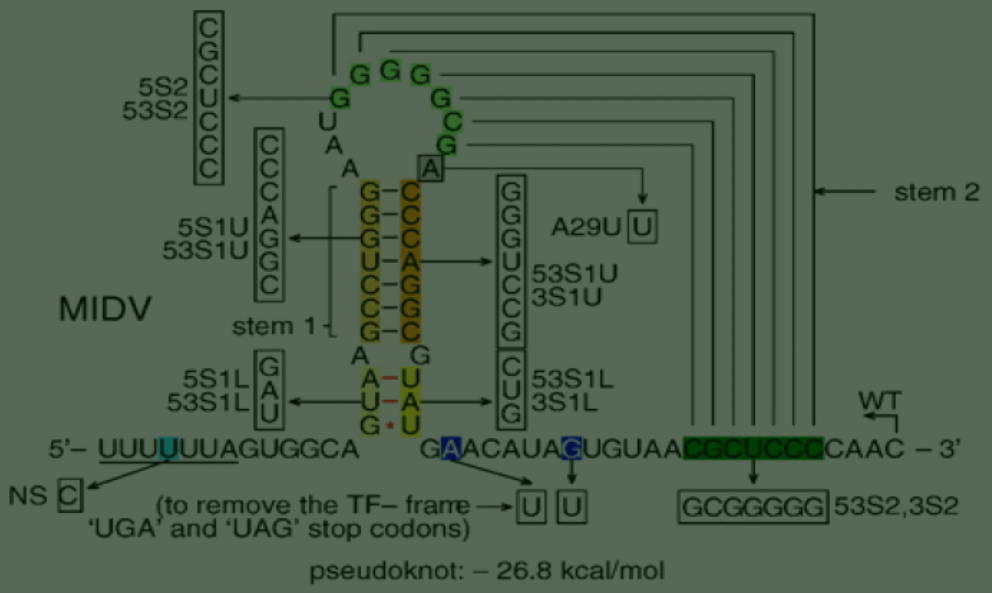


**Figure 7. Structure representation of MIDV frameshifting pseudoknot. The dark and light green shaded sequences are base-paired to form S2. Orange shaded region indicates upper S1 while yellow shaded region indicates unstable lower S1. Boxed sequences are the mutations made by Chung and colleagues. (Taken from Chung *et al.*, 2010)**

nt L1, 13 nt L2, and a single adenosine in between the two stems, reminiscent of the MMTV frameshifting pseudoknot. Interestingly, destabilizing the lower part of S1 resulted in comparable frameshifting efficiency whereas stabilizing it decreased frameshifting 4-fold (102). This is similar to the HIV-1 frameshifting hairpin that requires a lower stem to position the translating ribosomes (see below). Modifying the A between the stems to U has no significant effect suggesting that this nucleotide is only necessary to span the major groove. Intriguingly, the first 6 nt of the spacer together with the slippery sequence (U.UU_U.UU_A) are somehow capable of inducing 5% of frameshifting. In some Alfaviruses frameshifting seems to occur without apparent stimulatory structures (102). How this is achieved is not yet known.

### 2.3 Group 3: odd pseudoknots

An example of a B-type, bulge type, pseudoknot is found in the overlapping region of ORF1 and ORF 2 of *Barley yellow dwarf virus* (BYDV), an RNA plant virus belonging to the genus Luteovirus of the Tombusviridae. In this pseudoknot 6 nts that are located four thousand nucleotides more downstream can base pair to a bulge loop of the hairpin structure (Figure 8) adjacent to the GGGUUUU slippery sequence in the ORF1/2 overlap (103, 104). This long-distance interaction is not only conserved in a BYDV-like virus, *Soybean dwarf virus* (SbDV) (Figure 8) (104) but has also recently been discovered in *Red clover necrotic mosaic virus* (RCNMV), a member of

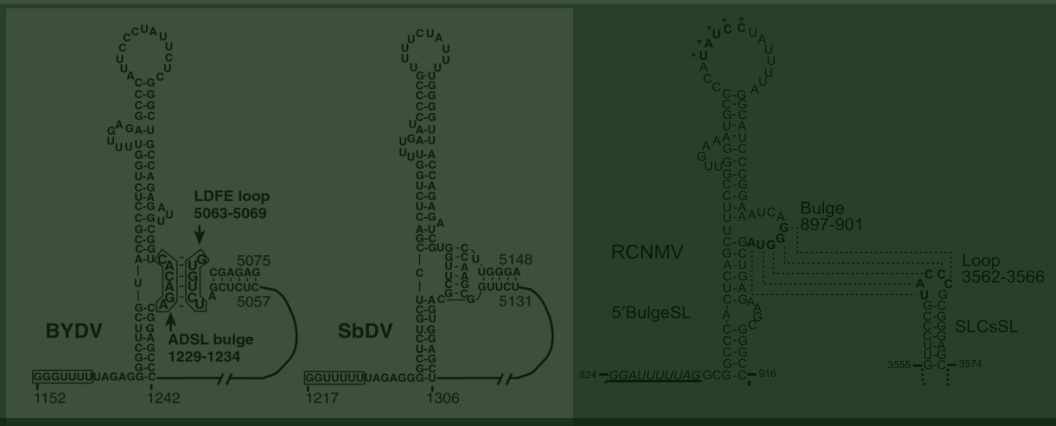


**Figure 8. Three representative bulge-apical loop frameshifting pseudoknots in plant viruses. The bulge residing in main stem-loop structure base pairs with the apical loop of another stem-loop in 3'UTR thousands nucleotides downstream. The numbers indicate the nucleotide positions in each RNA virus genome (figures of BYDV and SbDV are taken from Barry *et al.*, 2002; figure of RCNMV is taken from Tajima *et al.*, 2011).**

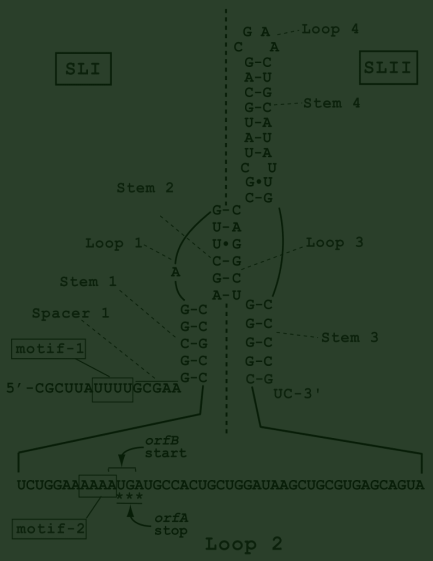


**Figure 9. Structure representation of apical loop-internal loop frameshifting pseudoknot. The apical loop from stem-loop structure 1 (SLI) forms a 6 bp stem with the internal loop of the 45 nts downstream stem-loop 2 (SLII) to induce frameshifting over the UUUU (motif-1) slippery sequence in IS*3411*. (taken from Mazauric *et al*., 2008)**

the genus Dianthovirus, also of the Tombusviridae (Figure 8) (105). This and anotherlong-distance interaction that stimulates translation initiation of BYDV are proposed to be involved in regulation of competition between translation andtranscription, an important issue for all (+) strand RNA viruses (104).

A novel type of frameshifting pseudoknot of which the S2 is formed by base pairing of the apical loop and internal loop of two stem-loop structures was identified by Mazauric *et. al.* in IS*3411*, a transposon of the IS*51* group of insertion sequences in eubacteria (Figure 9) (106). It was shown that the stability of the structure corrrelated with frameshifting efficiency and transposition, indicating that this new type of pseudoknot is of biological relevance. Interestingly, when the second hairpin (Figure 9, SLII) was cloned into the anticodon arm of a tRNA and expressed together with the remainder

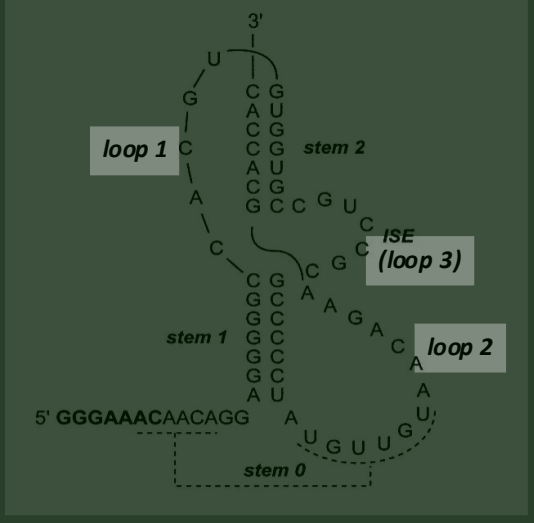


**Figure 10. Structure representation of VMV frameshifting pseudoknot. The slippery sequence is shown in bold. A possible interaction of spacer with loop 2 is indicated by dashed line (stem 0). The relatively large 7 nt loop3, interstem element (ISE) is the unique feature of this pseudoknot. (adapted from Pennell *et al.*, 2008)**

of the pseudoknot located on the mRNA, frameshifting was observed only when the 6 bp in stem 2 could form.

The frameshifting stimulator of the ovine lentivirus Visna-Maedi retrovirus (VMV) was confirmed to be a pseudoknot instead of a simple stem-loop (Figure 10) (107). Two interesting structural features were identified. First, a 5 nt L1, which is generally 1 or 2 nt in reported frameshifting pseudoknots to connect S1 and S2 is present. There are two cytidines in L1 that have potential to form $C^+ \cdot G$-C triples with S2. However, only one deletion mutant in which the last three nts were removed was examined and it was shown to be inactive in frameshifting, implying that L1 is not only for bridging but unknown interactions to stabilize VMV pseudoknot. Furthermore, a relatively large 7 nt L3 termed interstem element (ISE) is present in between S1 and S2, and this GC rich fragment was also shown to be crucial in inducing frameshifting. Either shortening or lengthing ISE dramatically reduced frameshifting efficiency. Changing the ISE sequence to alternate purine/pyrimidine bases while maintaning the stem length still resulted in a 5-fold decrease in frameshifting efficiency, indicating that

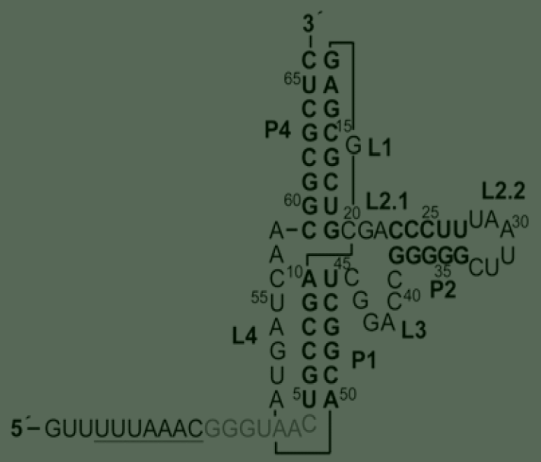


**Figure 11. Structure representation of three-stemmed pseudoknot aptamer of SAH riboswitch located 7 nt dowstream of UUUAAAC slippery sequence. The elements of this pseudoknot are indicated. A large and structured L2 (the L3 in this thesis) is present in between two stems. (taken from Chou *et al.*, 2010)**

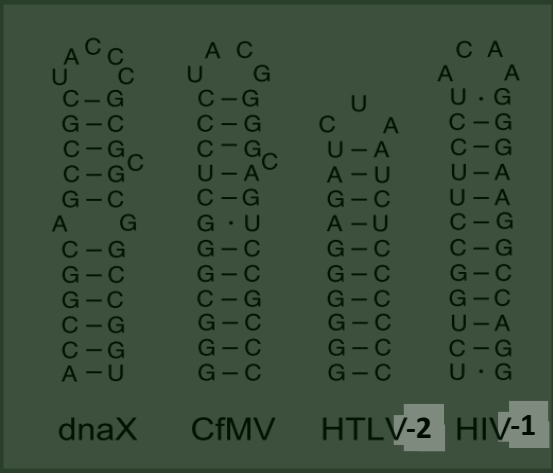


**Figure 12. Structure representation of four different frameshift-inducing hairpins. (adapted from Yu *et al.*, 2011)**

both the identity and the length of the sequence are important.

An interesting example of ametabolite-responsive frameshifting signal was recently reported. The three-stemmed pseudoknot (Figure 11) of an S-adenosylhomocysteine (SAH) riboswitch can specificly respond to ligand concentrations to induce different levels of frameshifting in *vitro* and in *vivo* (108). The ligand has been shown to stabilize the junctions between the different stems, which are dynamic in the absence of SAH. Although this is not a natural frameshifting pseudoknot, the finding of inducible frameshifting suggests that cellular factors may regulate -1 PRF through a mechanism that so far has only been found in +1 PRF (8).

**3. Stem-loop structures**

It has long been considered that a hairpin stimulates frameshifting to a lesser extent than a pseudoknot, although both RNA structures can pause ribosomes to a similar degree (109–111). Certain exceptions, however, were found upon testing identical frameshifting constructs in *E. coli* (112) or a modified wheat germ (WG) *in vitro* translation system (113). Nevertheless, there are several frameshifting inducing stem-loop structures identified, including *gag-pol* junction of lentiviruses HIV-1 and *Simian immunodeficiency virus* (SIV)/HIV-2 (114–117), the *gag-pro* junction of *Human T-cell leukemia virus type II* (HTLV-2) (118, 119), the junction between ORF 2a and ORF 2b of *Cocksfoot mottle virus* (CfMV) (120–122), and in decoding two *dnaX* products gamma ( $\gamma$ ) and tau ( $\tau$ ), two subunits of DNA polymerase III of *E. coli* (123, 124). Decoding of *dnaX* is an unusual type of frameshifting in the sense that the frameshift leads to a protein $\gamma$, which is shorter than the non-shifted protein, $\tau$, while in other cases of programmed frameshifting it is the opposite. The frameshifting signals consist of (i) a SD-like sequence upstream of highly slippery sequence AAAAAAG, reminiscent of +1 frameshifting of RF2 in *E coli* (11) and probably responsible to further stall translating ribosomes over slippery sequence; (ii) a downstream stem-loop structure. All of them are necessary to synthesize $\gamma$ and $\tau$ in an 1:1 ratio. The chemical probing analysis showed that the frameshift-inducing

hairpin (Figure 12) features an 11 bp stem with a A · G mismatch in the middle, a C bulge at the 3' side of the stem located 3 bp from the closing base pair (cbp), and a UACCC pentaloop (124). Mutational analysis *in vivo* demonstrated that removing the C bulge, restoring A · G to C-G, or adding a G to pair with the bulged C, all lead to higher frameshifting efficiency. Combined with results of other mutants, the authors concluded that the calculated stability of the stem-loop structure is positively correlated with frameshifting efficiency with and without SD-like stimulatory sequence. An independent study of assaying frameshifing efficiency of six HIV-1 hairpin mutants in yeast and cultured cells reached the same conclusion although with limited number of constructs (125).

The viral protease VPg and RNA-dependent RNA polymerase (RdRp) of the plant virus CfMV are expressed from two overlapping ORFs by means of -1 PRF (126). The stimulatory signal is characterized as a 12 bp stem with a C bulge at the 3' side positioned 3 bp away from the stable UACG tetraloop (Figure 12) (120). The location of the bulge is similar as in the frameshifting hairpin of *dnaX*, but whereas adding an complementary G increased frameshifting efficiency in *dnaX* construct (124) it had no effect on frameshifting in the CfMV construct (122) assayed in an WG *in vitro* translation system. Enlarging the loops of the *dnaX* and CfMV hairpins by 6 and 3 nts, respectively, slightly elevated their frameshifting efficiency. Remarkably, deletion of the C bulge, although not affecting frameshifting efficiency *in vitro*, proved to be deleterious to CfMV infection activity whereas the 3 nts enlarged-loop mutant kept a wt level of infectivity (122), suggesting that the specific RNA structure may be critical in physiological function of virus and can not be simply concluded by frameshifting efficiency. On the other hand, the effect of a modified RdRp peptide sequence by the C deletion needs to be taken into account. Moreover, co-expression of P27 viral protease but not replicase reduced production of the downstream reporter when the minimal frameshifting signal was present (127). This phenomenon is similar to the feedback regulation of antizyme synthesis (21), RF2 (11), and the eRF1 interaction with reverse transcriptase of *Moloney murine leukemia virus* (MuLV) (128), but the mechanism in CfMV still needs to be investigated.

The frameshift-inducing element in HTLV-2 is a 10 bp perfect stem capped by a CUA triloop (Figure 12) (119). On the basis of an extensive mutational analysis by shuffling of HIV-1 and HTLV-2 frameshifting RNA elements in a background of HIV-1 or HTLV-2 sequences, it was proposed that the frameshifting efficiency is not only determined by slippery sequences and stimulatory secondary structures but also largely affected by sequences upstream of slip site and the sequence of the spacer

region (119). However, closer examination of the correlation between frameshifting efficiency and the identity of the first nucleotide of the spacer shows no similar trend as proposed by Fayet's lab that the strong stacking of purine may stabilize the codon-anticodon interaction at the A site of slippery sequence thereby reducing frameshifting efficiency (129).

The discovery that -1 PRF is responsible for gag-pol polyprotein expression in HIV-1 was made more than 20 years ago (33) but the exact nature of the stimulatory structure has long been debated. Through extensive mutational and structure probing studies, combined with sequence alignments and NMR structure analysis (114–117, 130), the frameshift stimulator of HIV-1 is generally believed to be a 11 bp stem with a highly ordered ACAA tetra loop rather than a pseudoknot structure (Figure 12) (131, 132). An additional 8 bp unstable lower stem was later proposed to contribute to the frameshift efficiency (116). Considering that the ribosome has to be positioned over the slippery sequence when stalled by the hairpin, the lower stem should be melted during -1 PRF. Hence, the exact function of the lower stem is unknown. It was proposed that the lower stem acts as a "positioning element" to allow the upper 11 bp hairpin to pause ribosomes which in turn mediates translocation perturbations via an unknown mechanism (116). It is well known that subtle modulations of Gag/Gag-Pol ratio have profound negative effects on HIV infection activity (133, 134). Hence, it has been proposed that the finding of either cellular proteins (135, 136) or small molecules (137, 138) that may interact with the HIV frameshifting hairpin and affect its frameshifting efficiency, have the potential to become anti-HIV drugs.

HIV-2 and SIV, belonging to the genus lentiviruses like HIV-1, have nearly identical frameshifting stimulatory structures but somewhat distinct from the HIV-1 frameshifting stem-loop (139). The major difference is the 12 nts loop of HIV-2/SIV, which has been proposed to incorporate a sheared G-A base pair, a cross-strand adenosine stacking, two G-C base pairs, and a novel CYC (Y = C in SIV, Y = U in HIV-2) triloop sequence. The spacer between slip site and "main" frameshifting hairpin comprises a C : C mismatch, a 4 bp helical stem, and 4 (SIV) or 5 nts (HIV-2) single stranded region making it one (SIV) or two (HIV-2) nucleotides longer than the spacer of HIV-1. Noticeably, the stem length of SIV/HIV-2 and HIV-1 is 11 bp which is similar to the S1 of the IBV frameshifting pseudoknot. Since a full helical turn A-form RNA duplex is 11 bp, it may imply a similar mechanism to stimulate frameshifting for these RNA structures (41, 48). Although it was suggested that SIV/HIV-2 frameshifting signal is a hairpin, extending the signal by another 12 nts increased frameshifting from 8.3 to 12.2% (Figure 13). Interestingly, this extended

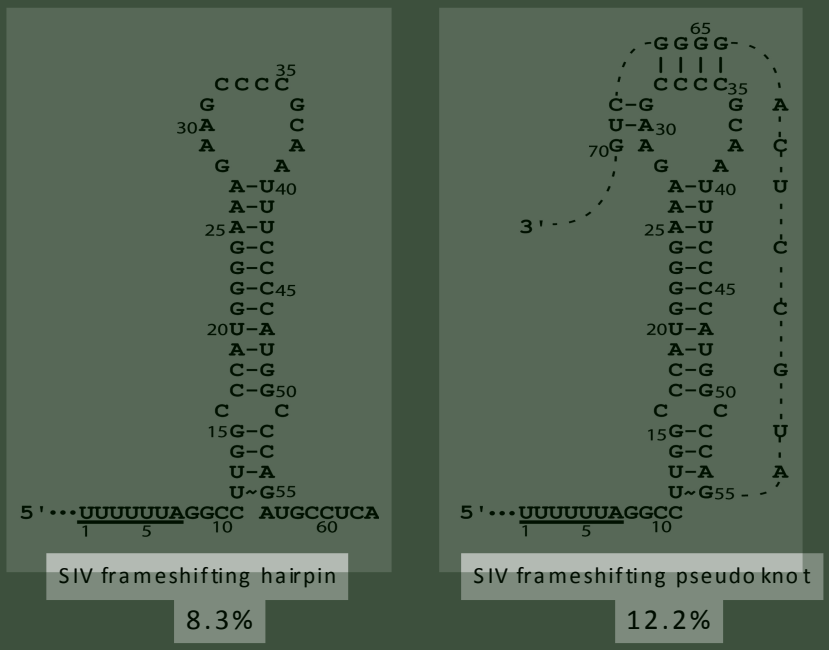


**Figure 13. Structure representation of predicted SIV frameshifting hairpin and frameshifting pseudoknot. The reported frameshifting efficiencies *in vitro* are indicated. (adapted from Marcheschi *et al.*, 2007)**

sequence can form a pseudoknot by base pairing with the 5'-AGCCCC- 3' sequence in the loop. This pseudoknot is conserved in all published strains (Olsthoorn, personal communication). So, similar to the HIV-1 group O retroviruses that make use of a pseudoknot instead of a simple stem-loop structure to regulate expression (140) the signal in SIV and HIV-2 retroviruses may be a pseudoknot as well. Why Butcher's lab has chosen to solve the structure of the less relevant hairpin structure remains unclear.

## 4. Antisense oligonucleotides (AONs)

Apart from natural examples of frameshifting structures, a novel finding has been the demonstration that synthetic AONs, annealed 3' of the slippery sequence and thereby mimicking a hairpin structure, are able to stimulate frameshifting *in vitro* (141, 142) and *in vivo* (143). In addition, AONs can also simulate triple helix (80) or kissing loop structures (106) to promote -1 PRF. These interesting results suggest that AONs act as physical barriers to stall ribosomes to stimulate ribosomal frameshifting and therefore are useful to dissect the mechanism of -1 PRF. Moreover, the great flexibility of AONs may have potential to treat frameshifting diseases.

## Conclusion

A wide variety of structures are able to induce ribosomal frameshifting. Their

efficiency depends much on their thermodynamic stability but additonally kinetic and mechanical aspects should be considered. As a rule of thumb it can be postulated that the smaller the structures the more additional interactions i.e. base triples and quadruples they need to withstand the ribosomal helicase. The pseudoknot may be a perfect platform to bring together such interactions. Whether these structures are actively involved in the recoding event or merely a physical barrier that increases the time for tRNAs to repair remains a matter of debate.

## Reference

1. Baranov,P.V., Gesteland,R.F. and Atkins,J.F. (2002) Recoding: translational bifurcations in gene expression. *Gene*, **286**, 187-201.

2. Gesteland,R.F., Weiss,R.B. and Atkins,J.F. (1992) Recoding: reprogrammed genetic decoding. *Science*, **257**, 1640-1641.

3. Namy,O., Hatin,I. and Rousset,J.-P. (2001) Impact of the six nucleotides downstream of the stop codon on translation termination. *EMBO Rep.*, **2**, 787-793.

4. Namy,O., Duchateau-Nguyen,G., Hatin,I., Hermann-Le Denmat,S., Termier,M. and Rousset,J.-P. (2003) Identification of stop codon readthrough genes in Saccharomyces cerevisiae. *Nucleic Acids Res.*, **31**, 2289-2296.

5. Bidou,L., Rousset,J.-P. and Namy,O. (2010) Translational errors: from yeast to new therapeutic targets. *FEMS Yeast Res.*, **10**, 1070-1082.

6. Hatfield,D.L. and Gladyshev,V.N. (2002) How selenium has altered our understanding of the genetic code. *Mol. Cell Biol.*, **22**, 3565-3576.

7. Howard,M.T., Aggarwal,G., Anderson,C.B., Khatri,S., Flanigan,K.M. and Atkins,J.F. (2005) Recoding elements located adjacent to a subset of eukaryal selenocysteine-specifying UGA codons. *EMBO J.*, **24**, 1596-1607.

8. Namy,O., Rousset,J.P., Napthine,S. and Brierley,I. (2004) Reprogrammed genetic decoding in cellular gene expression. *Mol. Cell*, **13**, 157-168.

9. Xu,J., Hendrix,R.W. and Duda,R.L. (2004) Conserved translational frameshift in dsDNA bacteriophage tail assembly genes. *Mol. Cell*, **16**, 11-21.

10. Baranov,P.V., Gesteland,R.F. and Atkins,J.F. (2004) P-site tRNA is a crucial

initiator of ribosomal frameshifting. *RNA*, **10**, 221-230.

11. Márquez,V., Wilson,D.N., Tate,W.P., Triana-Alonso,F. and Nierhaus,K.H. (2004) Maintaining the Ribosomal Reading Frame:: The Influence of the E Site during Translational Regulation of Release Factor 2. *Cell*, **118**, 45 – 55.

12. Devaraj,A. and Fredrick,K. (2010) Short spacing between the Shine-Dalgarno sequence and P codon destabilizes codon-anticodon pairing in the P site to promote +1 programmed frameshifting. *Mol. Microbiol.*, **78**, 1500-1509.

13. Curran,J.F. (1993) Analysis of effects of tRNA:message stability on frameshift frequency at the Escherichia coli RF2 programmed frameshift site. *Nucleic Acids Res.*, **21**, 1837-1843.

14. Adamski,F.M., Donly,B.C. and Tate,W.P. (1993) Competition between frameshifting, termination and suppression at the frameshift site in the Escherichia coli release factor-2 mRNA. *Nucleic Acids Res.*, **21**, 5074-5078.

15. Mansell,J.B., Guévremont,D., Poole,E.S. and Tate,W.P. (2001) A dynamic competition between release factor 2 and the tRNA(Sec) decoding UGA at the recoding site of Escherichia coli formate dehydrogenase H. *EMBO J.*, **20**, 7284-7293.

16. Belcourt,M.F. and Farabaugh,P.J. (1990) Ribosomal frameshifting in the yeast retrotransposon Ty: tRNAs induce slippage on a 7 nucleotide minimal site. *Cell*, **62**, 339-352.

17. Farabaugh,P.J., Zhao,H. and Vimaladithan,A. (1993) A novel programed frameshift expresses the POL3 gene of retrotransposon Ty3 of yeast: frameshifting without tRNA slippage. *Cell*, **74**, 93-103.

18. Guarraia,C., Norris,L., Raman,A. and Farabaugh,P.J. (2007) Saturation mutagenesis of a +1 programmed frameshift-inducing mRNA sequence derived from a yeast retrotransposon. *RNA*, **13**, 1940-1947.

19. Ivanov,I.P. and Atkins,J.F. (2007) Ribosomal frameshifting in decoding antizyme mRNAs from yeast and protists to humans: close to 300 cases reveal remarkable diversity despite underlying conservation. *Nucleic Acids Res.*, **35**, 1842-1858.

20. Petros,L.M., Howard,M.T., Gesteland,R.F. and Atkins,J.F. (2005) Polyamine sensing during antizyme mRNA programmed frameshifting. *Biochem. Biophys.*

*Res. Commun.*, **338**, 1478-1489.

21. Matsufuji,S., Matsufuji,T., Miyazaki,Y., Murakami,Y., Atkins,J.F., Gesteland,R.F. and Hayashi,S. (1995) Autoregulatory frameshifting in decoding mammalian ornithine decarboxylase antizyme. *Cell*, **80**, 51-60.

22. Ivanov,I.P., Anderson,C.B., Gesteland,R.F. and Atkins,J.F. (2004) Identification of a new antizyme mRNA +1 frameshifting stimulatory pseudoknot in a subset of diverse invertebrates and its apparent absence in intermediate species. *J. Mol. Biol.*, **339**, 495-504.

23. Namy,O., Galopier,A., Martini,C., Matsufuji,S., Fabret,C. and Rousset,J.-P. (2008) Epigenetic control of polyamines by the prion [PSI+]. *Nat. Cell Biol.*, **10**, 1069-1075.

24. Park,H.J., Park,S.J., Oh,D.-B., Lee,S. and Kim,Y.-G. (2009) Increased -1 ribosomal frameshifting efficiency by yeast prion-like phenotype [PSI+]. *FEBS Lett.*, **583**, 665-669.

25. Jacks,T. and Varmus,H.E. (1985) Expression of the Rous sarcoma virus pol gene by ribosomal frameshifting. *Science*, **230**, 1237-1242.

26. Baranov,P.V., Fayet,O., Hendrix,R.W. and Atkins,J.F. (2006) Recoding in bacteriophages and bacterial IS elements. *Trends in Genetics*, **22**, 174-181.

27. Farabaugh,P.J. (1996) Programmed translational frameshifting. *Microbiol. Rev.*, **60**, 103-34.

28. Larsen,B., Gesteland,R.F. and Atkins,J.F. (1997) Structural probing and mutagenic analysis of the stem-loop required for Escherichia coli dnaX ribosomal frameshifting: programmed efficiency of 50%. *J. Mol. Biol.*, **271**, 47-60.

29. Wills,N.M. (2006) A Functional -1 Ribosomal Frameshift Signal in the Human Paraneoplastic Ma3 Gene. *J. Biol. Chem.*, **281**, 7082-7088.

30. Manktelow,E., Shigemoto,K. and Brierley,I. (2005) Characterization of the frameshift signal of Edr, a mammalian example of programmed- 1 ribosomal frameshifting. *Nucleic Acids Res.*, **33**, 1553-1563.

31. Clark,M.B., Janicke,M., Gottesbuhren,U., Kleffmann,T., Legge,M., Poole,E.S. and Tate,W.P. (2007) Mammalian Gene PEG10 Expresses Two Reading

Frames by High Efficiency -1 Frameshifting in Embryonic-associated Tissues. *J. Biol. Chem.*, **282**, 37359-37369.

32. Brierley,I., Jenner,A.J. and Inglis,S.C. (1992) Mutational analysis of the "slippery-sequence" component of a coronavirus ribosomal frameshifting signal. *J. Mol. Biol.*, **227**, 463-479.

33. Jacks,T., Power,M.D., Masiarz,F.R., Luciw,P.A., Barr,P.J. and Varmus,H.E. (1988) Characterization of ribosomal frameshifting in HIV-1 gag-pol expression. *Nature*, **331**, 280-283.

34. ten Dam,E.B., Pleij,C.W. and Bosch,L. (1990) RNA pseudoknots: translational frameshifting and readthrough on viral RNAs. *Virus Genes*, **4**, 121-136.

35. Tu,C., Tzeng,T.H. and Bruenn,J.A. (1992) Ribosomal movement impeded at a pseudoknot required for frameshifting. *Proc. Natl. Acad. Sci. U.S.A.*, **89**, 8636-8640.

36. Lopinski,J.D., Dinman,J.D. and Bruenn,J.A. (2000) Kinetics of ribosomal pausing during programmed -1 translational frameshifting. *Mol. Cell. Biol.*, **20**, 1095-1103.

37. Kontos,H., Napthine,S. and Brierley,I. (2001) Ribosomal pausing at a frameshifter RNA pseudoknot is sensitive to reading phase but shows little correlation with frameshift efficiency. *Mol. Cell. Biol.*, **21**, 8657-8670.

38. Namy,O., Moran,S.J., Stuart,D.I., Gilbert,R.J.C. and Brierley,I. (2006) A mechanical explanation of RNA pseudoknot function in programmed ribosomal frameshifting. *Nature*, **441**, 244-247.

39. Cornish,P.V., Ermolenko,D.N., Noller,H.F. and Ha,T. (2008) Spontaneous intersubunit rotation in single ribosomes. *Mol. Cell*, **30**, 578-588.

40. Qu,X., Wen,J.-D., Lancaster,L., Noller,H.F., Bustamante,C. and Tinoco,I.,Jr (2011) The ribosome uses two active mechanisms to unwind messenger RNA during translation. *Nature*, **475**, 118-121.

41. Giedroc,D.P., Theimer,C.A. and Nixon,P.L. (2000) Structure, stability and function of RNA pseudoknots involved in stimulating ribosomal frameshifting1. *J. Mol. Biol.*, **298**, 167-185.

42. Rietveld,K., Van Poelgeest,R., Pleij,C.W., Van Boom,J.H. and Bosch,L. (1982)

The tRNA-like structure at the 3' terminus of turnip yellow mosaic virus RNA. Differences and similarities with canonical tRNA. *Nucleic Acids Res.*, **10**, 1929-1946.

43. Dam,E., Pleij,K. and Draper,D. (1992) Structural and functional aspects of RNA pseudoknots. *Biochemistry*, **31**, 11665-11676.

44. Brierley,I., Pennell,S. and Gilbert,R.J.. (2007) Viral RNA pseudoknots: versatile motifs in gene expression and replication. *Nat. Rev. Microbiol.*, **5**, 598 - 610.

45. Egli,M., Minasov,G., Su,L. and Rich,A. (2002) Metal ions and flexibility in a viral RNA pseudoknot at atomic resolution. *Proc. Natl. Acad. Sci. U.S.A.*, **99**, 4302-4307.

46. Nixon,P.L., Cornish,P.V., Suram,S.V. and Giedroc,D.P. (2002) Thermodynamic analysis of conserved loop-stem interactions in P1-P2 frameshifting RNA pseudoknots from plant Luteoviridae. *Biochemistry*, **41**, 10665-10674.

47. Chen,X., Kang,H., Shen,L.X., Chamorro,M., Varmus,H.E. and Tinoco,I.,Jr (1996) A characteristic bent conformation of RNA pseudoknots promotes -1 frameshifting during translation of retroviral RNA. *J. Mol. Biol.*, **260**, 479-483.

48. Giedroc,D.P. and Cornish,P.V. (2009) Frameshifting RNA pseudoknots: structure and mechanism. *Virus research*, **139**, 193-208.

49. Wilkinson,S.R. and Been,M.D. (2005) A pseudoknot in the 3' non-core region of the glmS ribozyme enhances self-cleavage activity. *RNA*, **11**, 1788-1794.

50. Montange,R.K. and Batey,R.T. (2008) Riboswitches: emerging themes in RNA structure and function. *Annu. Rev. Biophys*, **37**, 117-133.

51. Gilley,D. and Blackburn,E.H. (1999) The telomerase RNA pseudoknot is critical for the stable assembly of a catalytically active ribonucleoprotein. *Proc. Natl. Acad. Sci. U.S.A.*, **96**, 6621-6625.

52. Wang,C., Le,S.Y., Ali,N. and Siddiqui,A. (1995) An RNA pseudoknot is an essential structural element of the internal ribosome entry site located within the hepatitis C virus 5' noncoding region. *RNA*, **1**, 526-537.

53. Kolupaeva,V.G., Pestova,T.V. and Hellen,C.U. (2000) Ribosomal binding to the internal ribosomal entry site of classical swine fever virus. *RNA*, **6**, 1791-1807.

54. Pestova,T.V., Lomakin,I.B. and Hellen,C.U.T. (2004) Position of the CrPV IRES on the 40S subunit and factor dependence of IRES/80S ribosome assembly. *EMBO Rep.*, **5**, 906-913.

55. Philippe,C., Eyermann,F., Bénard,L., Portier,C., Ehresmann,B. and Ehresmann,C. (1993) Ribosomal protein S15 from Escherichia coli modulates its own translation by trapping the ribosome on the mRNA initiation loading site. *Proc. Natl. Acad. Sci. U.S.A.*, **90**, 4394-4398.

56. Chamorro,M., Parkin,N. and Varmus,H.E. (1992) An RNA pseudoknot and an optimal heptameric shift site are required for highly efficient ribosomal frameshifting on a retroviral messenger RNA. *Proc. Natl. Acad. Sci. U.S.A.*,**89**, 713-717.

57. ten Dam,E., Brierley,I., Inglis,S. and Pleij,C. (1994) Identification and analysis of the pseudoknot-containing gag-pro ribosomal frameshift signal of simian retrovirus-1. *Nucleic Acids Res.*, **22**, 2304-2310.

58. Su,L., Chen,L., Egli,M., Berger,J.M. and Rich,A. (1999) Minor groove RNA triplex in the crystal structure of a ribosomal frameshifting viral pseudoknot. *Nat. Struct. Biol.*, **6**, 285-292.

59. Shen,L.X. and Tinoco,I.,Jr (1995) The structure of an RNA pseudoknot that causes efficient frameshifting in mouse mammary tumor virus. *J. Mol. Biol.*, **247**, 963-978.

60. Chen,X., Chamorro,M., Lee,S.I., Shen,L.X., Hines,J.V., Tinoco,I.,Jr and Varmus,H.E. (1995) Structural and functional studies of retroviral RNA pseudoknots involved in ribosomal frameshifting: nucleotides at the junction of the two stems are important for efficient ribosomal frameshifting. *EMBO J.*, **14**, 842-852.

61. Chen,X., Kang,H., Shen,L.X., Chamorro,M., Varmus,H.E. and Tinoco,I.,Jr (1996) A characteristic bent conformation of RNA pseudoknots promotes -1 frameshifting during translation of retroviral RNA. *J. Mol. Biol.*, **260**, 479-483.

62. Kang,H. and Tinoco,I.,Jr (1997) A mutant RNA pseudoknot that promotes ribosomal frameshifting in mouse mammary tumor virus. *Nucleic Acids Res.*, **25**, 1943-1949.

63. Kang,H., Hines,J.V. and Tinoco,I.,Jr (1996) Conformation of a non-frameshifting RNA pseudoknot from mouse mammary tumor virus. *J. Mol. Biol.*, **259**, 135-147.

64. Morikawa,S. and Bishop,D.H. (1992) Identification and analysis of the gag-pol ribosomal frameshift site of feline immunodeficiency virus. *Virology*, **186**, 389-397.

65. Sung,D. and Kang,H. (1998) Mutational analysis of the RNA pseudoknot involved in efficient ribosomal frameshifting in simian retrovirus-1. *Nucleic Acids Res.*, **26**, 1369 -1372.

66. Du,Z., Holland,J.A., Hansen,M.R., Giedroc,D.P. and Hoffman,D.W. (1997) Base-pairings within the RNA pseudoknot associated with the simian retrovirus-1 gag-pro frameshift site. *J. Mol. Biol.*, **270**, 464-470.

67. Michiels,P.J., Versleijen,A.A., Verlaan,P.W., Pleij,C.W., Hilbers,C.W. and Heus,H.A. (2001) Solution structure of the pseudoknot of SRV-1 RNA, involved in ribosomal frameshifting1. *J. Mol. Biol.*, **310**, 1109-1123.

68. ten Dam,E.B., Verlaan,P.W. and Pleij,C.W. (1995) Analysis of the role of the pseudoknot component in the SRV-1 gag-pro ribosomal frameshift signal: loop lengths and stability of the stem regions. *RNA*, **1**, 146-154.

69. Olsthoorn,R.C., Reumerman,R., Hilbers,C.W., Pleij,C.W. and Heus,H.A. (2010) Functional analysis of the SRV-1 RNA frameshifting pseudoknot. *Nucleic Acids Res.*, **38**, 7665-7672.

70. Wang,Y., Wills,N.M., Du,Z., Rangan,A., Atkins,J.F., Gesteland,R.F. and Hoffman,D.W. (2002) Comparative studies of frameshifting and nonframeshifting RNA pseudoknots: a mutational and NMR investigation of pseudoknots derived from the bacteriophage T2 gene 32 mRNA and the retroviral gag-pro frameshift site. *RNA*, **8**, 981-996.

71. Su,L., Chen,L., Egli,M., Berger,J.M. and Rich,A. (1999) Minor groove RNA triplex in the crystal structure of a ribosomal frameshifting viral pseudoknot. *Nat. Struct. Mol. Biol.*, **6**, 285-292.

72. Egli,M., Minasov,G., Su,L. and Rich,A. (2002) Metal ions and flexibility in a viral RNA pseudoknot at atomic resolution. *Proc. Natl. Acad. Sci. U.S.A.*, **99**, 4302-4307.

73. Pallan,P.S., Marshall,W.S., Harp,J., Jewett,F.C.,3rd, Wawrzak,Z., Brown,B.A.,2nd, Rich,A. and Egli,M. (2005) Crystal structure of a luteoviral RNA pseudoknot and model for a minimal ribosomal frameshifting motif. *Biochemistry*, **44**, 11315-11322.

74. Nixon,P.L., Rangan,A., Kim,Y.-G., Rich,A., Hoffman,D.W., Hennig,M. and Giedroc,D.P. (2002) Solution structure of a luteoviral P1-P2 frameshifting mRNA pseudoknot. *J. Mol. Biol.*, **322**, 621-633.

75. Giedroc,D.P., Cornish,P.V. and Hennig,M. (2003) Detection of scalar couplings involving 2'-hydroxyl protons across hydrogen bonds in a frameshifting mRNA pseudoknot. *J. Am. Chem. Soc*, **125**, 4676-4677.

76. Cornish,P.V., Stammler,S.N. and Giedroc,D.P. (2006) The global structures of a wild-type and poorly functional plant luteoviral mRNA pseudoknot are essentially identical. *RNA*, **12**, 1959-1969.

77. Kim,Y.G., Maas,S., Wang,S.C. and Rich,A. (2000) Mutational study reveals that tertiary interactions are conserved in ribosomal frameshifting pseudoknots of two luteoviruses. *RNA*, **6**, 1157-1165.

78. Nixon,P.L. and Giedroc,D.P. (2000) Energetics of a strongly pH dependent RNA tertiary structure in a frameshifting pseudoknot. *J. Mol. Biol.*, **296**, 659-671.

79. Nixon,P.L., Cornish,P.V., Suram,S.V. and Giedroc,D.P. (2002) Thermodynamic analysis of conserved loop-stem interactions in P1-P2 frameshifting RNA pseudoknots from plant Luteoviridae. *Biochemistry*, **41**, 10665-10674.

80. Chou,M.-Y. and Chang,K.-Y. (2010) An intermolecular RNA triplex provides insight into structural determinants for the pseudoknot stimulator of -1 ribosomal frameshifting. *Nucleic Acids Res.*, **38**, 1676-1685.

81. Cornish,P.V., Hennig,M. and Giedroc,D.P. (2005) A loop 2 cytidine-stem 1 minor groove interaction as a positive determinant for pseudoknot-stimulated -1 ribosomal frameshifting. *Proc. Natl. Acad. Sci. U.S.A.*, **102**, 12694-12699.

82. Cornish,P.V., Stammler,S.N. and Giedroc,D.P. (2006) The global structures of a wild-type and poorly functional plant luteoviral mRNA pseudoknot are essentially identical. *RNA*, **12**, 1959-1969.

83. Cornish,P.V. and Giedroc,D.P. (2006) Pairwise coupling analysis of helical junction hydrogen bonding interactions in luteoviral RNA pseudoknots.

*Biochemistry*, **45**, 11162-11171.

84. Plant,E.P., Rakauskaite,R., Taylor,D.R. and Dinman,J.D. (2010) Achieving a Golden Mean: Mechanisms by Which Coronaviruses Ensure Synthesis of the Correct Stoichiometric Ratios of Viral Proteins. *J. Virol.*, **84**, 4330-4340.

85. Brierley,I., Digard,P. and Inglis,S.C. (1989) Characterization of an efficient coronavirus ribosomal frameshifting signal: requirement for an RNA pseudoknot. *Cell*, **57**, 537-547.

86. Brierley,I. and Pennell,S. (2001) Structure and function of the stimulatory RNAs involved in programmed eukaryotic-1 ribosomal frameshifting. *Cold Spring Harb. Symp. Quant. Biol.*, **66**, 233-248.

87. Brierley,I., Rolley,N.J., Jenner,A.J. and Inglis,S.C. (1991) Mutational analysis of the RNA pseudoknot component of a coronavirus ribosomal frameshifting signal. *J. Mol. Biol.*, **220**, 889-902.

88. Pleij,C.W., Rietveld,K. and Bosch,L. (1985) A new principle of RNA folding based on pseudoknotting. *Nucleic Acids Res.*, **13**, 1717-1731.

89. Napthine,S., Liphardt,J., Bloys,A., Routledge,S. and Brierley,I. (1999) The role of RNA pseudoknot stem 1 length in the promotion of efficient -1 ribosomal frameshifting. *J. Mol. Biol.*, **288**, 305-320.

90. Liphardt,J., Napthine,S., Kontos,H. and Brierley,I. (1999) Evidence for an RNA pseudoknot loop-helix interaction essential for efficient -1 ribosomal frameshifting. *J. Mol. Biol.*, **288**, 321-335.

91. Cate,J.H., Gooding,A.R., Podell,E., Zhou,K., Golden,B.L., Szewczak,A.A., Kundrot,C.E., Cech,T.R. and Doudna,J.A. (1996) RNA tertiary structure mediation by adenosine platforms. *Science*, **273**, 1696-1699.

92. Kolk,M.H., van der Graaf,M., Wijmenga,S.S., Pleij,C.W., Heus,H.A. and Hilbers,C.W. (1998) NMR structure of a classical pseudoknot: interplay of single- and double-stranded RNA. *Science*, **280**, 434-438.

93. Bredenbeek,P.J., Pachuk,C.J., Noten,A.F., Charité,J., Luytjes,W., Weiss,S.R. and Spaan,W.J. (1990) The primary structure and expression of the second open reading frame of the polymerase gene of the coronavirus MHV-A59; a highly conserved polymerase is expressed by an efficient ribosomal frameshifting mechanism. *Nucleic Acids Res.*, **18**, 1825-1832.

94. Herold,J. and Siddell,S.G. (1993) An "elaborated" pseudoknot is required for high frequency frameshifting during translation of HCV 229E polymerase mRNA. *Nucleic Acids Res.*, **21**, 5838-5842.

95. Thiel,V., Ivanov,K.A., Putics,A., Hertzig,T., Schelle,B., Bayer,S., Weissbrich,B., Snijder,E.J., Rabenau,H., Doerr,H.W., et al. (2003) Mechanisms and enzymes involved in SARS coronavirus genome expression. *J. Gen. Virol.*, **84**, 2305-2315.

96. Brierley,I. and Dos Ramos,F.J. (2006) Programmed ribosomal frameshifting in HIV-1 and the SARS-CoV. *Virus research*, **119**, 29-42.

97. Baranov,P.V., Henderson,C.M., Anderson,C.B., Gesteland,R.F., Atkins,J.F. and Howard,M.T. (2005) Programmed ribosomal frameshifting in decoding the SARS-CoV genome. *Virology*, **332**, 498-510.

98. Plant,E.P., Pérez-Alvarado,G.C., Jacobs,J.L., Mukhopadhyay,B., Hennig,M. and Dinman,J.D. (2005) A Three-Stemmed mRNA Pseudoknot in the SARS Coronavirus Frameshift Signal. *Plos Biol.*, **3**, e172.

99. Su,M.-C., Chang,C.-T., Chu,C.-H., Tsai,C.-H. and Chang,K.-Y. (2005) An atypical RNA pseudoknot stimulator and an upstream attenuation signal for -1 ribosomal frameshifting of SARS coronavirus. *Nucleic Acids Res.*, **33**, 4265-4275.

100. Plant,E.P. and Dinman,J.D. (2008) The role of programmed-1 ribosomal frameshifting in coronavirus propagation. *Frontiers in bioscience: a journal and virtual library*, **13**, 4873.

101. Firth,A.E., Chung,B.Y., Fleeton,M.N. and Atkins,J.F. (2008) Discovery of frameshifting in Alphavirus 6K resolves a 20-year enigma. *Virol. J.*, **5**, 108.

102. Chung,B.Y.-W., Firth,A.E. and Atkins,J.F. (2010) Frameshifting in alphaviruses: a diversity of 3'stimulatory structures. *J. Mol. Biol.*, **397**, 448-456.

103. Paul,C.P., Barry,J.K., Dinesh-Kumar,S.P., Brault,V. and Miller,W.A. (2001) A sequence required for -1 ribosomal frameshifting located four kilobases downstream of the frameshift site. *J. Mol. Biol.*, **310**, 987-999.

104. Barry,J.K. and Miller,W.A. (2002) A -1 ribosomal frameshift element that requires base pairing across four kilobases suggests a mechanism of regulating ribosome and replicase traffic on a viral RNA. *Proc. Natl. Acad. Sci. U.S.A.*,

**99**, 11133-11138.

105. Tajima,Y., Iwakawa,H.-O., Kaido,M., Mise,K. and Okuno,T. (2011) A long-distance RNA-RNA interaction plays an important role in programmed -1 ribosomal frameshifting in the translation of p88 replicase protein of Red clover necrotic mosaic virus. *Virology*, **417**, 169-178.

106. Mazauric,M.-H., Licznar,P., Prère,M.-F., Canal,I. and Fayet,O. (2008) Apical loop-internal loop RNA pseudoknots: a new type of stimulator of -1 translational frameshifting in bacteria. *J. Biol. Chem.*, **283**, 20421-20432.

107. Pennell,S., Manktelow,E., Flatt,A., Kelly,G., Smerdon,S.J. and Brierley,I. (2008) The stimulatory RNA of the Visna-Maedi retrovirus ribosomal frameshifting signal is an unusual pseudoknot with an interstem element. *RNA*, **14**, 1366-1377.

108. Chou,M.-Y., Lin,S.-C. and Chang,K.-Y. (2010) Stimulation of -1 programmed ribosomal frameshifting by a metabolite-responsive RNA pseudoknot. *RNA*, **16**, 1236-1244.

109. Somogyi,P., Jenner,A.J., Brierley,I. and Inglis,S.C. (1993) Ribosomal pausing during translation of an RNA pseudoknot. *Mol. Cell. Biol.*, **13**, 6931-6940.

110. Kontos,H., Napthine,S. and Brierley,I. (2001) Ribosomal pausing at a frameshifter RNA pseudoknot is sensitive to reading phase but shows little correlation with frameshift efficiency. *Mol. Cell Biol.*, **21**, 8657-8670.

111. Namy,O., Moran,S.J., Stuart,D.I., Gilbert,R.J.C. and Brierley,I. (2006) A mechanical explanation of RNA pseudoknot function in programmed ribosomal frameshifting. *Nature*, **441**, 244-247.

112. Brierley,I., Meredith,M.R., Bloys,A.J. and Hagervall,T.G. (1997) Expression of a coronavirus ribosomal frameshift signal in Escherichia coli: influence of tRNA anticodon modification on frameshifting. *J. Mol. Biol.*, **270**, 360-373.

113. Napthine,S., Vidakovic,M., Girnary,R., Namy,O. and Brierley,I. (2003) Prokaryotic-style frameshifting in a plant translation system: conservation of an unusual single-tRNA slippage event. *EMBO J.*, **22**, 3941-3950.

114. Dulude,D., Baril,M. and Brakier-Gingras,L. (2002) Characterization of the frameshift stimulatory signal controlling a programmed -1 ribosomal frameshift in the human immunodeficiency virus type 1. *Nucleic Acids Res.*,

**30**, 5094-5102.

115. Staple,D.W. and Butcher,S.E. (2003) Solution structure of the HIV-1 frameshift inducing stem-loop RNA. *Nucleic Acids Res.*, **31**, 4326-4331.

116. Staple,D.W. and Butcher,S.E. (2005) Solution structure and thermodynamic investigation of the HIV-1 frameshift inducing element. *J. Mol. Biol.*, **349**, 1011-1023.

117. Gaudin,C., Mazauric,M.-H., Traïkia,M., Guittet,E., Yoshizawa,S. and Fourmy,D. (2005) Structure of the RNA signal essential for translational frameshifting in HIV-1. *J. Mol. Biol.*, **349**, 1024-1035.

118. Kollmus,H., Honigman,A., Panet,A. and Hauser,H. (1994) The sequences of and distance between two cis-acting signals determine the efficiency of ribosomal frameshifting in human immunodeficiency virus type 1 and human T-cell leukemia virus type II in vivo. *J. Virol.*, **68**, 6087-6091.

119. Kim,Y.G., Maas,S. and Rich,A. (2001) Comparative mutational analysis of cis-acting RNA signals for translational frameshifting in HIV-1 and HTLV-2. *Nucleic Acids Res.*, **29**, 1125-1131.

120. Lucchesi,J., Mäkeläinen,K., Merits,A., Tamm,T. and Mäkinen,K. (2000) Regulation of -1 ribosomal frameshifting directed by cocksfoot mottle sobemovirus genome. *Eur. J. Biochem.*, **267**, 3523-3529.

121. Mäkinen,K., Tamm,T., Naess,V., Truve,E., Puurand,U., Munthe,T. and Saarma,M. (1995) Characterization of cocksfoot mottle sobemovirus genomic RNA and sequence comparison with related viruses. *J. Gen. Virol.*, **76**, 2817-2825.

122. Tamm,T., Suurväli,J., Lucchesi,J., Olspert,A. and Truve,E. (2009) Stem-loop structure of Cocksfoot mottle virus RNA is indispensable for programmed -1 ribosomal frameshifting. *Virus Res.*, **146**, 73-80.

123. Tsuchihashi,Z. and Kornberg,A. (1990) Translational frameshifting generates the gamma subunit of DNA polymerase III holoenzyme. *Proc. Natl. Acad. Sci. U.S.A.*, **87**, 2516-2520.

124. Larsen,B., Gesteland,R.F. and Atkins,J.F. (1997) Structural probing and mutagenic analysis of the stem-loop required for Escherichia coli dnaX ribosomal frameshifting: programmed efficiency of 50%. *J. Mol. Biol.*, **271**,

47-60.

125. Bidou,L., Stahl,G., Grima,B., Liu,H., Cassan,M. and Rousset,J.P. (1997) In vivo HIV-1 frameshifting efficiency is directly related to the stability of the stem-loop stimulatory signal. *RNA*, **3**, 1153-1158.

126. Mäkinen,K., Naess,V., Tamm,T., Truve,E., Aaspõllu,A. and Saarma,M. (1995) The putative replicase of the cocksfoot mottle sobemovirus is translated as a part of the polyprotein by -1 ribosomal frameshift. *Virology*, **207**, 566-571.

127. Mäkeläinen,K. and Mäkinen,K. (2005) Factors affecting translation at the programmed -1 ribosomal frameshifting site of Cocksfoot mottle virus RNA in vivo. *Nucleic Acids Res.*, **33**, 2239-2247.

128. Orlova,M., Yueh,A., Leung,J. and Goff,S.P. (2003) Reverse transcriptase of Moloney murine leukemia virus binds to eukaryotic release factor 1 to modulate suppression of translational termination. *Cell*, **115**, 319-331.

129. Bertrand,C., Prère,M.F., Gesteland,R.F., Atkins,J.F. and Fayet,O. (2002) Influence of the stacking potential of the base 3'of tandem shift codons on -1 ribosomal frameshifting used for gene expression. *RNA*, **8**, 16-28.

130. Baril,M., Dulude,D., Gendron,K., Lemay,G. and Brakier-Gingras,L. (2003) Efficiency of a programmed -1 ribosomal frameshift in the different subtypes of the human immunodeficiency virus type 1 group M. *RNA*, **9**, 1246-1253.

131. Le,S.Y., Shapiro,B.A., Chen,J.H., Nussinov,R. and Maizel,J.V. (1991) RNA pseudoknots downstream of the frameshift sites of retroviruses. *Genet. Anal. Tech. Appl*, **8**, 191-205.

132. Dinman,J.D., Richter,S., Plant,E.P., Taylor,R.C., Hammell,A.B. and Rana,T.M. (2002) The frameshift signal of HIV-1 involves a potential intramolecular triplex RNA structure. *Proc. Natl. Acad. Sci. U.S.A.*, **99**, 5331-5336.

133. Shehu-Xhilaga,M., Crowe,S.M. and Mak,J. (2001) Maintenance of the Gag/Gag-Pol ratio is important for human immunodeficiency virus type 1 RNA dimerization and viral infectivity. *J. Virol.*, **75**, 1834-1841.

134. Telenti,A., Martinez,R., Munoz,M., Bleiber,G., Greub,G., Sanglard,D. and Peters,S. (2002) Analysis of natural variants of the human immunodeficiency virus type 1 gag-pol frameshift stem-loop structure. *J. Virol.*, **76**, 7868-7873.

135. Mazauric,M.-H., Seol,Y., Yoshizawa,S., Visscher,K. and Fourmy,D. (2009) Interaction of the HIV-1 frameshift signal with the ribosome. *Nucleic Acids Res.*, **37**, 7654-7664.

136. Kobayashi,Y., Zhuang,J., Peltz,S. and Dougherty,J. (2010) Identification of a cellular factor that modulates HIV-1 programmed ribosomal frameshifting. *J. Biol. Chem.*, **285**, 19776-19784.

137. Marcheschi,R.J., Mouzakis,K.D. and Butcher,S.E. (2009) Selection and characterization of small molecules that bind the HIV-1 frameshift site RNA. *ACS Chem. Biol.*, **4**, 844-854.

138. Marcheschi,R.J., Tonelli,M., Kumar,A. and Butcher,S.E. (2011) Structure of the HIV-1 Frameshift Site RNA Bound to a Small Molecule Inhibitor of Viral Replication. *ACS Chem. Biol.*, 6, 857-864.

139. Marcheschi,R.J., Staple,D.W. and Butcher,S.E. (2007) Programmed ribosomal frameshifting in SIV is induced by a highly structured RNA stem-loop. *J. Mol. Biol.*, **373**, 652-663.

140. Baril,M., Dulude,D., Steinberg,S.V. and Brakier-Gingras,L. (2003) The frameshift stimulatory signal of human immunodeficiency virus type 1 group O is a pseudoknot. *J. Mol. Biol.*, **331**, 571-583.

141. Olsthoorn,R.C.L., Laurs,M., Sohet,F., Hilbers,C.W., Heus,H.A. and Pleij,C.W.A. (2004) Novel application of sRNA: stimulation of ribosomal frameshifting. *RNA*, **10**, 1702-1703.

142. Howard,M.T., Gesteland,R.F. and Atkins,J.F. (2004) Efficient stimulation of site-specific ribosome frameshifting by antisense oligonucleotides. *RNA*, **10**, 1653-1661.

143. Henderson,C.M., Anderson,C.B. and Howard,M.T. (2006) Antisense-induced ribosomal frameshifting. *Nucleic Acids Res.*, **34**, 4302-4310.

# Chapter III

## Stem-loop structures can effectively substitute for an RNA pseudoknot in -1 ribosomal frameshifting

Chien-Hung Yu, Mathieu H.M. Noteborn, Cornelis W.A. Pleij, and René C.L. Olsthoorn.

Department of Molecular Genetics, Leiden Institute of Chemistry, Leiden University, PO Box 9502, 2300RA Leiden, The Netherlands.

Nucleic Acids Res., 2011, **39**:8952-9.

### Abstract

–1 programmed ribosomal frameshifting (PRF) in synthesizing gag/pro precursor polyprotein in *Simian retrovirus type-1* (SRV-1) is stimulated by a classical H-type pseudoknot which forms an extended triple helix involving base-base and base-sugar interactions between loop and stem nucleotides. Recently we showed that mutation of bases involved in triple helix formation affected frameshifting, again emphasizing the role of the triple helix in –1 PRF. Here, we investigated the efficiency of hairpins of similar base pair composition as the SRV-1 gag/pro pseudoknot. Although not capable of triple helix formation they proved worthy stimulators of frameshifting. Subsequent investigation of ~30 different hairpin constructs revealed that next to thermodynamic stability, also loop size and composition, and stem irregularities can influence frameshifting. Interestingly, hairpins carrying the stable GAAA tetraloop were significantly less shifty than other hairpins, including those with a UUCG motif. The data are discussed in relation to natural shifty hairpins.

## Introduction

Ribosomal frameshifting is a translational recoding event in which a certain percentage of ribosomes are forced to shift to another reading frame in order to synthesize an alternative protein. This switch occurs at a specific position on the mRNA, called the slip site or slippery sequence, and can be either forwards (+1) or backwards (–1). The nature and efficiency of frameshifting depends on several factors, including tRNA availability and modifications, and mRNA primary and secondary structure [see (1) and (2) for reviews].

The signals that are responsible for –1 frameshifting comprise two elements: a slippery sequence where the actual reading shift takes place, and a downstream located structural element which greatly stimulates the efficiency of frameshifting. Although the mechanism is still elusive, the present view is that the downstream structure forms a physical barrier that blocks EF-2 function and causes ribosomes to stall in their translocation step. This "roadblock" puts tension on the mRNA–tRNA interaction. The tension can be relieved by the realigning of A-site and P-site tRNAs in the 5′-direction, whereafter EF-2 can do its work and the ribosome resumes translation in the −1 reading frame (3).

In general, a pseudoknot is more efficient in stimulating frameshifting than a hairpin of the same sequence composition. This difference is likely related to a higher thermodynamic stability of the pseudoknot. Indeed, from thermodynamic analysis it appears that pseudoknots are more stable than their hairpin counterparts (4-6). Recent studies employing mechanical 'pulling' of frameshifter pseudoknots have shown a correlation between the mechanical strength of a pseudoknot and its frameshifting capacity (7,8), and the influence of major groove and minor groove triplex structures (9). The higher strength of a pseudoknot can be primarily attributed to the formation of base triples between the lower stem S1 and loop 2 (Fig. 1a), making it more resistant against unwinding by an elongating ribosome (8,10). Base triples in several pseudoknots, such as *Beet western yellows virus* (BWYV) p1-p2 (11), *Pea enation mosaic virus type-1* (PEMV-1) p1-p2 (6), *Sugarcane yellow leaf virus* (ScYLV) p1-p2 (12), and *Simian retrovirus type-1* gag-pro (SRV-1) (13,14) have been shown to play an essential role in frameshifting. For pseudoknots with a longer stem S1 of 10-11 base pairs (bp), like that of *Infectious Bronchitis Virus* (IBV), base triples do not appear to contribute to frameshifting (15)

Although a hairpin is considered to be a less efficient frameshift-inducing secondary structure than a pseudoknot, some viruses like *Human immunodeficiency virus* (HIV) (16), *Human T-lymphotropic virus type-2* (HTLV-2) (17), and *Cocksfoot mottle virus* (CfMV) (18) make use of a simple hairpin to stimulate substantial levels

of frameshifting. In addition, frameshifting in the prokaryotic *dnaX* gene, requires, next to an upstream enhancer, the presence of a hairpin as well (19). A few studies have investigated a correlation between hairpin stability and frameshift efficiency of natural shifty hairpins (19,20). Nonetheless, certain studies have shown that a hairpin composed of the same base pairs as a frameshifter pseudoknot is not efficient in inducing frameshifting in mammalian cells and lysates (21-23) but is in other systems (24).

Here we have carried out a systematic analysis of the frameshift-inducing efficiency of hairpins derived from the SRV-1 gag-pro frameshifter pseudoknot. Investigation of about 30 different hairpin constructs revealed that next to thermodynamic stability, also loop size and composition, and stem irregularities can significantly influence frameshifting. Our data showed that there exists no base specific contacts between the hairpin and the ribosome during frameshifting and suggests that the hairpin primarily serves as a barrier to allow repositioning of tRNAs at the slippery site.

## Materials and methods

### Plasmids construction

Mutations in the SRV-1 gag-pro frameshifting signal were made in an abridged version of plasmid SF2 (25) which is derivative of pSFCASS5 (26), a frameshift reporter construct. In this version the entire BglII-NcoI fragment of pSF2 was replaced by a synthetic dsDNA fragment (5'-GATCTTAATACGACTCACTATAGGGCTCA**TTTAAAC**TAGTTGAGGGGC CATATTTCGC-3', a SpeI restriction site is underlined). This yielded plasmid pSF208 in which the original GGGAAAC slippery sequence has been replaced by the more slippery UUUAAAC sequence (26). pSF208 was digested with SpeI and NcoI, and sets of complementary oligonucleotides corresponding to the various mutants were inserted. A list of oligonucleotides is available upon request. All constructs were verified by automated dideoxy sequencing using chain terminator dyes (LGTC, Leiden).

### *In vitro* transcription

DNA templates were linearized by BamHI digestion and purified by successive phenol/chloroform extraction and column filtration (Qiagen, Benelux). SP6 polymerase directed transcriptions were carried out in 50 µl reactions containing ~2 µg linearized DNA, 10 mM NTPs, 40 mM Tris-HCl (pH 7.9), 10 mM NaCl, 10 mM

DTT, 6 mM $MgCl_2$, 2 mM spermidine, 6 units of RNase inhibitor (RNAsin, Promega, Benelux), and 15 units of SP6 polymerase (Promega, Benelux). After an incubation period of 2 hr at 37ºC, samples were taken and run on agarose gels to determine the quality and quantity of the transcripts. Appropriate dilutions of the reaction mix in water were directly used for *in vitro* translations. Alternatively, transcripts were purified by phenol/chloroform extraction and isopropanol precipitation and quantified by UV absorption as described previously (14).

**_In vitro_ translation**

Experiments were carried out in duplicate using serially - in water - diluted mRNAs with final concentrations of 5 nM. Reactions contained 4 µl of an RNA solution, 4.5 µl of rabbit reticulocyte lysate (RRL, Promega), 0.25 - 1 µl of $^{35}S$ methionine (Amersham, *in vitro* translation grade), 0.5 µl of 1 mM amino acids lacking methionine and were incubated for 60 min. at 28°C. Samples were boiled for 3 min. in 2x Laemmli buffer and loaded onto 12% SDS polyacrylamide gels. Gels were dried and exposed to phosphoimager screens. Band intensity of 0-frame and –1 frameshift products was measured using a Molecular Imager FX and Quantity One software (Biorad). Frameshift percentages were calculated as the amount of –1 frameshift product divided by the sum of 0 and –1 frame products, corrected for the number of methionines (10 in the 0-frame product and 28 in the fusion product), multiplied by 100.

**Frameshift assays in mammalian cells**

Candidates of interest were constructed in a dual luciferase vector, pDUAL-HIV(0), essentially as described previously (14,27). In short, pDUAL-HIV(0) was digested by KpnI and BamHI, followed by insertion of complementary oligonucleotides to clone mutants with SRV-1 gag/pro pseudoknot, different lengths of stem of hairpins, and 9bp stems capped with the indicated loops (Figure 2c and 5). An in-frame control was constructed by inserting an A-residue upstream of the cytosine in the UUUAAAC slippery sequence of a 12bp hairpin frameshift construct and the negative control (NC) was constructed by inserting of scrambled sequence of complementary oligonucleotides without apparent secondary structure downstream of slippery sequence. Hela cells were cultured in DMEM/high glucose/stable glutamine (PAA Laboratories GmbH, Germany) and supplemented with 10% fetal calf serum and 100 U/ml penicillin and 100 µg/ml streptomycin. Cells were kept in a humidified atmosphere containing 5% CO2 at 37°C. Assay protocols were described previously (14). Briefly, cells were transfected with 300 ng of plasmid using 1 µl of lipofectamine-2000 (Invitrogen) in a 24-well plate. Cells were lysed 24 hr after

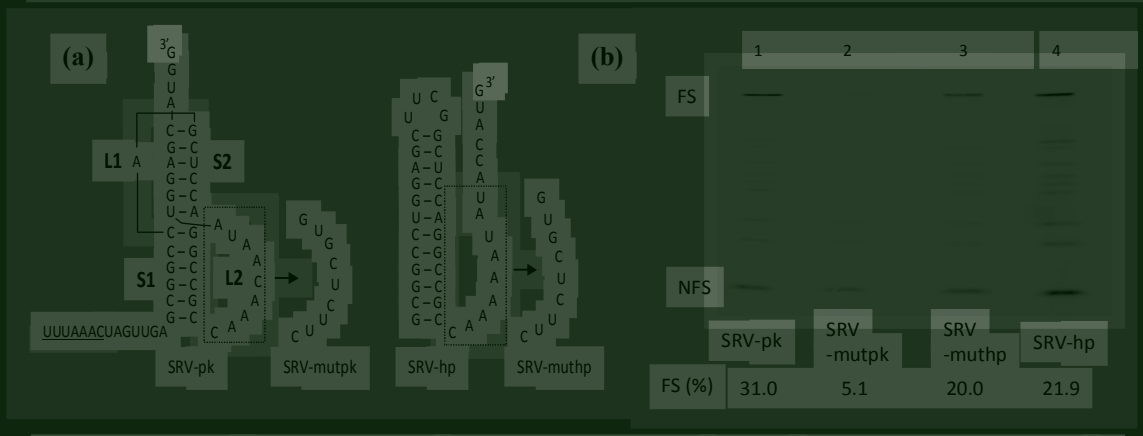


**Figure 1. Hairpin derivative of the Simian retrovirus type-1 (SRV-1) frameshift pseudoknot is an efficient frameshift stimulator. (a) Schematic representation of the SRV-1 pseudoknot (SRV-pk) and its hairpin derivative (SRV-hp). Mutations in SRV-pk loop 2 (L2) and SRV-hp are indicated. The slippery sequence is underlined. (b) SDS-PAGE analysis of 35S-methionine labeled translation products in rabbit reticulocyte lysate (RRL). -1 ribosomal frameshifting is monitored by appearance of the 65-kD product (FS). The non-shifted zero-frame product is indicated by NFS. Quantitative analysis of frameshifting efficiency [FS (%)] is described in Materials and**

transfection and luciferase activities were quantified by Glomax-multidetector (Promega, Benelux) according to manufacturer's protocol. Frameshifting efficiency was calculated by dividing the ratio of Renilla luciferase (RL) over Firefly luciferase (FL) activity of the mutant by the RL/FL ratio of the in-frame control, multiplied by 100.

## Results

### Hairpin derived from the SRV-1 gag-pro pseudoknot is an efficient frameshift stimulator

In contrast to earlier reports involving the IBV frameshifting pseudoknot (21,22), we found that in the case of the SRV-1 gag-pro frameshift inducing pseudoknot a hairpin of similar composition as the pseudoknot did stimulate frameshifting *in vitro* (Fig. 1a and 1b). The 12 bp hairpin derivative of the SRV-1 gag-pro pseudoknot (SRV-hp) showed 22% frameshifting efficiency, whereas the SRV-1 gag-pro pseudoknot (SRV-pk) in this context yielded 31%. The pseudoknot in these experiments is a modified version of the wild-type SRV-1 gag-pro pseudoknot previously used for NMR and functional analysis (14). We note that the UUUAAAC slippery sequence was used to enhance the sensitivity of the *in vitro* frameshifting assay. This sequence is approximately 1.5 fold more slippery than the wild-type GGGAAAC slippery sequence (28). In the latter context, the hairpin was indeed less efficient (data not

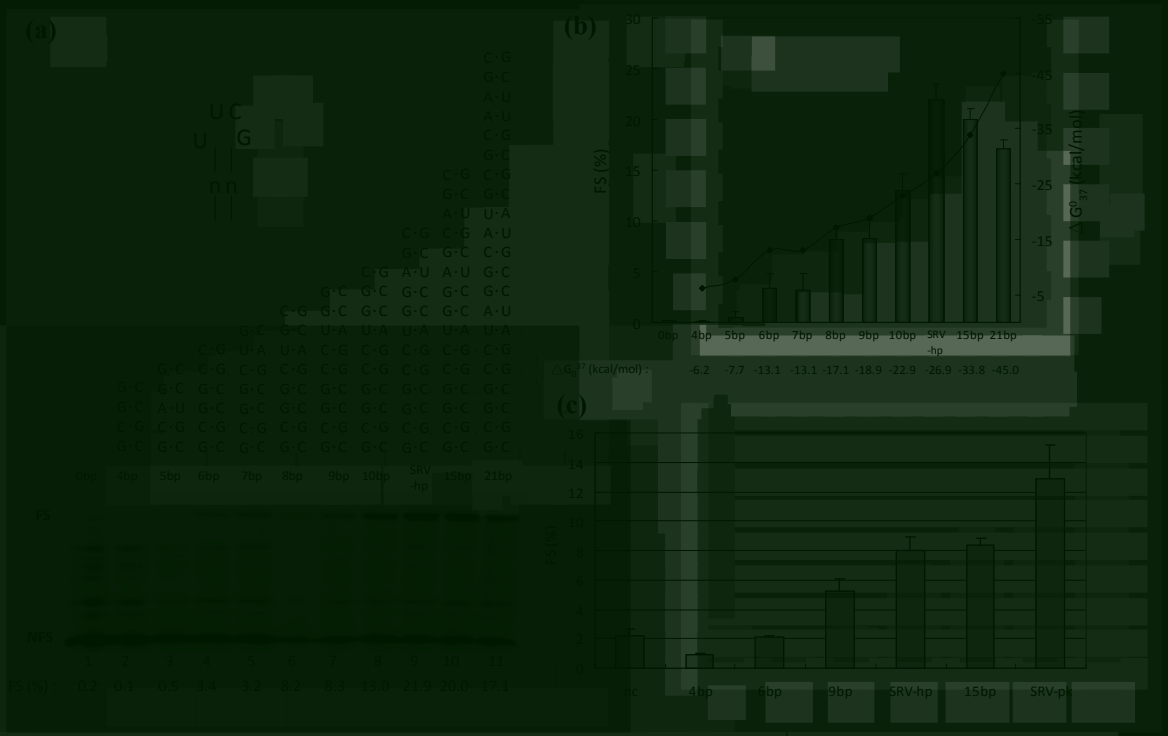


**Figure 2. Influence of stem length of UUCG-capped hairpins on –1 ribosomal frameshifting efficiency *in vitro* and *in vivo*. (a) SDS-PAGE analysis of $^{35}$S-methionine labeled translation products in RRL using mRNAs with hairpins of various stem lengths. See legend to Figure 1(b) for more details. The base composition of the various stems is shown. The 0bp is the control without a hairpin. (b) Graph showing the relation between frameshifting efficiency (indicated by bars) on the left y-axis and predicted thermodynamic stability by MFOLD (indicated by a solid diamond (◆) on the right y-axis. The average FS (%) and error bars were from at least three independent experiments. (c) Selected hairpins with different lengths of stem were assayed for their ability to induce -1 ribosomal frameshifting in Hela cells. The frameshifting efficiency was obtained by measuring dual-luciferase activity of a frameshift reporter construct (see Materials and Methods). The *in vivo* experiments were done at least three times in triplicate.**

shown) while a non-slippery variant, GGGAAGC, was not effective at all (<0.2%, data not shown). Two other known efficient slip sites, AAAAAAC and UUUUUUA, caused 23 and 27%, respectively, of ribosomes to switch frame in the presence of the 12bp hairpin (data not shown). These data showed that the 12bp hairpin is a genuine stimulator of frameshifting.

Since the hairpin construct also contained sequences resembling those of L2 of the pseudoknot construct, it was theoretically possible that these nucleotides could take part in the same base triples. To investigate this possibility, we replaced the downstream sequence in the hairpin construct (SRV-muthp). This did not affect the frameshift efficiency of the hairpin construct. By contrast, the same mutations in the pseudoknot context (SRV-mutpk) reduced its activity about 6 fold (Fig. 1b). Thus, it is

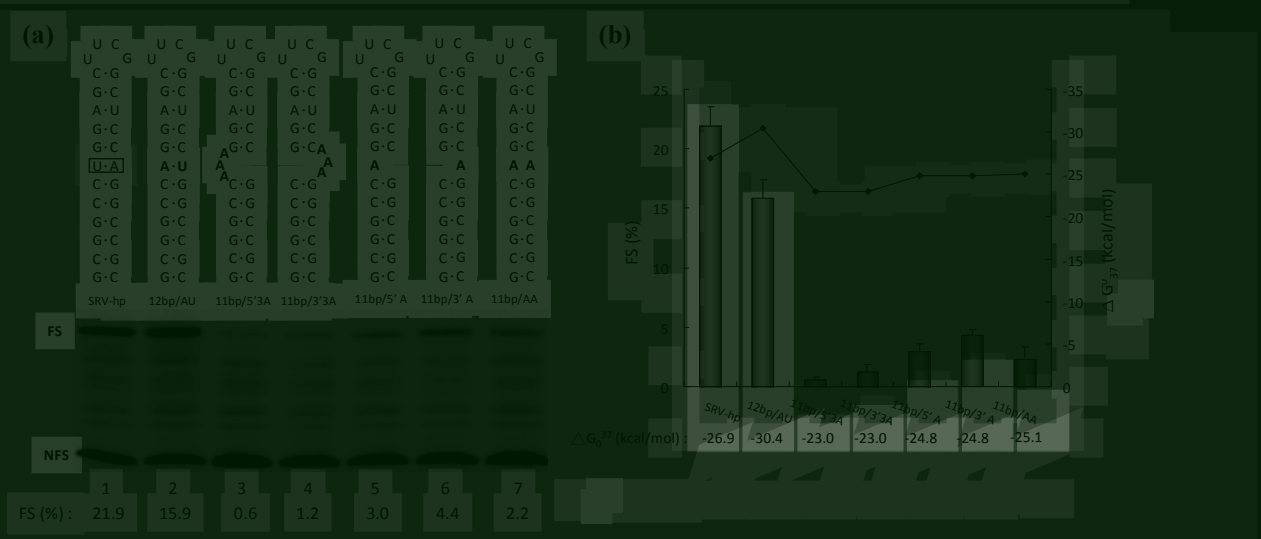


**Figure 3. Influence of bulges and mismatches in the middle part of the hairpin on frameshifting efficiency. (a) SDS-PAGE analysis of $^{35}$S-methionine labeled translation products in RRL using mRNAs containing the indicated hairpins. See legend to Figure 1(b) for more details. (b) Graph showing the relation between the predicted thermodynamic stability and frameshift efficiency. See legend to Figure 2(b) for more details.**

unlikely that triple helix formation or other tertiary interactions contribute to hairpin-dependent frameshifting; the hairpin as such seems to be sufficient.

**Effect of hairpin stem size on frameshifting efficiency**

Next, we investigated the role of stem length on frameshifting efficiency. Increasing the stem size from 12 to 15 or 21bp did not significantly alter frameshifting (Fig. 2a). On the other hand, decreasing stem size led to a steady decrease in frameshifting efficiency which seemed to vanish around a stem size of 5bp or $\Delta G^{37}$ of -7.7 kcal/mol (Fig. 2b). Thermodynamic stabilities were calculated at the MFOLD website using version 2.3 parameters (http://mfold.rna.albany.edu/?q=mfold/RNA-Folding-Form2.3), as these were previously shown to better fit *in vivo* hairpin stabilities (29). These data support the notion that downstream structures serve as barriers to stall translating ribosomes to stimulate frameshifting, and demonstrate that there is a correlation between the thermodynamic stability of a hairpin and its frameshift inducing capacity.

A selection of above hairpins was cloned into a dual-luciferase reporter plasmid and their frameshifting efficiency assayed in mammalian cells (Fig. 2c). Although the absolute level of frameshifting was lower than in vitro, the trend was similar and showed maximal frameshifting of ~8% around 12-15 bp. The pseudoknot in these assays was 1.6 times more efficient than the 12 and 15 bp hairpins, close to the *in vitro* ratio of 1.4 (see above). Thus, the hairpin derivative can effectively substitute for the SRV-1 gag-pro pseudoknot in -1 ribosomal frameshifting.

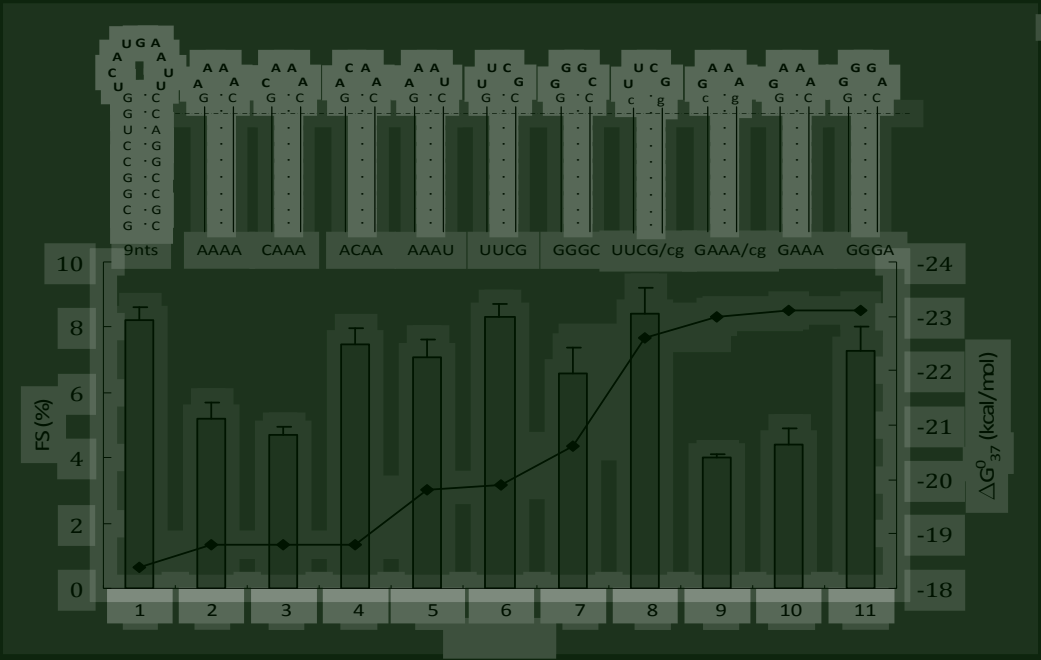


**Figure 4. Influence of loop sequence and closing base pair (cbp) on –1 ribosomal frameshifting efficiency. The composition of various loops capping a 9bp stem is shown in bold, and CG-cbps are shown in lower case. The constructs are named after their loop sequence followed by the "/cg" extension when the cbp was changed from G-C to C-G. Slippery sequence and spacer are the same as in the construct shown in Figure 1(a). Graph is similar to that of Figure 2(b) except that on the right y-axis $\Delta G$ starts from –18 kcal/mol.**

## Bulges and mismatches decrease frameshifting efficiency

Bulges and mismatches are known to change twisting and bending of a regular stem and are thus expected to influence the way in which a ribosome encounters a hairpin structure (11,30). To investigate a possible effect of helical twisting and bending on frameshifting, we introduced mismatches and bulges in the 12bp stem at a position corresponding to the junction in the SRV gag-pro pseudoknot (Fig. 3a). Introduction of an A •A mismatch half-way the stem (11bp/AA) decreased frameshifting about 10 fold, although its predicted thermodynamic stability of –25.1 kcal/mol is comparable to that of a regular hairpin of 10bp, yielding 13% frameshifting (Fig. 3b). The frameshift inducing ability was recovered when the base pair was restored to A-U (12bp/AU).

We also introduced a single or triple adenosine bulge at either side of the stem, to investigate potential bending effects on frameshifting. Figure 3a and b show that the single adenosine bulge mutant decreased frameshifting, depending on the location of the bulge, five to seven fold compared to the 12bp hairpin construct. When the bulge was enlarged to three adenosines the frameshifting was almost abolished. Interestingly, the effect of bulges at the 3' side of the stem was less dramatic than those at the 5'

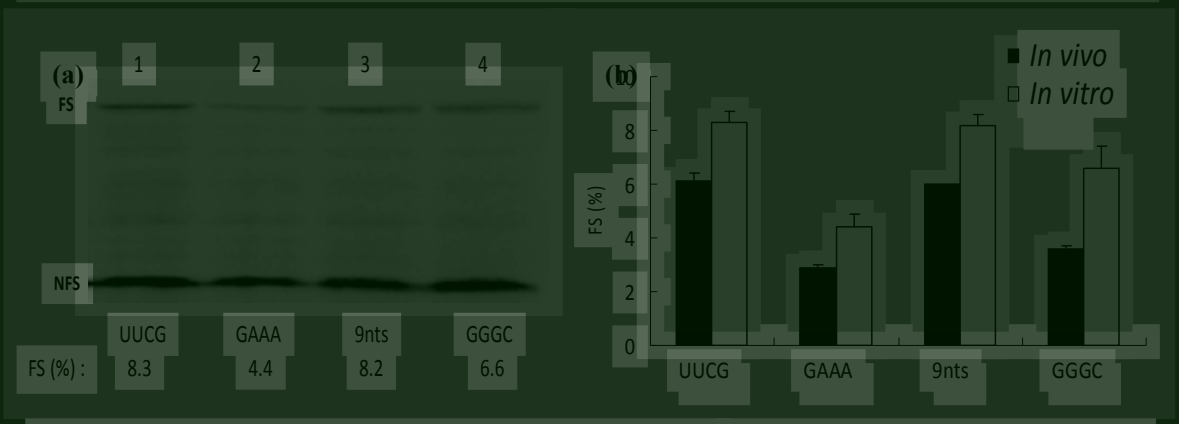


**Figure 5. Comparison of in vitro and in vivo frameshifting efficiencies induced by four selected 9bp hairpins with different loops. (a) SDS-PAGE analysis of 35S-methionine labeled translation products in RRL of mRNAs containing the 9bp hairpin with the indicated loop sequence. See legend to Figure 1(b) for more details. (b) Comparison of –1 ribosomal frameshifting in vitro and in vivo. The in vitro efficiency (white bar) was obtained by quantifying autoradiograms and averaging of at least three independent experiments. In vivo frameshifting efficiency (black bar) was obtained by measuring dual-luciferase activity of a frameshift reporter construct in Hela cells (see Materials and Methods). The in vivo experiments were done at least three times in triplicate.**

side.

**Loop composition affects frameshifting efficiency**

The loop composition plays a major role in hairpin stability, RNA/RNA, and RNA/protein interaction. These factors may directly influence hairpin-induced ribosomal frameshifting efficiency. To explore the correlation between loop composition and frameshifting efficiency, a number of loop mutations were introduced in the context of a 9bp stem (Fig. 4). We note that the UUCG tetraloop with a CG closing base pair (cbp) has higher stability (approximately 2 kcal/mol) than that with a GC cbp (31). Therefore, we first tested if this different cbp affected frameshifting efficiency. Our results showed that there is no difference in frameshifting efficiency between UUCG and UUCG/cg constructs (Fig. 4, bars 6 and 8). Replacing the UUCG tetraloop by GGGC which, due to its high content of purines, is among the most disfavored tetraloops (32) had only a marginal effect on frameshifting (Fig. 4, compare bars 6 and 7 and Fig. 5a, lanes 1 and 4). Interestingly, increasing the loop size to 9nt, which is predicted to lower the stability of stem did not affect frameshifting (Fig. 4, bar 1; Fig. 5a, lane 3).

Substituting UUCG by another stable tetraloop sequence (GAAA) resulted in a 2-fold decrease in frameshifting (Fig. 5a, lanes 1 and 2) either with GC (Fig. 4, bar 10) or CG cbp (Fig. 4, bar 9). We designed another five loop mutants to try to explain the

low efficiency of the GAAA tetraloop constructs. Constructs AAAA and CAAA induced 5.2% and 4.7% frameshifting, respectively (Fig. 4, bars 2 and 3), which is close to that of the GAAA constructs. The efficiency of two other A-rich loop mutants, ACAA and AAAU, was 7.5% and 7.1%, respectively (Fig. 4, bars 4 and 5), thereby closely matching that of the UUCG constructs. Finally, the GGGA tetraloop construct, belonging to the stable GNRA tetraloop family, induced 1.7-times more frameshifting than its GAAA sibling (Fig. 4, bar 11). These data suggest that the presence of 3 or 4 adenines at the 3' side of a tetraloop is unfavorable for frameshifting.

### Loop composition affects frameshifting efficiency *in vivo*

To further examine the role of the loop identity or size in ribosomal frameshifting, we cloned some of the above loop mutants into a dual-luciferase reporter plasmid and assayed their frameshifting efficiency in mammalian cells (Fig. 5b). Our data show that the effects of loop nucleotides are comparable *in vitro* and *in vivo*. The stable GAAA tetraloop construct again had the lowest frameshifting efficiency (Fig. 5b, 2.9%), which was half that of the UUCG construct (Fig. 5b, 6.1%).

## Discussion

Most RNA viruses that make use of ribosomal frameshifting employ pseudoknot structures instead of simple hairpins for this job. The reason for this may be the presence of a triple helix interaction between S1 and L2 in most frameshifter pseudoknots, which has been suggested to be a poor substrate for the ribosomal helicase (13,33) and hence increases ribosomal pausing and the time window for slippage. Although pausing is critical, it is not sufficient for efficient frameshifting (34). Previously, it was shown that a 17bp hairpin with a calculated stability of –31.2 kcal/mol derived from the minimal IBV pseudoknot induced 5 to 10-fold less frameshifting in RRL (22) even though both the hairpin and the pseudoknot can pause ribosomes at the same position and to a similar extent (34). In the present study, a 12bp hairpin derivative of the SRV-1 gag-pro pseudoknot with a calculated stability of –26.9 kcal/mol was capable of inducing 22% of frameshifting, which is only 1.4-fold less than its pseudoknotted counterpart. This indicated that a non-natural hairpin can be an efficient frameshift stimulator, at least in the SRV-1 model. Furthermore, our results showed that the frameshifting efficiency increased upon elongation of the length of the hairpin up to 12-15 bp, which is consistent with our previous data using antisense oligonucleotides of 12-15 nts to induce ribosomal frameshifting (35). More importantly, the frameshift inducing ability of these hairpin

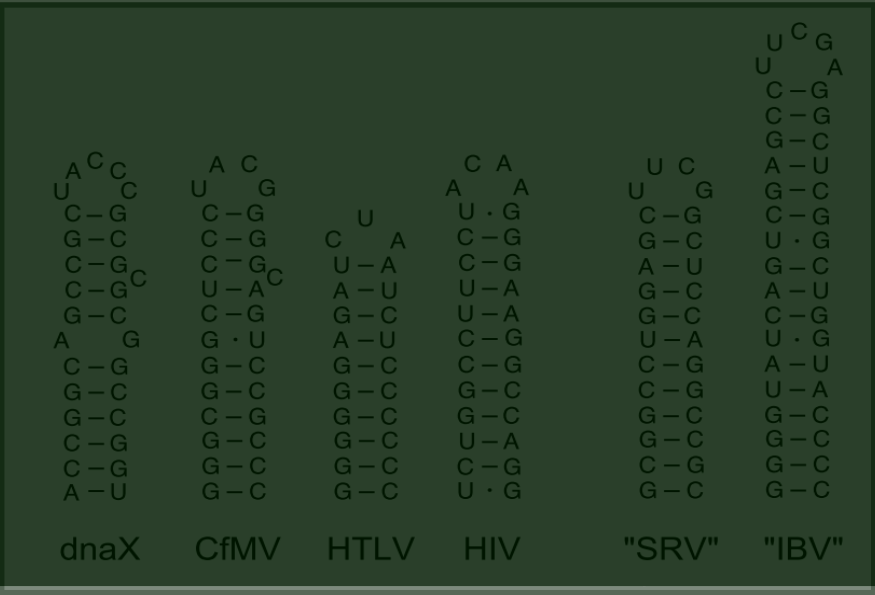


**Figure 6. Overview of naturally occurring hairpins involved in –1 ribosomal frameshifting and two synthetic pseudoknot-derived hairpins (SRV and IBV). Abbreviations: HIV, Human immunodeficiency virus type 1; HTLV, Human T-lymphotropic virus type 2; CfMV, Cocksfoot mottle virus; IBV, Infectious bronchitis virus; SRV, Simian retrovirus type 1.**

constructs with a perfect stem linearly correlated with the calculated thermodynamic stability, in agreement with two previous reports (19,20).

In the experiments of Bidou *et al.* (20) studying the HIV-1 gag-pol frameshift hairpin the stem-length was kept at 11bp while its stability was varied between –3.4 to –22.1 kcal/mol (recalculated using MFOLD 2.3) by changing the number of AU and GC base pairs in a small set of 6 hairpins. In the case of the *dnaX* gene of *E. coli* 22 variants of the wild type 11bp hairpin were tested for their ability to stimulate –1 PRF at the AAAAAAG slippery sequence. Hairpin stabilities varied between –10.4 and –27 kcal/mol and a positive correlation ($R^2$=0.72) between frameshifting efficiency and calculated stability was observed (19). The *dnaX* gene with the highly efficient (prokaryotic) AAAAAAG slippery sequence is not directly comparable to our *in vitro* system; a 6bp hairpin in the dnaX gene displayed 17% of frameshifting whereas a 6bp hairpin in our system induced only 3.5% of frameshifting.

In the HIV-1 gag-pol gene Bidou *et al.* (20) observed a 15-20% decrease in frameshifting *in vivo* with their most stable hairpin, similar to our results with the 21bp hairpin. However, in our case the stability at which this happened was –45 kcal/mol much higher than their most stable hairpin of –22.1 kcal/mol. It is possible that this difference is due to the different experimental systems. Although it has been suggested that too stable stems increase the time for tRNAs to shift back into the 0-frame again (20) we believe that our 21bp hairpin is less efficient because it has more AU bps in the middle of the stem compared to the 12 and 15 bp hairpins (Figure

2a). The experiments with hairpins harboring bulges or mismatches halfway the stem demonstrated that this region is quite important for frameshifting (Figure 3a and b). Even though the overall stability of these constructs was comparable to that of a hairpin of 9 or 10 bp, their frameshift activity was equal or lower than that of a 6bp hairpin of –13.1 kcal/mol: as if the mismatch or bulge after the 6$^{th}$ base pair disconnected the upper part of the stem. This observation is reminiscent of the overall destabilizing effect of mismatches in DNA hairpins. In a pioneer single-molecule pulling study it was shown that introducing a mismatch in a 20bp DNA hairpin shifted its transition state close to the location of the mismatch (36). Our data also comply with this mechanical study and suggest that mechanical stability may be a better parameter than thermodynamic stability to describe the frameshift efficiency of hairpins.

In addition to the mentioned dnaX and HIV-1 gag-pol hairpins, other examples of frameshifter hairpins are found in HTLV-2 and CfMV (Figure 6). HTLV-2 gag-pro features a perfect 10bp hairpin with CUA tri-loop which induces 9% frameshifting in RRL (16). The CfMV 2a-2b frameshifting hairpin consists of 12bp, one cytidine bulge close to the top, and a stable UACG tetraloop and is capable of inducing 11% of frameshifting in a wheat germ cell-free system (WGE) (17). What these hairpins have in common is their length of 10-12 bp, their relatively low number of mismatches and bulges, their small loops and their high GC content especially in the bottom 6 bp. These features are also applicable to the good frameshifters from our dataset. Interestingly, these features do not all apply to the minimal IBV hairpin (Figure 6) that is derived from the so-called minimal IBV pseudoknot. Despite its large size of 17bp, absence of mismatches and bulges, presence of a small loop, the stability of the middle part of the hairpin, i.e. bps 5 to 9, is not very high. This could be the reason why its activity in RRL is 5-10 fold lower (22) than of its parent pseudoknot, whose activity is 46% (15). Surprisingly, in our assays the frameshift-inducing efficiency of minimal IBV hairpin was 26% (data not shown), which is far more than the 4-8% reported by Brierley and co-workers (22). Since in the latter experiments in-house prepared RRL and capped transcripts were used and a 6-nt spacer, as opposed to a 7-nt spacer in our constructs, if these differences could account for the large discrepancy remains to be investigated.

Remarkably, in WGE the minimal IBV hairpin has been reported to induce high levels (34%) of frameshifting versus 51% for the minimal IBV pseudoknot (24). Whilst these two eukaryotic translation systems may not be fully equivalent such a large discrepancy in frameshift efficiency is remarkable. It should be noted that the 1.5-fold difference between the frameshift efficiencies of the minimal IBV pseudoknot and hairpin in WGE is actually very close to the 1.4 and 1.6 ratio we

obtained for SRV in vitro and in vivo, respectively. This ratio may reflect the additional interactions, like base triples, in a pseudoknot that make it a better frameshift stimulator than a hairpin. In this respect, the 26% we obtained for the minimal IBV hairpin versus 46% for the IBV pseudoknot (15) or a ratio of 1.6 may be relevant. Note that this does not imply the existence of base triples in the IBV pseudoknot, since there are no data to support this.

In addition to stem size, loop composition is another determinant of hairpin stability. An important subgroup of hairpin loops is the tetraloop, which is the most common loop size in 16S and 23S ribosomal RNAs (37). The tetraloops with consensus UNCG, GNRA, or CUUG loop sequence form stable loop conformations (38,39). As opposed to the mentioned stable tetraloops, purine-rich (32) and larger loops (40) are considered to be less favorable for hairpin formation. Our results showed that the GGGC loop is indeed less efficient in inducing frameshifting but the larger loop construct (9bp/9nt), although having a lower thermodynamic stability, showed comparable frameshifting efficiency to the stable UUCG tetraloop hairpin. This is consistent with previous studies that showed that increasing the size of the loop in a hairpin or pseudoknot can increase frameshift-inducing ability to a certain extent (21,41). Although larger loops seem efficient in inducing frameshifting, in known examples of frameshifter hairpins, there are no loop sizes of more than 5 nucleotides. This could relate to hairpin folding kinetics (40) or to nuclease sensitivity.

Intriguingly, we found that a 9bp stem capped with a GAAA tetraloop is 2-fold less efficient in inducing frameshifting than its UUCG counterpart *in vitro* and *in vivo*. It has been reported that GAAA tetraloops are frequently involved in RNA tertiary interactions (42). We hypothesize that the GAAA tetraloop may be involved in an unknown RNA tertiary structure with ribosomal RNA thereby interfering with frameshifting. The fact that in the known natural examples of frameshifter hairpins, the GAAA tetraloop, despite its high stability, is absent can be taken as support for this hypothesis (Olsthoorn, unpublished data). Further investigation of this observation may lead to new insights in ribosomal frameshifting.

In conclusion, our data show that hairpins of various base composition in stem and loop can act as efficient frameshift stimulators. Combined with our previous studies on antisense-induced frameshifting (43), these data support the notion that downstream structures primarily serve as barriers to stall translating ribosomes to stimulate frameshifting. Although there exists a linear relationship between calculated stability and frameshifting, local destabilizing elements like bulges or mismatches in a hairpin can greatly influence frameshift-inducing activity. Future experiments addressing the mechanical strength of these hairpins (7-9) may help to improve our understanding of the basics of ribosomal frameshifting.

## Acknowledgements

We thank Fabien Sohet and Maarten Laurs for their initial contributions to this subject.

## References

1. Farabaugh,P.J. (2000) Translational frameshifting: implications for the mechanism of translational frame maintenance. *Prog. Nucleic Acid Res. Mol. Biol.*, **64**, 131-170.
2. Giedroc,D.P. and Cornish,P.V. (2009) Frameshifting RNA pseudoknots: structure and mechanism. *Virus Res.*, **139**, 193-208.
3. Namy,O., Moran,S.J., Stuart,D.I., Gilbert,R.J. and Brierley,I. (2006) A mechanical explanation of RNA pseudoknot function in programmed ribosomal frameshifting. *Nature*, **441**, 244-247.
4. Nixon,P.L. and Giedroc,D.P. (2000) Energetics of a strongly pH dependent RNA tertiary structure in a frameshifting pseudoknot. *J. Mol. Biol.*, **296**, 659-671.
5. Giedroc,D.P., Theimer,C.A. and Nixon,P.L. (2000) Structure, stability and function of RNA pseudoknots involved in stimulating ribosomal frameshifting. *J. Mol. Biol.*, **298**, 167-185.
6. Nixon,P.L., Rangan,A., Kim,Y.G., Rich,A., Hoffman,D.W., Henning,M. and Giedroc,D.P. (2002) Solution structure of a luteoviral P1-P2 frameshifting mRNA pseudoknot. *J. Mol. Biol.*, **322**, 621-633.
7. Hansen,T.M., Reihani,S.N., Oddershede,L.B. and Sørensen,M.A. (2007) Correlation between mechanical strength of messenger RNA pseudoknots and ribosomal frameshifting. *Proc. Natl. Acad. Sci. U.S.A.*, **104**, 5830-5835.
8. Green,L., Kim,C.H., Bustamante,C. and Tinoco,I.Jr. (2008) Characterization of the mechanical unfolding of RNA pseudoknots. *J Mol Biol.*, **375**, 511-528.
9. Chen,G., Chang,K.Y., Chou,M.Y., Bustamante,C. and Tinoco,I.Jr. (2009) Triplex structures in an RNA pseudoknot enhance mechanical stability and increase efficiency of -1 ribosomal frameshifting. *Proc. Natl. Acad. Sci. U.S.A.*, **106**, 12706-12711.
10. Plant,E.P. and Dinman,J.D. (2005) Torsional restraint: a new twist on frameshifting pseudoknots. *Nucleic Acids Res.*, **33**, 1825-1833.
11. Kim,Y.G., Su,L., Maas,S., O'Neill,A. and Rich,A. (1999) Specific mutations in a viral RNA pseudoknot drastically change ribosomal frameshifting efficiency. *Proc. Natl. Acad. Sci. U.S.A.*, **96**, 14234-14239.

12. Cornish,P.V., Hennig,M. and Giedroc,D.P. (2005) A loop 2 cytidine-stem1 minor groove interaction as a positive determinant for pseudoknot-stimulated -1 ribosomal frameshifting. *Proc. Natl Acad. Sci. U.S.A.*, **102**, 12694-12699.

13. Michiels,P.J., Versleijen,A.A., Verlaan,P.W., Pleij,C.W., Hilbers,C.W. and Heus,H.A. (2001) Solution structure of the pseudoknot of SRV-1 RNA, involved in ribosomal frameshifting. *J. Mol. Biol.,* **310**, 1109-1123.

14. Olsthoorn,R.C., Reumerman,R., Hilbers,C.W., Pleij,C.W. and Heus,H.A. (2010) Functional analysis of the SRV-1 RNA frameshifting pseudoknot. *Nucleic Acids Res.*, **38**, 7665-7672.

15. Napthine, S., Liphardt, J., Bloys, A., Routledge, S, and Brierley, I. (1999) The role of RNA pseudoknot stem 1 length in the promotion of efficient -1 ribosomal frameshifting. *J. Mol. Biol.*, 288, 305-320.

16. Gaudin,C., Mazauric,M.H., Traïkia,M., Guittet,E., Yoshizawa,S. and Fourmy,D. (2005) Structure of the RNA signal essential for translational frameshifting in HIV-1. *J. Mol. Biol.*, **349**, 1024-1035.

17. Kim,Y.G., Maas,S. and Rich,A. (2001) Comparative mutational analysis of cis-acting RNA signals for translational frameshifting in HIV-1 and HTLV-2. *Nucleic Acids Res.*,**29**, 1125-1131.

18. Lucchesi,J., Mäkeläinen,K., Merits,A., Tamm,T. and Mäkinen,K. (2000) Regulation of -1 ribosomal frameshifting directed by cocksfoot mottle sobemovirus genome. *Eur. J. Biochem.*, **267**, 3523-3529.

19. Larsen,B., Gesteland,R.F. and Atkins,J.F. (1997) Structural probing and mutagenic analysis of the stem-loop required for Escherichia coli dnaX ribosomal frameshifting: programmed efficiency of 50%. *J. Mol. Biol.*, **271**, 47-60.

20. Bidou,L., Stahl,G., Grima,B., Liu,H., Cassan,M.,and Rousset,J.P. (1997) In vivo HIV-1 frameshifting efficiency is directly related to the stability of the stem-loop stimulatory signal. *RNA*, **3**, 1153-1158.

21. Brierley,I., Rolley,N.J., Jenner,A.J. and Inglis,S.C. (1991) Mutational analysis of the RNA pseudoknot component of a coronavirus ribosomal frameshifting signal. *J. Mol. Biol.* 220, 889-902.

22. Somogyi,P., Jenner,A.J., Brierley,I. and Inglis,S.C. (1993) Ribosomal pausing during translation of an RNA pseudoknot. *Mol. Cell Biol.,***13**, 6931-6940.

23. Marczinke, B, Hagervall, T, and Brierley, I. (2000) The Q-base of asparaginyl-tRNA is dispensable for efficient -1 ribosomal frameshifting in eukaryotes. *J. Mol. Biol.*. **295**, 179-191.

24. Napthine, S., Vidakovic, M., Girnary, R., Namy, O., and Brierley, I. (2004) Prokaryotic-style frameshifting in a plant translation system: conservation of an unusual single-tRNA slippage event. *EMBO J.,* 22, 3941-3950.

25. Brierley,I., Jenner,A.J. and Inglis,S.C. (1992) Mutational analysis of the "slippery-sequence" component of a coronavirus ribosomal frameshifting signal. *J. Mol. Biol.*. **227**, 463-479.

26. ten Dam,E.B., Brierley,I., Inglis S. and Pleij,C.W. (1994) Identification and analysis of the pseudoknot-containing gag-pro ribosomal frameshift signal of simian retrovirus-1. *Nucleic Acids Res.*, **22**, 2304-2310.

27 Grentzmann, G., Ingram , J.A., Kelly, P.J., Gesteland, R.F., and Atkins, J.F. (1998) A dual-luciferase reporter system for studying recoding signals. *RNA*, 4, 479-486.

28. ten Dam,E.B., Verlaan,P.W. and Pleij,C.W. (1995) Analysis of the role of the pseudoknot component in the SRV-1 gag-pro ribosomal frameshift signal: loop lengths and stability of the stem regions. *RNA*, **1**, 146-154.

29. de Smit,M.H. van Duin,J. (2003) Translational standby sites: how ribosomes may deal with the rapid folding kinetics of mRNA. *J. Mol. Biol.,* **331**, 737-743.

30. Chen,X., Kang,H., Shen,L.X., Chamorro,M., Varmus, H.E. and Tinoco,I.Jr. (1996) A characteristic bent conformation of RNA pseudoknots promotes -1 frameshifting during translation of retroviral RNA. *J. Mol. Biol.*, **260**, 479-483.

31. Blose,J.M., Proctor,D.J., Veeraraghavan,N., Misra,V.K. and Bevilacqua,P.C. (2009) Contribution of the closing base pair to exceptional stability in RNA tetraloops: roles for molecular mimicry and electrostatic factors. *J. Am. Chem. Soc.*,**131**, 8474-8484.

32. Nagel,J.H., Flamm,C., Hofacker,I.L., Franke,K., de Smit,M.H., Schuster,P. and Pleij,C.W. (2006) Structural parameters affecting the kinetics of RNA hairpin formation. *Nucleic Acids Res.* **34**, 3568-3576.

33. Marcheschi,R.J., Staple,D.W. and Butcher,S.E. (2007) Programmed ribosomal frameshifting in SIV is induced by a highly structured RNA stem-loop. *J. Mol. Biol.*, **373**, 652-663.

34. Kontos,H., Napthine,S. and Brierley,I. (2001) Ribosomal pausing at a frameshifter RNA pseudoknot is sensitive to reading phase but shows little correlation with frameshift efficiency. *Mol. Cell Biol.*, **21**, 8657-8670.

35. Yu,C.H., Noteborn,M.H. and Olsthoorn,R.C. (2010) Stimulation of ribosomal frameshifting by antisense LNA. *Nucleic Acids Res.*, **38**, 8277-8283.

36. Woodside,M.T., Anthony,P.C., Behnke-Parks,W.M., Larizadeh,K., Herschlag,D. and Block,S.M. (2006) Direct measurement of the full, sequence-dependent folding landscape of a nucleic acid. *Science*, **314**, 1001-1004.

37. Gutell,R.R., Weiser,B., Woese,C.R. and Noller,H.F. (1985) Comparative anatomy of 16-S-like ribosomal RNA. *Prog. Nucleic Acids Res. Mol. Biol.,* **32**, 155-216.

38. Cheong,C., Varani,G. and Tinoco,I.Jr. (1990) Solution structure of an unusually stable RNA hairpin, 5'GGAC(UUCG)GUCC. *Nature*, **346**, 680-682.

39. Heus,H.A. and Pardi,A. (1991) Structural features that give rise to the unusual stability of RNA hairpins containing GNRA loops. *Science*, **253**, 191-194.

40. Kuznetsov,S.V., Ren,C.C., Woodson,S.A. and Ansari,A. (2008) Loop dependence of the stability and dynamics of nucleic acid hairpins. *Nucleic Acids Res.*, **36**, 1098-1112.

41. Tamm,T., Suurväli,J., Lucchesi,J., Olspert,A. and Truve,E. (2009) Stem-loop structure of Cocksfoot mottle virus RNA is indispensable for programmed -1 ribosomal frameshifting. *Virus Res.*, **146**, 73-80.

42. Cate,J.H., Gooding,A.R., Podell,E., Zhou,K., Golden,B.L., Szewczak,A.A., Kundrot,C.E., Cech,T.R. and Doudna,J.A. (1996) RNA tertiary structure mediation by adenosine platforms. *Science,* **273**, 1696-1699.

43. Olsthoorn,R.C., Laurs,M., Sohet,F., Hilbers,C.W., Heus,H.A. and Pleij, C.W. (2004) Novel application of sRNA: stimulation of ribosomal frameshifting. *RNA*, **10**, 1702-1703.

# Chapter IV

## Stimulation of ribosomal frameshifting by antisense LNA

Chien-Hung Yu, Mathieu H.M. Noteborn, and René C.L. Olsthoorn.

Department of Molecular Genetics, Leiden Institute of Chemistry, Leiden University, PO Box 9502, 2300RA Leiden, The Netherlands.

Nucleic Acids Res., 2010, **38**:8277-83.

### Abstract

Programmed ribosomal frameshifting is a translational recoding mechanism commonly used by RNA viruses to express two or more proteins from a single mRNA at a fixed ratio. An essential element in this process is the presence of an RNA secondary structure, such as a pseudoknot or a hairpin, located downstream of the slippery sequence. Here, we have tested the efficiency of RNA oligonucleotides annealing downstream of the slippery sequence to induce frameshifting *in vitro*. Maximal frameshifting was observed with oligonucleotides of 12-18 nucleotides. Antisense oligonucleotides bearing locked nucleid acid (LNA) modifications also proved to be efficient frameshift-stimulators in contrast to DNA oligonucleotides. The number, sequence, and location of LNA bases in an otherwise DNA oligonucleotide have to be carefully manipulated to obtain optimal levels of frameshifting. Our data favor a model in which RNA stability at the entrance of the ribosomal tunnel is the major determinant of stimulating slippage rather than a specific three-dimensional structure of the stimulating RNA element.

## Introduction

Programmed ribosomal frameshifting is a translational recoding event that increases the versatility of gene expression. It is mainly utilized by eukaryotic RNA viruses (1-3), though some prokaryotic (4) and mammalian genes (5-7) are also controlled by ribosomal frameshifting. The requirements for -1 ribosomal frameshifting are the presence of a slippery heptanucleotide sequence X XXY YYZ [where X can be A, U, G, or C; Y can be A or U; and Z does not equal Y; the spaces indicate the original reading frame] (8) followed by a downstream structural element, such as a pseudoknot, a hairpin, or an antisense oligonucleotide duplex (for reviews, see 9). Although the mechanism of frameshifting is still elusive, a promising model has been proposed by Brierley and co-workers using cryo-electron microscopy to image mammalian 80S ribosomes (10). In their model, the ribosome is paused by its inability to unwind a pseudoknot structure resulting in a blockage of the A-site by eEF-2. During translocation, the P-site tRNA is bent in the 3' direction by opposing forces. To release the tension, the P-site tRNA may un-pair and subsequently re-pair in the -1 frame with a certain frequency, followed by A-site tRNA delivery into the new -1 reading frame. These and other recent data obtained by mechanical unfolding of frameshifter pseudoknots suggest that mRNA secondary structures with certain conformational features that resist ribosomal helicase-mediated unwinding and eEF-2 catalyzed translocation are key players in ribosomal frameshifting.

Small oligonucleotides have been used for several years to regulate gene expression by RNaseH-dependent RNA degradation (11), blocking translation (12), or re-directing splicing (13). More recently, microRNAs (miRNAs) (14) and small interfering RNAs (siRNAs) have appeared on the scene of post-transcriptional gene regulation (15). siRNAs may be effective in treatment of chronic hepatitis-B virus infection (16), HIV infection (17), cancer (18), and age-related macular degeneration (19). Very few antisense oligonucleotides, for example against the *bcl-2* oncogene have reached the stage of clinical trials (20) or have actually been approved by the FDA, for instance for the treatment of human cytomegalovirus (CMV) retinitis (21).

Enhancing the stability of small oligonucleotides to prolong circulation and meanwhile increasing target specificity are major concerns for therapeutic applications. Various kinds of modifications in backbones, sugars, or even analogs have already been studied extensively (for reviews, see 22,23) to meet these requirements. LNA (locked nucleic acid) is a rather novel nucleic acid analog comprising a class of bicyclic high-affinity RNA analogues in which the furanose ring of LNA monomers is conformationally locked in an RNA-mimicking C3′-*endo*/*N*-type conformation (24). The LNA modification also resists degradation

by cellular nucleases. Furthermore, introducing LNA into DNA or RNA oligonucleotides improves the affinity for complementary sequences and increases the melting temperature by several degrees (25). A recent study showed that LNA/DNA mix-mers against miRNA-122 can be acutely administered at high dosage with long lasting effects without any evidence of LNA-associated toxicities or histopathological changes in the studied animals (26). These data suggests that LNA is a promising candidate for small oligonucleotide applications.

We and others have demonstrated that small RNA oligonucleotides are able to mimic the function of frameshifter pseudoknots or hairpins by redirecting ribosomes into new reading frames (27, 28). In this paper, we have investigated the length and concentration of RNA oligonucleotides for optimal frameshifting, as well as the effects of introducing LNA-type sugars in DNA oligonucleotides.

## Materials and Methods

### Frameshift reporter construct and oligonucleotides

The -1 ribosomal frameshifting events were monitored by the SF reporter construct described previously (27). Complementary oligonucleotides (Eurogentec, Liege, Belgium) SF462 (CTAGTTGACCTCAACCCTTGGAA) and SF463 (CATGTTCCAAGGGTTGAGGTCAA) and SF468 (CTAGTTGAGCGCGCTGGAGGCCATGG) and SF469 (CATGCCATGGCCTCCAGCGCGCTCA) were annealed and ligated into SpeI/NcoI digested SF reporter to construct the SF462 and SF468 templates, respectively. All constructs were verified by DNA sequencing on a ABI PRISM® 3730xl analyzer (LGTC, Leiden, The Netherlands). RNA oligonucleotides (except for RNA13 which was obtained from Invitrogen) were purchased from Dharmacon (Lafayette, USA). The RNAs from Dharmacon carried a 2'-O-ACE protection group, which was removed by incubation with 100mM acetic acid pH 3.8 and TEMED at 60 ºC for 30 min. The sequences of RNA oligos were as follows: RNA6: GCGCGC, RNA9: CCAGCGCGC, RNA12: CCUCCAGCGCGC, RNA15: UGGCCUCCAGCGCGC, RNA18: CCAUGGCCUCCAGCGCGC, 18RNA: GCGCGCUGGAGGCCAUGG, and RNA13: CCAAGGGGUUGAGG.

DNA and LNA/DNA mix-mers were synthesized by Eurogentec. Custom oligonucleotides were extracted by phenol/chloroform followed by ethanol precipitated before use. The sequences of DNA and LNA/DNA mix-mers were as follows (lower case represents the LNA modification and capital represents DNA): DNA18: CCATGGCCTCCAGCGCGC. DNA13: CCAAGGGTTGAGG, LNA2:

CCATGGCCTCCAGCGCgc, LNA4: CCATGGCCTCCAGCgcgc, LNA6: CCATGGCCTCCAgcgcgc, LNA2-1: CCATGGCCTCCAGCgcGC, LNA2-2: CCATGGCCTCCAgcGCGC, LNA2-3: ccATGGCCTCCAGCGCGC, LNA2-4: CCATGGCCTCCAGCgCGc, LD1: CCAAGGGTTGAGg, LD2: CCAAGGGTTGAgg, LD4: CCAAGGGTTgagg, LD6: CCAAGGGttgagg.

**_In vitro_ transcription**

Plasmids were linearized by BamHI and purified by phenol/chloroform extraction followed by ethanol precipitation. *In vitro* transcription was conducted by SP6 RNA polymerase and carried out in the 30 μL reaction mixture of: 1 μg of linearized template, 5 mM of rNTPs, 20 units of RNase inhibitor, and 15 units of SP6 RNA polymerase with buffer (all from Promega, Benelux). After 2 hours incubation at 37ºC, the integrity and quantity of transcripts were checked by agarose gel and appropriate amount of the RNA were diluted in nuclease free water for *in vitro* translation.

**_In vitro_ translation**

*In vitro* translations were carried out in nuclease treated rabbit reticulocyte lysate (RRL) (Promega). The amount of mRNA was 0.025 pmole and different amounts of oligonucleotides (0.025-15.625 pmole) were mixed with template for 20 minutes at room temperature. After incubation, 4 μl of RRL, 0.01 mM amino acids mixture except methionine, 2 μCi of $^{35}$S methionine (10 mCi/ml, MP Biomedicals, *in vitro* translational grade) were added in total volume of 10 μL and incubated at 28℃ for 1 hour. After translation, samples were mixed with 2X Laemmli buffer, boiled at 90℃ for 5 minutes and resolved by 13% SDS polyacrylamide gels. Gels were fixed in 10% acetic acid and 30% methanol for 20 minutes, dried under vacuum, and exposed to phosphoimager screens (Biorad). The screen was scanned and quantified the 0 frame and -1 frameshift protein products by Quantity One software (Biorad). Frameshift percentages were calculated by the amount of -1 frameshift product divided by the amount of 0-frame product after correction for the number of methionines in the protein sequence, and multiplied by 100.

**Determination of the melting temperature of oligonucleotide duplexes**

RNA oligonucleotide 18RNA (5'GCGCGCUGGAGGCCAUGG3', Dharmacon, Lafayette, USA) was mixed in a 1:1 molar ratio with RNA18, DNA18 or one of the various DNA/LNA mix-mers. in UV-melting buffer (100 mM NaCl, 10 mM Cacodylate acid, pH 6.8). The analysis was performed on a Varian Cary 300 spectrophotometer using temperature ramps of 0.25℃/min during heating and cooling. The absorbance at 260 nm was recorded and normalized to the blank control.

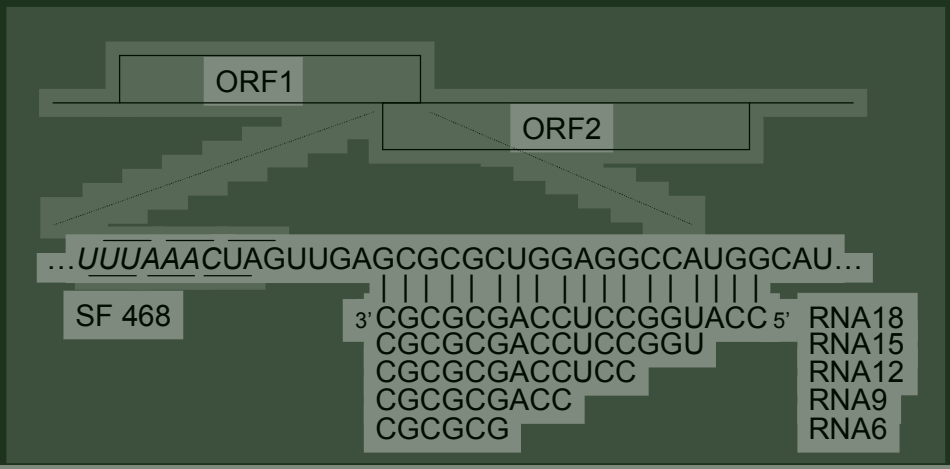


**Figure 1. Schematic representation of frameshift reporter constructs. ORF1 (19 kD) is in the 0 frame and ORF2 (46 kD) is in the -1 translational frame with respect to ORF1. The appearance of the 65 kD fusion protein represents the occurrence of -1 frameshifting. The UUUAAAC slippery sequence is indicated in italics. The 0-reading frame and -1 reading frames codons are indicated above and below the sequences, respectively. RNA18, 12, 15, 9, and 6 are antisense RNA oligonucleotides complementary to the indicated region downstream of the slippery sequence in SF468 mRNA.**

## Results

### Length-dependent RNA oligonucleotide-induced ribosomal frameshifting

Although antisense oligonucleotides were found to induce ribosomal frameshifting (27,28), the optimal number of base pairs has not been addressed yet. To investigate this we designed antisense RNA oligonucleotides that are 6, 9, 12, 15, and 18 bases complementary to the region downstream of an UUUAAAC slippery sequence in our reporter plasmid | SF468 | (Fig. 1). | First, titration | with | RNA6 and RNA9 oligonucleotides revealed that a 625-fold molar excess of oligonucleotides over mRNA resulted in the highest level of frameshifting (Fig. 2a); this ratio was used in the following experiments. The shortest oligonucleotide, RNA6, was not capable of inducing significant levels of frameshifting (Fig. 2b), whereas RNA9 induced about 3.5 % of frameshifting. Maximum levels were obtained with RNA12, RNA15, and RNA18; all three induced about 12% of frameshifting. In the following experiments oligonucleotides between 12 and 18 nts in length were used.

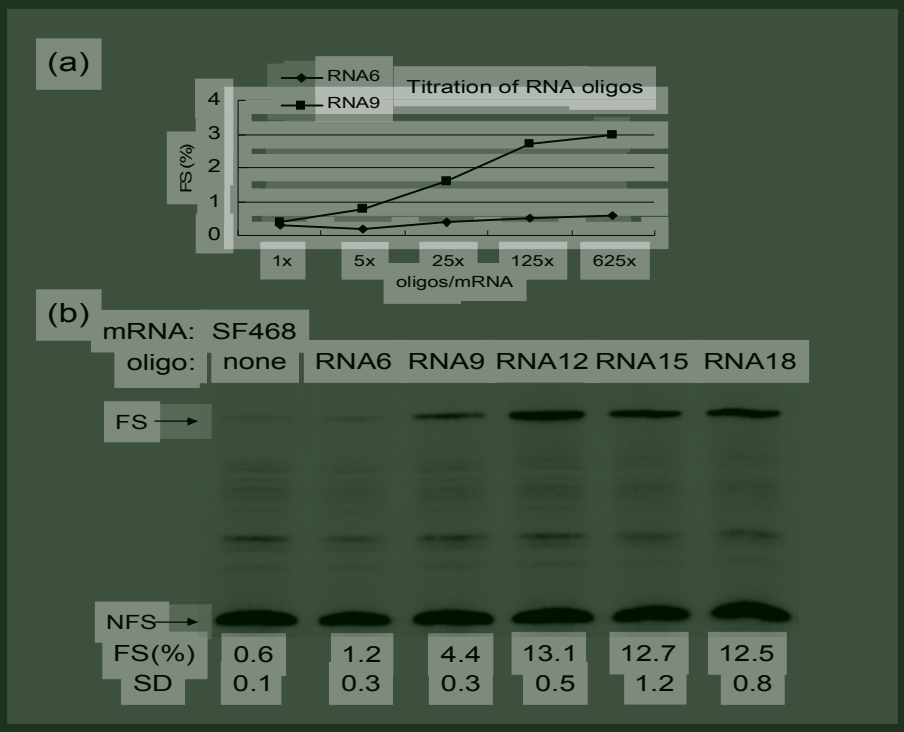


**Figure 2. Optimizing the ratio and lengths of frameshift-inducing RNA oligonucleotides. (a) 0.05 pmol of SF468 mRNA were mixed with 0.05, 0.25, 1.25, 6.25, 31.25 pmol of RNA6 and RNA9 oligonucleotides, respectively. Mixtures were subsequently translated in the presence of 35S-methionine and the labeled proteins were examined by 13% SDS-PAGE. Frameshift efficiencies [FS (%)] were calculated after quantification and correction of in-frame and frameshifted product. (b) 625 molar excess of different lengths of RNA oligos (RNA6, 9, 12, 15, 18, respectively) and control without added oligonucleotide were mixed with 0.05 pmol of SF468 mRNA. Mixtures were translated and examined by 13% SDS-PAGE. In-frame and frameshifted protein products are indicated by NFS and FS, respectively. Frameshifting efficiency [FS (%)] and standard deviation (SD) of three independent duplicate assays are indicated below each lane.**

## LNA/DNA mix-mers induced-ribosomal frameshifting

Since we have absent knowledge about the efficacy of LNA-induced ribosomal frameshifting, LNA/DNA mix-mers of 18 nts in length were designed to investigate this (Fig. 3).[1] A DNA oligonucleotide, as expected, was less capable (3.5%) of inducing frameshift due to the lower thermodynamic stability of RNA-DNA duplexes, see also below. Surprisingly, substituting the 3' cytosine and guanosine in this DNA oligonucleotide by their LNA analogs enhanced its frameshift inducing capacity to 8.7%, i.e. as high as an RNA oligonucleotide (8.8%). Increasing the LNA content of this oligonucleotide further did not lead to higher frameshifting. On the contrary, the efficiency of LNA4 was with 7.7% lower than that of LNA2 and that of LNA6 was a mere 1.1%. Since the overall translation efficiency seemed not affected by LNA6 we suspected an effect of the oligonucleotide itself (see below).

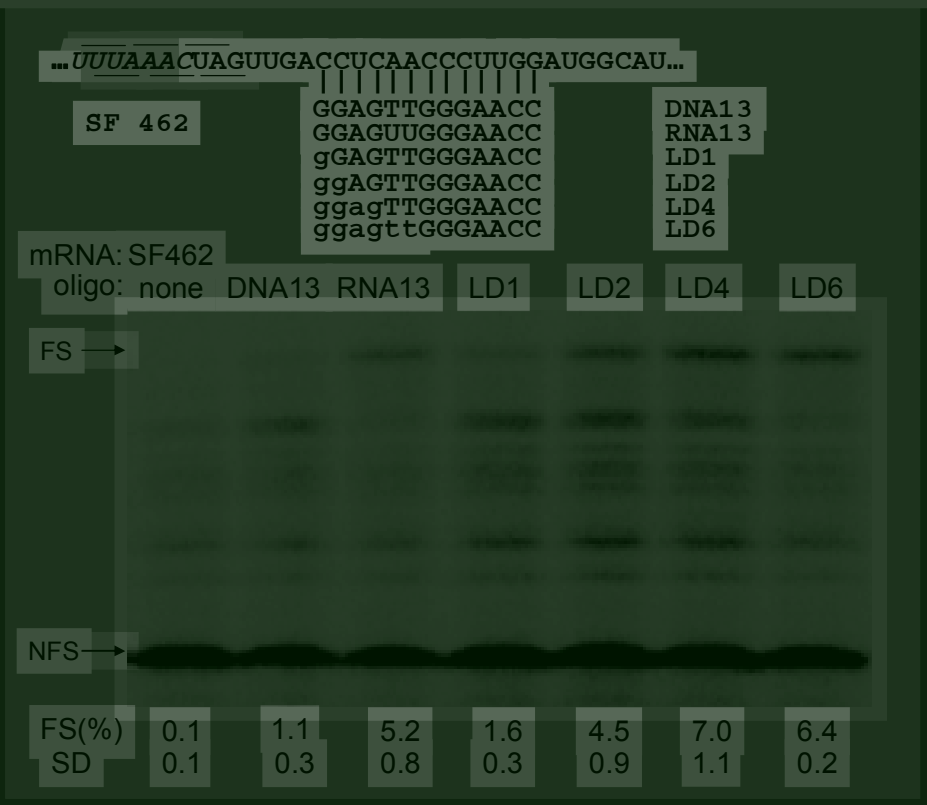


**Figure 3. Effect of LNA substitutions on oligonucleotide-induced frameshifting. SF468 mRNA was translated in the presence of a 625-fold molar excess of DNA, RNA or LNA substituted DNA oligonucleotides in rabbit reticulocyte lysate. DNA and RNA oligonucelotides are indicated in capital and LNA substitutions are denoted by lowercase. See legend to Figure 2 for more details.**

## The effectiveness of LNA/DNA mix-mers is universal

To demonstrate that the enhanced effect of LNA oligonucleotides is a general feature we designed another construct (SF462) in which the target sequence was replaced by an unrelated sequence (Fig. 4). LNA/DNA mix-mers were designed in which nucleotides starting from the 3' end were gradually replaced by LNA (Fig. 4). Increasing the number of LNAs from 1 to 2 and 4 in these DNA oligonucleotides improved their frameshift inducing ability, reaching an apparent optimum of 7.0 % with 4 LNA substitutions. Further increase of the LNA content to 6 nts (LD6) did not improve frameshift efficiency, but, on the other hand, LD6 also did not lead to the dramatic decrease as observed above for the LNA6 oligonucleotide applied in the SF468 construct. We suspected that (partial) self-complementarity may be limiting the effective concentration of free LNA/DNA oligonucleotides. To check this possibility, we ran all the oligonucleotides on a non-denaturing polyacrylamide gel. Figure 5 showed that the LNA6 oligonucleotide indeed migrated more slowly indicative of partial dimer formation, presumably by intermolecular base pairing of the palindromic GCGCGC sequences in each oligonucleotide (compare the migration to that of the full dimer formed by annealing of oligonucleotides DNA18 and 18DNA). The LD

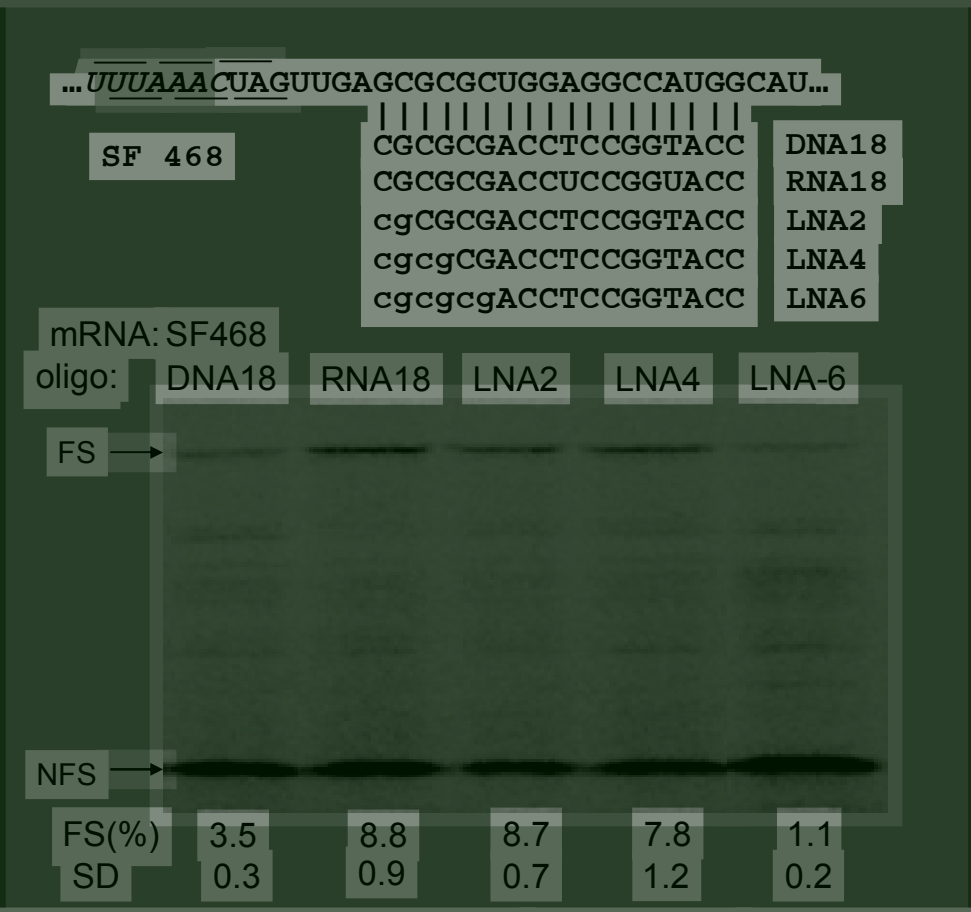


**Figure 4. Frameshift enhancing activity of LNA-substituted deoxy-oligonucleotides. mRNA SF462 was translated in the absence or presence of 625-fold molar excess of DNA, RNA or LNA substituted DNA oligonucleotides, which were denoted in lowercase, in rabbit reticulocyte lysate. See legend to Figure 2 for more details.**

series, as predicted, migrated as monomers. We noted that LD2, though loaded in equal amount, based on its UV absorbance, showed a higher affinity to ethidium bromide than its counterparts. At present we have no explanation for this unexpected behaviour of LD2, since its migration and therefore its conformation was identical to the other LNA/DNA mix-mers.

These results demonstrate that LNA modifications indeed enhance the antisense-induced frameshifting efficiency probably due to higher thermodynamic stability and RNA-like structural properties. This phenomenon appears to be general, at least in our experiments.

**Position effect of LNA substitutions**

To investigate which positions in a DNA oligonucleotide would exert the largest effect when substituted by an LNA analog, we designed LNA/DNA mix-mer mutants based on LNA2, which is the most efficient LNA/DNA mix-mer in our experiments and would give a good read-out. When the two LNA substitutions were moved 2 positions

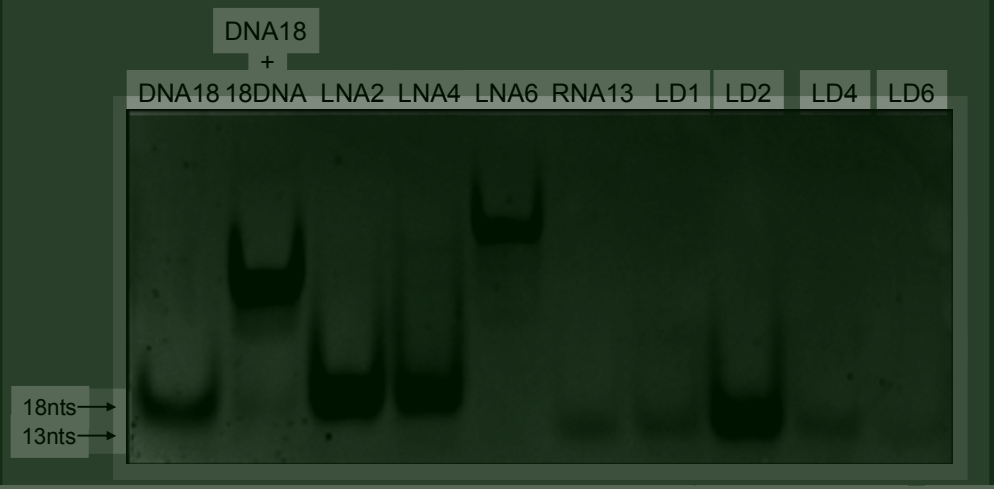


**Figure 5. Self-dimerization of frameshift-inducing oligonucleotides. 31.25 pmol of the indicated oligonucleotides were left at room temperature for 10 min. and then loaded on a 15% non-denaturing polyacrylamide gel. After electrophoresis, the gel was stained by EtBr and photographed under UV-light.**

more inward (L2-1) compared to LNA2, the frameshift efficiency decreased to 6.7% (Fig. 6). However, when the LNA modifications were moved another 2 positions more inward (L2-2), activity dropped to 2.7% (Fig. 6) which is comparable to an unmodified DNA oligonucleotide. Similarly, when the LNA groups were introduced at the other end of the oligonucleotide, activity was as low as DNA18 (Fig. 6). Finally, L2-4, in which the 1st and 4th position were LNA, was only half as efficient as LNA2. These results indicate that the choice of the location of the LNA modifications is crucial for the frameshift-inducing efficiency of an oligonucleotide.

**Thermodynamic stability of frameshift-inducing oligonucleotides**

Theoretically the position effect of the LNA substitutions could simply be explained by differences in thermodynamic stability of the resulting mRNA/oligonucleotide duplexes. To investigate this possibility we carried out UV-melting studies of the 18-nt LNA oligonucleotides in a 1:1 complex with an 18-nt RNA (18RNA) representing the mRNA. The melting temperatures ($T_m$) are shown in Table 1. The $T_m$ of the 18RNA/RNA18 duplex was the highest with 82˚C in agreement with its high frameshifting efficiency. The 18RNA/DNA18 duplex had a much lower $T_m$ of 72˚C, which is expected for an RNA/DNA hybrid, and also agreed with the lower frameshifting efficiency. The LNA substituted oligonucleotides, all had higher $T_m$s (+4 to +9 ˚C) than DNA18. The $T_m$ of L2-2 was with 81˚C almost as high as that of RNA18. Remarkably there was no correlation between the $T_m$ of the LNA oligonucleotides and their frameshifting inducing capacity. For example, the Tm of LNA2 was rather low with 76˚C but it had the highest frameshifting activity, and L2-2,

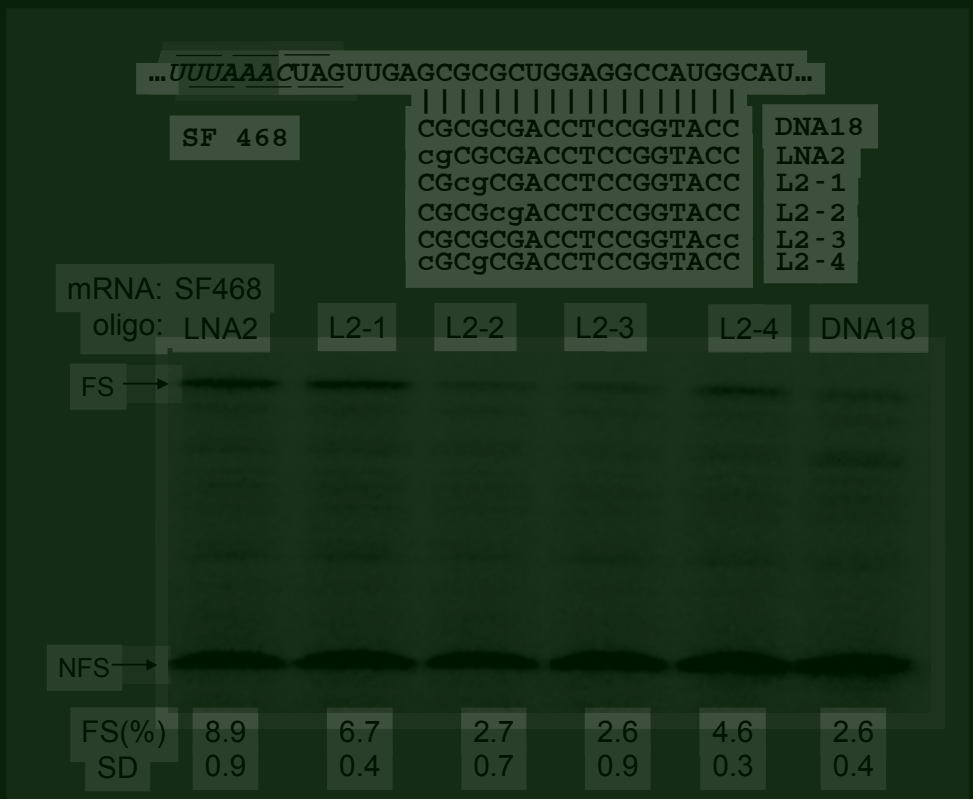


**Figure 6. Position effect of LNA substitutions on their frameshift-inducing activity. LNA substitutions are denoted by lowercase. See legend to Figure 2 for more details.**

which had the highest $T_m$, actually had the lowest frameshifting activity. $T_m$s of L2-3 and L2-4 were identical but their frameshifting activity were 2.3 and 4.6%, respectively. We also noted that both L2-2 and L2-3 were comparable to DNA18 in frameshifting activity but formed far more stable duplexes. These data suggest that the position effect of the LNA substitutions is related to the mechanism of frameshifting and not per se to their thermodynamic stability.

| Frameshift-inducing oligo | *Tm* (℃) |
|---|---|
| DNA18 | 72 |
| RNA18 | 82 |
| LNA2 | 76 |
| LNA2-1 | 80 |
| LNA2-2 | 81 |
| LNA2-2 | 78 |
| LNA2-4 | 78 |

**Table 1. $T_m$ measurements of frameshift-inducing oligos hybridized to complementary RNA.**

# Discussion

Previously, we have demonstrated that antisense oligonucleotides can induce high levels of -1 frameshifting (27). The optimal length of small antisense oligonucleotides, however, was not investigated. Understanding the optimal length of trans-acting oligonucleotides that can induce the most efficient frameshifting and, at the same time, escape RNAi interference will be an important issue for future *in vivo* applications. Here we found that maximum levels of frameshifting were obtained with oligonucleotides of 12 nt and more. This is comparable to the stem lengths (S1+S2) of known examples of highly frameshift inducing H-type pseudoknots, such as the 6+6 base pairs of the Simian retrovirus type-1 pseudoknot (29), the 11+6 base pairs of the minimal Infectious Bronchitis virus (IBV) pseudoknot (30), and the 6+6 base pairs chimeric Mouse Mammary Tumor virus (MMTV)-IBV pseudoknot (31). In addition, in known examples of hairpin-induced frameshift, the stem length of hairpins is around 12 base pairs (32-34). This may imply that a full helical turn of an RNA helix either in one single stem or in two stacking stems of a pseudoknot (S1+S2) is selected by viruses to induce efficient ribosomal frameshifting.

In addition to RNA oligonucleotides, we demonstrated that LNA/DNA mix-mers are also capable of stimulating efficient -1 ribosomal frameshifting in contrast to DNA oligonucleotides. Replacing two nts in a DNA oligonucleotide by LNA was already sufficient to reach the same level of frameshifting as with a comparable RNA oligonucleotide. However, the excellent affinity of LNA oligonucleotides could be a double-edged sword in certain cases. In our experimental system, the oligonucleotides are partly self-complementary and this resulted in the formation of dimers (Fig. 5), which were apparently unable to induce frameshifting (LNA6, Fig. 3). Hence, LNA substitutions should be optimized in a sequence that is prone to form dimers. In our SF462 construct (Fig. 4), the optimal number of LNA substitutions to induce the most significant amount of frameshifting is four. LD6 with two additional LNA substitutions did not improve the efficiency. Thus, our results suggest that the first four base pairs are critical for antisense-induced frameshifting. A likely explanation is that when a ribosome that is translating the slippery sequence, the helicase active site is around position +11, with respect to the first nucleotide of the P-site, which is close to the first base pair of the mRNA/oligonucleotide duplex (35). Increasing the local thermodynamic stability in this region may prevent ribosomes to unwind RNA structures, causing ribosomal pausing at the slippery sequence, and finally results in a higher frequency of ribosomal frameshifting.

Our data also showed that a single LNA modification is not sufficient to turn a DNA oligonucleotide into an efficient frameshift inducer but that a second LNA is

needed. The best position for the second modification appeared to be also close to the 3' end of the oligonucleotide. Although one could expect that spacing of two LNA groups by two non-modified sugars as applied in probes for miRNAs, results in the optimal induction of the 3' endo conformation in the neigboring sugars (36), this was not the case in our frameshift assays. Here such a spacing was less efficient (see data for L2-4, Fig. 6). However, we have not investigated if possible differences of self-dimerization behaviour of these oligonucleotides accounts for the different stimulating activities, since such effects were only observed when six LNA modifications were introduced in an oligonucleotide of this sequence.

The observation that different positions of LNA substitutions induced different levels of ribosomal frameshifting is interesting. Even though the overall thermodynamic stability of these oligonucleotides is roughly the same, they still create different degrees of barriers for ribosomes to unwind and these differences could be the reason for different level of induced frameshifting.

The finding that local stability at the 3' end of the LNA/DNA mix-mers is important for frameshifting is in agreement with the observation that in natural examples of frameshift stimulators, most of them have high GC content in the first few nucleotides (1). Hence, our data support the notion that the stability of the 3' end of the oligonucleotide, which may reside in the active site of the ribosomal helicase, is critical for frameshift-inducing structural elements. In pseudoknots this stability is probably attained by triple interactions, since nature has no other way to increase the stability of a GC-rich A-type helix. Triplex structures have been documented for a number of frameshifter pseudoknots, e.g. BWYV (37), SRV-1 (38), and in a telomerase pseudoknot (39).

Several models of ribosomal frameshifting have been proposed (1,40,41). The consistency from these studies is that ribosomal pausing at shifty sites by downstream structural elements is important but that pausing caused by RNA secondary structure, does not always result in frameshifting. In addition, a lack of correlation between the extent of pausing and the efficiency of frameshifting by IBV pseudoknots has been observed (42). A recent study also showed that pseudoknots with a similar global structure can still induce very different levels of frameshifting although their thermodynamic stabilities were different (43). These data complicate the view on the role of the downstream structure. Experiments involving simple oligonucleotides such as shown here may be better alternatives to elucidate the role of the downstream element.

Several groups have correlated the mechanical force of unfolding of a pseudoknot with its frameshifting efficiency by using optical tweezers (39,44-46) and suggest that frameshift efficiency is dependent on the unfolding force rather than on differences of

thermodynamic stability between folded and unfolded states. Since we showed here that antisense oligonucleotides can induce frameshifting presumably by serving as a physical barrier for the elongating ribosome, it will be interesting to measure the strength of these linear oligonucleotides in complex with (a piece of) mRNA by optical tweezers and see if there is a correlation with their frameshifting efficiency.

Finally, several properties of LNA, including its good aqueous solubility, low toxicity, highly efficient binding to complementary nucleic acids, high biostability, and, improved mismatch discrimination relative to natural nucleic acid (47) make LNA a promising candidate for *in vivo* applications of antisense-induced frameshifting.

## References


1. Giedroc, D.P., Theimer, C.A., and Nixon, P.L. (2000) Structure, stability and function of RNA pseudoknots involved in stimulating ribosomal frameshifting. *J. Mol. Biol.*, **298**, 167-185.
2. Brierley I. and Dos Ramos, F.J. (2006) Programmed ribosomal frameshifting in HIV-1 and the SARS-CoV. *Virus Res.*, **119**, 29-42.
3. Dinman, J.D., Icho, T. and Wickner, R.B. (1991) A -1 ribosomal frameshift in a double-stranded RNA virus of yeast forms a gag-pol fusion protein. *Proc. Natl. Acad. Sci. U.S.A.*, **88**, 174-178.
4. Baranov, P.V., Fayet, O., Hendrix, R.W. and Atkins, J.F. (2006) Recoding in bacteriophages and bacterial IS elements. *Trends Genet.*, **22**, 174-81.
5. Wills, N.M., Moore, B., Hammer, A., Gesteland, R.F. and Atkins, J.F. (2006) A functional -1 ribosomal frameshift signal in the human paraneoplastic Ma3 gene. *J. Biol. Chem.*, **281**, 7082-7088.
6. Manktelow, E., Shigemoto, K. and Brierley, I. (2005) Characterization of the frameshift signal of Edr, a mammalian example of programmed -1 ribosomal frameshifting. *Nucleic Acids Res.*, **33**, 1553-1563.
7. Clark, M.B., Jänicke, M., Gottesbühren, U., Kleffmann, T., Legge, M., Poole, E.S. and Tate, W.P. (2007) Mammalian gene PEG10 expresses two reading frames by high efficiency -1 frameshifting in embryonic-associated tissues. *J Biol. Chem.*, **282**, 37359-37369.
8. Brierley, I., Jenner, A.J. and Inglis, S.C. (1992) Mutational analysis of the "slippery-sequence" component of a coronavirus ribosomal frameshifting signal. *J. Mol. Biol.*, **227**, 463-479.
9. Giedroc, D.P. and Cornish, P.V. (2009) Frameshifting RNA pseudoknots: structure

and mechanism. *Virus Res.*, **139**, 193-208.
10. Namy, O., Moran, S.J., Stuart, D.I., Gilbert, R.J. and Brierley, I. (2006) A mechanical explanation of RNA pseudoknot function in programmed ribosomal frameshifting. Nature, **441**, 244-247.
11. Crooke, S.T. (2004) Progress in antisense technology. *Annu. Rev. Med.*, **55**:61-95.
12. Heasman J. (2002) Morpholino oligos: making sense of antisense? *Dev. Biol.*, **243**, 209-214.
13. Lu, Q.L., Mann, C.J., Lou, F., Bou-Gharios, G., Morris, G.E., Xue, S.A., Fletcher, S., Partridge, T.A. and Wilton, S.D. (2003) Functional amounts of dystrophin produced by skipping the mutated exon in the mdx dystrophic mouse. *Nat. Med.*, **9**, 1009-1014.
14. Bartel D.P. (2009) MicroRNAs: target recognition and regulatory functions. *Cell*, **136**, 215-233.
15. Ghildiyal, M. and Zamore, P.D. (2009) Small silencing RNAs: an expanding universe. *Nat. Rev. Genet.*, **10**, 94-108.
16. Morrissey, D.V., Lockridge, J.A., Shaw, L., Blanchard, K., Jensen, K., Breen, W., Hartsough, K., Machemer, L., Radka, S., Jadhav, V., Vaish, N., Zinnen, S., Vargeese, C., Bowman, K., Shaffer, C.S., Jeffs, L.B., Judge, A., MacLachlan, I. and Polisky, B. (2005) Potent and persistent in vivo anti-HBV activity of chemically modified siRNAs. *Nat. Biotechnol.*, **23**, 1002-1007.
17. Berkhout, B. (2004) RNA interference as an antiviral approach: targeting HIV-1. *Curr. Opin. Mol. Ther.*, **6**, 141-145.
18. Huang, C., Li, M., Chen, C. and Yao, Q. (2008) Small interfering RNA therapy in cancer: mechanism, potential targets, and clinical applications. *Expert Opin. Ther. Targets.* **12**, 637-645.
19. Fattal, E. and Bochot, A. (2006) Ocular delivery of nucleic acids: antisense oligonucleotides, aptamers and siRNA. *Adv. Drug Deliv. Rev.*, **58**(11):1203-1223.
20. Moreira, J.N., Santos, A. and Simões, S. (2006) Bcl-2-targeted antisense therapy (Oblimersen sodium): towards clinical reality. *Rev. Recent Clin. Trials.*, **1**, 217-235.
21. Perry, C.M. and Balfour, J.A. (1999) *Fomivirsen. Drugs*, **57**, 375-380.
22. Sahu, N.K., Shilakari, G., Nayak, A. and Kohli, D.V. (2007) Antisense technology: a selective tool for gene expression regulation and gene targeting. *Curr. Pharm. Biotechnol.*, **8**, 291-304.
23. Corey, D.R. (2007) Chemical modification: the key to clinical application of RNA interference? *J. Clin. Invest.*, **117**, 3615-3622.
24. Vester, B. and Wengel, J. (2004) LNA (locked nucleic acid): high-affinity targeting of complementary RNA and DNA. *Biochemistry*, **43**, 13233-13241.

25. Braasch, D.A. and Corey, D.R. (2001) Locked nucleic acid (LNA): fine-tuning the recognition of DNA and RNA. *Chem. Biol.*, **8**, 1-7.
26. Elmén, J., Lindow, M., Schütz, S., Lawrence, M., Petri, A., Obad, S., Lindholm, M., Hedtjärn, M., Hansen, H.F., Berger, U., Gullans, S., Kearney, P., Sarnow, P., Straarup, E.M. and Kauppinen, S. (2008) LNA-mediated microRNA silencing in non-human primates. *Nature*, **452**, 896-899.
27. Olsthoorn, R.C., Laurs, M., Sohet, F., Hilbers, C.W., Heus, H.A. and Pleij, C.W. (2004) Novel application of sRNA: stimulation of ribosomal frameshifting. *RNA*, **10**, 1702-1703.
28. Howard, M.T., Gesteland, R.F. and Atkins, J.F. (2004) Efficient stimulation of site-specific ribosome frameshifting by antisense oligonucleotides. *RNA*, **10**, 1653-1661.
29. ten Dam, E., Brierley, I., Inglis, S. and Pleij, C. (1994) Identification and analysis of the pseudoknot-containing gag-pro ribosomal frameshift signal of simian retrovirus-1. *Nucleic Acids Res.*, **22**, 2304-2310.
30. Liphardt, J., Napthine, S., Kontos, H. and Brierley, I. (1999) Evidence for an RNA pseudoknot loop-helix interaction essential for efficient -1 ribosomal frameshifting. *J. Mol. Biol.*, **288**, 321-335.
31. Napthine, S., Liphardt, J., Bloys, A., Routledge, S. and Brierley, I. (1999) The role of RNA pseudoknot stem 1 length in the promotion of efficient -1 ribosomal frameshifting. *J. Mol. Biol.*, **288**, 305-320.
32. Dulude, D., Baril, M. and Brakier-Gingras, L. (2002) Characterization of the frameshift stimulatory signal controlling a programmed -1 ribosomal frameshift in the human immunodeficiency virus type 1. *Nucleic Acids Res.*, **30**, 5094-5102.
33. Lucchesi, J., Mäkeläinen, K., Merits, A., Tamm, T. and Mäkinen, K. (2000) Regulation of -1 ribosomal frameshifting directed by cocksfoot mottle sobemovirus genome. *Eur. J. Biochem.*, **267**, 3523-3529.
34. Larsen, B., Gesteland, R.F. and Atkins, J.F. (1997) Structural probing and mutagenic analysis of the stem-loop required for Escherichia coli dnaX ribosomal frameshifting: programmed efficiency of 50%. *J. Mol. Biol.*, **271**, 47-60.
35. Takyar, S., Hickerson, R.P. and Noller, H.F. (2005) mRNA helicase activity of the ribosome. *Cell*, **120**, 49-58.
36. Válóczi, A., Hornyik, C., Varga, N., Burgyán, J., Kauppinen, S. and Havelda, Z. (2004) Sensitive and specific detection of microRNAs by northern blot analysis using LNA-modified oligonucleotide probes. *Nucleic Acids Res.*, **32**, e175.
37. Su, L., Chen, L., Egli, M., Berger, J.M. and Rich, A. (1999) Minor groove RNA triplex in the crystal structure of a ribosomal frameshifting viral pseudoknot. *Nat. Struct. Biol.*, **6**, 285-292.

38. Michiels, P.J., Versleijen, A.A., Verlaan, P.W., Pleij, C.W., Hilbers, C.W. and Heus, H.A. (2001) Solution structure of the pseudoknot of SRV-1 RNA, involved in ribosomal frameshifting. *J. Mol. Biol.*, **310**, 1109-1123.
39. Chen, G., Chang, K.Y., Chou, M.Y., Bustamante, C. and Tinoco, I. Jr. (2009) Triplex structures in an RNA pseudoknot enhance mechanical stability and increase efficiency of -1 ribosomal frameshifting. *Proc. Natl. Acad. Sci. U.S.A.* **106**, 12706-12711.
40. Brierley, I. and Pennell, S. (2001) Structure and function of the stimulatory RNAs involved in programmed eukaryotic-1 ribosomal frameshifting. *Cold Spring Harb. Symp. Quant. Biol.*, **66**, 233-48.
41. Plant, E.P., Jacobs, K.L., Harger, J.W., Meskauskas, A., Jacobs, J.L., Baxter, J.L., Petrov, A.N. and Dinman, J.D. (2003) The 9-A solution: how mRNA pseudoknots promote efficient programmed -1 ribosomal frameshifting. *RNA*, **9**, 168-174.
42. Kontos, H., Napthine, S. and Brierley, I. (2001) Ribosomal pausing at a frameshifter RNA pseudoknot is sensitive to reading phase but shows little correlation with frameshift efficiency. *Mol. Cell Biol.*, **21**, 8657-8670.
43. Cornish, P.V., Stammler, S.N. and Giedroc, D.P. (2006) The global structures of a wild-type and poorly functional plant luteoviral mRNA pseudoknot are essentially identical. *RNA*, **12**, 1959-1969.
44. Hansen, T.M., Reihani, S.N., Oddershede, L.B. and Sørensen, M.A. (2007) Correlation between mechanical strength of messenger RNA pseudoknots and ribosomal frameshifting. *Proc. Natl. Acad. Sci. U.S.A.*, **104**, 5830-5835.
45. Mazauric, M.H., Seol, Y., Yoshizawa, S., Visscher, K. and Fourmy, D. (2009) Interaction of the HIV-1 frameshift signal with the ribosome. *Nucleic Acids Res.*, **37**, 7654-7664.
46. Green, L., Kim, C.H., Bustamante, C. and Tinoco, I. Jr. (2008) Characterization of the mechanical unfolding of RNA pseudoknots. *J. Mol. Biol.*, **375**, 511-528.
47. Grünweller, A. and Hartmann R.K. (2007) Locked nucleic acid oligonucleotides: the next generation of antisense agents? *BioDrugs*, **21**, 235-43.

# Chapter V

## Antisense oligonucleotides that mimic a pseudoknot are highly efficient in stimulating –1 ribosomal frameshifting

Chien-Hung Yu, Mathieu H.M. Noteborn, and René C.L. Olsthoorn.

Department of Molecular Genetics, Leiden Institute of Chemistry, Leiden University, PO Box 9502, 2300RA Leiden, The Netherlands.

Submitted to Nucleic Acid Res.

**Abstract**

Programmed –1 ribosomal frameshifting (–1 PRF) is stimulated by RNA structures like pseudoknots or hairpins. Previously, it was shown that antisense oligonucleotides (ONs) annealing downstream of the slippery sequence and mimicking the stem of a hairpin are capable of inducing efficient PRF. Pseudoknots generally induce higher levels of frameshifting as compared to hairpin structures partly due to the formation of triple interactions between bases in loop 2 (L2) and stem 1 (S1). Based on our knowledge of the *Simian Retrovirus type 1* (SRV-1) gag-pro frameshifting pseudoknot, we here designed ONs that after binding to mRNA would mimic pseudoknots. Our data demonstrate that pseudoknot-forming ONs do induce more frameshifting than duplex-forming ONs. Depending on the length of S1, this enhancement was affected by the identity of bases in L2. This finding was corroborated by testing the corresponding *in cis* pseudoknots, i.e. the frameshift-inducing ability of pseudoknots with longer S1 are less affected by the identity of L2 in a length dependent manner. The greater flexibility of using small ONs to study –1 PRF allows the use of non-natural modifications. For instance it was found that 2'ACE protected ONs carrying a bulky bis(2-hydroxyethoxy) methyl orthoester group at their 2' hydroxyls are fully capable of inducing frameshifting, implying functional extensions of this type of modification in gene regulation by ONs. Our findings are discussed in relation to natural frameshifter pseudoknots and other antisense induced frameshifting studies.

## Introduction

The genetic information has to be decoded into functional polypeptides through translation. Although the genetic code has been deciphered, it is still far from perfect to extrapolate protein sequences from the DNA information of the genome in living organisms. One of the reasons is that in certain genes standard rules of decoding are overruled by alternative ways of translation, named recoding, which are stimulated by various kinds of signals embedded in the mRNA (1). To date, several biologically important recoding events, including stop codon-redefinition, translational hopping, and programmed ribosomal frameshifting (PRF) have been characterized in all three kingdoms [for reviews, see (2, 3)].

During PRF, elongating ribosomes are re-directed at a defined frequency by specific RNA elements into alternative reading frames either one nucleotide (nt) into the 3' direction (+1 PRF), or one (–1 PRF) or two nts (–2 PRF) into the 5' direction. –1 PRF, among the most inviting and best characterized frameshifting events, is promoted by two *in cis* RNA signals: a heptameric slippery sequence, X.XX Y.YY Z., where the dots indicate the original reading frame and spaces the frame after –1 PRF; and a structural element, either a simple stem-loop or a pseudoknot structure generally located 5-7 nts downstream of the slippery sequence [for a review, see (4)]. Most cases of –1 PRF have been found in the genomes of eukaryotic RNA viruses and prokaryotic insertional sequences [for reviews, see (5, 6)] whereas one example of a cellular gene in *Escherichia coli* (7) and three cellular genes in mammalians (8–10) are known to be expressed through –1 PRF.

It is generally believed that –1 PRF is promoted by downstream secondary structures which stall elongating ribosomes over the slippery sequence followed by tandem or single tRNA slippage into the –1 reading frame. A recent study using cryo-electron microscopy to image mammalian ribosomes stalled by the *Infectious bronchitis virus* (IBV) frameshifting pseudoknot or its inactive hairpin derivative showed several interesting features that further elucidate the mechanism of –1 PRF (11). First, the pseudoknot, as expected, resides in the mRNA entrance channel and makes direct contact with the putative ribosomal helicase in agreement with previous assumptions (12). Strikingly, the A-site is occupied by eEF-2 while the P-site tRNA is strongly bent toward the 3' direction probably due to the opposing forces raised between translocation and the hard-to-melt pseudoknot during translation elongation. However, tRNA bending is not observed in the control experiment using a frameshift-inactive hairpin construct. These findings suggest that the P-site tRNA dissociates and re-pairs into the –1 reading frame to release the tension built up by the frameshifting pseudoknot that resists unwinding by the ribosomal helicase. Therefore,

it is assumed that the better frameshifter RNAs can more resist unwinding by ribosomal helicase. Recently developed methods using optical tweezers to probe mechanical stability of RNA structures have shown a promising correlation between stability and frameshifting efficiency (13, 14).

In addition to the mentioned –1 PRF inducing RNA secondary structures, antisense ONs annealing downstream of the slippery sequence and mimicking the stem of a hairpin were recently found to be capable of inducing efficient PRF (15, 16). Since pseudoknots generally induce higher levels of frameshifting as compared to stem-loop structures, we here attempted to design ONs that would mimic a pseudoknot using our knowledge of the SRV-1 gag-pro pseudoknot (17, 18). Our data demonstrate that pseudoknot-forming ONs do induce more frameshifting than duplex-forming ONs. Interestingly, depending on the length of stem 1 (S1), this enhancement is affected by the identity of bases in loop 2 (L2) of the pseudoknot. The latter result is discussed in relation to natural frameshifter pseudoknots.

## Materials and Methods

### Frameshift reporter construction and oligonucleotides

The –1 PRF reporter constructs in this report were based on plasmid pSF208 (19). Briefly, pSF208 was digested by SpeI and NcoI followed by ligation of sets of complementary oligonucleotides (Eurogentec, Liege, Belgium) with designed mutations. A list of oligonucleotides is available upon request. All constructs were verified by sequencing (LGTC, Leiden, The Netherlands).

Antisense RNA oligonucleotides were all purchased from Dharmacon (Lafayette, USA). Of the delivered RNA oligonucleotides, which carry bis(2-hydroxyethoxy) methyl orthoester protection groups on their 2'OH, half the amount was de-protected by incubating with 100 mM acetic acid pH 3.8 and N,N,N',N'-tetramethylethane-1,2-diamine (TEMED) at 60°C for 30 minutes.

### *In vitro* transcription

*In vitro* transcription reactions using a RiboMAX Large Scale RNA Production Systems kit (Promega, The Netherlands) were carried out as described before (19).

### *In vitro* translation

*In vitro* translations were carried out in nuclease-treated rabbit reticulocyte lysate (RRL) (Promega). Prior to translation transcripts (0.025 pmoles) were incubated without or with 15.625 pmoles of ONs for 20 minutes at room temperature. After

incubation, 4 µL of RRL, 0.01 mM amino acids mixture except methionine, 2 µCi of $^{35}$S methionine (10 mCi/ml, MP Biomedicals, *in vitro* translational grade) were added in a total volume of 10 µL and incubated at 28°C for 1 hour. After translation, samples were resolved by gel electrophoresis and frameshift percentages determined as described before (19).

**Determination of the melting temperature (*T*m) of oligonucleotide duplexes**

RNA oligonucleotide 18RNA (5'GCGCGCUGGAGGCCAUGG3') with and without 2'ACE modifications was mixed in a 1:1 molar ratio with RNA18 (5'CCAUGGCCUCCAGCGCGC3') also with and without 2'ACE modifications, in UV-melting buffer (100 mM NaCl, 10 mM Na-cacodylate, pH 6.8). The measurements were performed on a Varian Cary 300 spectrophotometer with a heating rate of 0.25°C/min over a temperature gradient of 30°C to 90°C. The absorbance at 260 nm was recorded and normalized to the blank control. Data was analyzed by fitting the transition to a two-state model with correcting sloping baselines using a nonlinear least-squares program to estimate *T*m.

## Results

***In trans* re-creation of the SRV-1 frameshifter pseudoknot by structured ONs**

It has previously been shown that linear ONs that bind downstream of a slippery sequence and mimic the double-stranded stem region of frameshifter hairpins, efficiently stimulate ribosomal frameshifting (15, 16). Since pseudoknots are better frameshifters than their hairpin derivatives (19, 20), we attempted to design pseudoknot-mimicking ONs based on structural (Fig. 1A) (17) and functional studies (18) with the aim to enhance ON-induced frameshifting. We first compared the frameshifting efficiency induced by a linear (R6b, hairpin-mimicking) and a structured (R28, pseudoknot-mimicking) RNA ONs (Fig. 1B). Figure 1C shows that R28 promoted 1.6% of ribosomes to switch frame at the UUUAAAC slippery sequence, compared to 0.8% by R6b. This 2-fold increase may be due to a more stabilized ON-mRNA interaction contributed by tertiary interactions between L2 and minor groove of S1 as in SRV-1 frameshifting pseudoknots (Fig. 1A). To support this idea we designed another two mutants (Figure 1B): M28C, which is reminiscent of the A26C mutation shown previously to reduce frameshifting more than 3 fold in the context of the wild-type *in cis* pseudoknot (18), and M28, in which most of the adenosines were replaced by uridines to disrupt potential triple interactions. The reduction in frameshifting obtained with M28C (Fig. 1C, lane 5) and M28 (lane 4), by

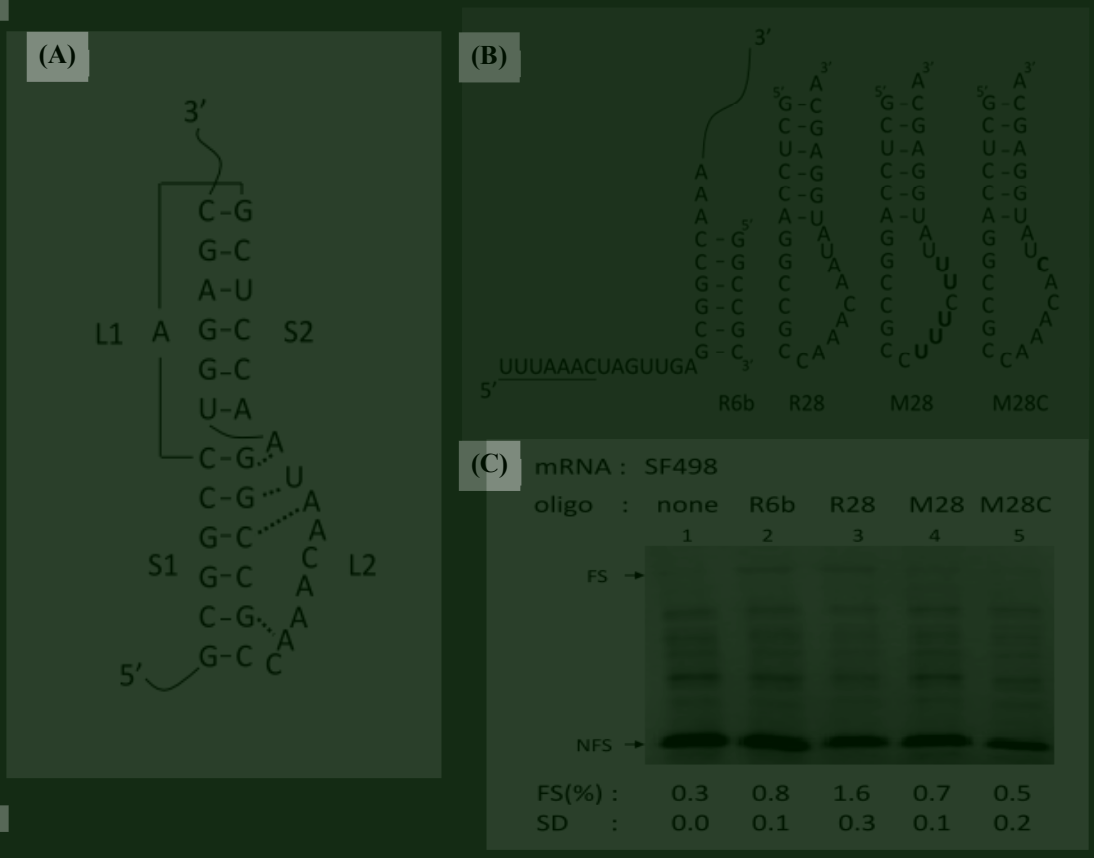


**Figure 1. –1 PRF induced by ONs mimicking the SRV-1 frameshifter pseudoknot. (A) Secondary structure of the SRV-1 frameshifting pseudoknot (18). Dashed lines represent base triples. The annotation of stems and loops is indicated. (B) Sequences of a linear ON mimicking the S1 region of the SRV-1 pseudoknot (R6b) and structured ONs mimicking the entire SRV-1 pseudoknot (R28, M28 and M28C) and binding 7 nts downstream of the UUUAAAC slip site (underlined) are shown. Changes with respect to R28 are shown in bold. (C) SDS-PAGE analysis of 35S-methionine labeled translation products in rabbit reticulocyte lysate. –1 PRF is monitored by appearance of a 65 kD shifted product (FS). The non-shifted in-frame 19 kD products are indicated by NFS. Quantitative analysis of frameshifting efficiency is described in Materials and Methods. The standard deviation (SD) shows the variation of the averaged frameshifting efficiency from at least three independent measurements.**

3.2 and 2.3 fold, respectively, is comparable to the effect of these mutations in the wild-type pseudoknot (18). These data suggest that binding of structured ONs can mimic stem-loop tertiary interactions in the minor groove of a pseudoknot stem 1, thereby enhancing frameshifting efficiency.

**Improving ON-induced frameshifting efficiency by structured oligonucleotides – a longer S1 version**

We previously reported that a linear ON of 12-18 nts has the optimal length to induce

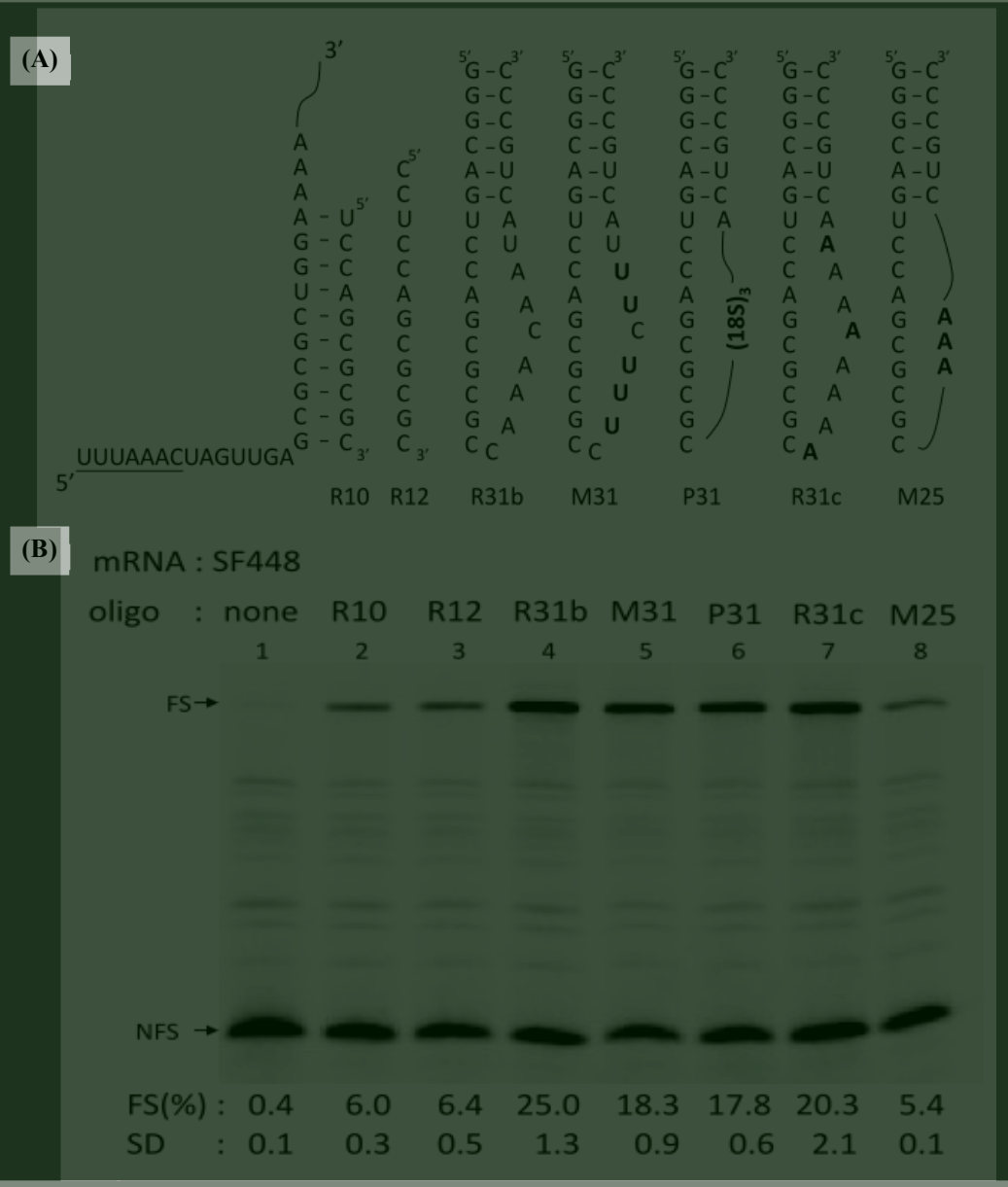


**Figure 2. –1 PRF induced by structured ONs mimicking a frameshifter pseudoknot with a 10 bp stem S1 and the effect of ACE modifications at the 2'-OH of the ribose in these ONs. (A) Sequences of linear ONs (R10 and R12) and structured ONs (R31b, M31, R31c, and M25) with 10 base complementarity to a region 7 nts downstream of UUUAAAC slip site (underlined) are shown. Changes with respect to R31b are shown in bold. (18S)3 is the abbreviation of three 18-atom spacers, which are composed of consecutive hexaethylene glycols. (B) SDS-PAGE analysis of 35S-methionine labeled translation products. The RNA molecules of each ON are de-protected by the protocol provided by the manufacturer. See legend to Figure 1C and Materials and Methods for more details. (C) SDS-PAGE analysis of 35S-methionine labeled translation products in RRL. The RNA molecules of each ON are protected by ACE groups at the 2'-OH of the ribose. See Figure 1C and Materials and Methods for more details.**

frameshifting, yielding an efficiency of 13% (21). It was worthwhile to test whether

we could increase this efficiency by introducing base-triples using structured ONs in a longer stem construct in R10 (Fig. 2A) similar to the R6 and R28 as described above. Building upon the data obtained with R28 and M28, we designed R31b, M31, and M25 structural ONs hybridized to an mRNA template used previously (19) to investigate the effect of base triples with an S1 of 10 bp (Fig. 2A). The results shown in Figure 2B indicate that R31b induces 25.0% of frameshifting, which is about 4-fold more efficient than linear R10 (6.0%) or R12 (6.4%). Next, we investigated what are the critical components of this "pseudo-pseudoknot" for frameshifting. Reducing the loop length to three nts (M25) was predicted to disrupt the pseudoknot-like structure since three nts are not sufficient to cross the minor groove of a 10 bp stem (22). Indeed, frameshifting was strongly reduced to a level (5.4%) that was close to that of R10 (Fig. 2A, lane 8). Interestingly, when the loop was replaced by a U-rich sequence (M31) with the aim to abrogate triple interactions as with M28, frameshifting decreased 1.4-fold compared to R31b (Fig. 2B, lanes 4 and 5), much less than the difference between R28 and M28 (2.3 fold). Although learning from natural pseudoknots that L2 is generally A-rich because triple interactions mainly occur through the amino groups of adenosines, we could not exclude the possibility of interactions through the U-rich loop. Therefore, we designed P31 of which the bases and riboses of L2 were replaced by polyethylene glycol (PEG) linkers to completely rule out the possibility of triplex formation (Fig. 2A). The frameshifting efficiency of P31 was also 1.4 fold less than that of R31b (Fig. 2B, lanes 4 and 6) further indicating the role of triple interactions of structured ONs in enhancing frameshifting. However, replacing all bases in L2 to adenines (R31c) caused a 5% decrease in frameshifting (Fig. 2B, lanes 4 and 7). Native gel electrophoresis of this ON showed a large fraction of R31c to form dimers, thereby reducing its effective concentration (data not shown).

**Effect of 2' bulky groups on frameshifting efficiency by affecting hairpin formation**

The ONs used in our assays were purchased with ACE [bis(2-acetoxyethoxy) methyl orthoester] protective groups at the 2'OH, which were removed according to manufacturer's instructions (see Materials and Methods). Since only half the amount of each ON was deprotected, the other half allowed us to investigate the effect of bulky 2' moieties on complex stability and frameshifting efficiency. It has been suggested that the 2' bulky group may prevent the formation of intra-molecular structure (23). The ACE version of RNA31b when used in the frameshift assay was nearly 4-fold less efficient than its non-modified form (Fig. 2C, lane 4). This suggested that the ACE side group interfered with the formation of the second stem. The same effect was observed for ONs M31, M25, and R31c, which all induced less

| *T*m (°C) | RNA18 with 2'ACE | RNA18 w/o 2'ACE |
|---|---|---|
| 18RNA with 2'ACE | 78 | 81 |
| 18RNA w/o 2'ACE | 80 | 82 |

**Table 1. *T*m measurements of AONs with and without 2'ACE modification.**

frameshifting than their non-protected counterparts (Fig. 2C, lanes 5, 7, and 8). Intriguingly, the P31 with ACE modification (Fig. 2C, lane 6) was as effective as its counterpart without protection. The reason for this is still under investigation. UV-melting experiments indeed showed that ACE-ACE duplexes were less stable than ACE-RNA and RNA-ACE duplexes (Table 1). Surprisingly, linear R10 and R12 ONs with ACE modification, although forming a less stable duplex with RNA, were ~1.6 fold more efficient than their non-modified versions (Fig. 2C, lane 1 and 2),

**The relation between S1 length and S1-L2 triple interactions in frameshifter pseudoknots**

Although the loop-stem interactions further stabilized the ON-mRNA interaction, their effect was less significant when the length of S1 was increased. This observation fits with the general belief that frameshifter pseudoknots with a long S1 (10-11 bp) are not dependent on the L2 sequence to induce efficient frameshifting; short S1 (4-6 bp) pseudoknots, however, rely on S1-L2 tertiary interactions to be efficient frameshifters (4, 24). To investigate the relation between S1 length and triple interactions in our experiments, we designed pseudoknots with different lengths of S1 (Fig. 3A) based on the above data with *in trans* ONs. We first modified the L2 sequence of the SRV-1 pseudoknot from A-rich (SF520) to U-rich (SF522) to disrupt triple interactions (Fig. 3A). This resulted in a 2.6-fold (from 37.6% to 14.6%) decrease in frameshifting efficiency (Fig. 3B, lanes 1 and 2), in accordance with our data using structured ONs (Fig. 1C, lane 3 and 4). In the context of another S1 sequence based on our previous publication (21), a more dramatic difference (about 3.6-fold) was observed as a result of the U-rich loop sequence (Fig. 3B, lanes 3 and 4). In the latter construct, extending S1 to 7 bp the difference in frameshift activity between the A-rich and U-rich L2 constructs was less than 3-fold [SF482 and SF484 (Fig. 3B, lanes 5 and 6)]. Further increasing S1 to 8 bp (Fig. 3B, lane 7 and 8) and 9 bp (Fig. 3B, lane 9 and 10) reduced the difference to 1.4-fold and 1.6-fold, respectively. Interestingly, at a stem length of 10 bp, there was no difference any more in the frameshifting efficiency between the two different kinds of L2 sequence (Fig. 3B, lanes 11 and 12). These *in cis* pseudoknot data correlate well with the *in trans* structured ON data and also

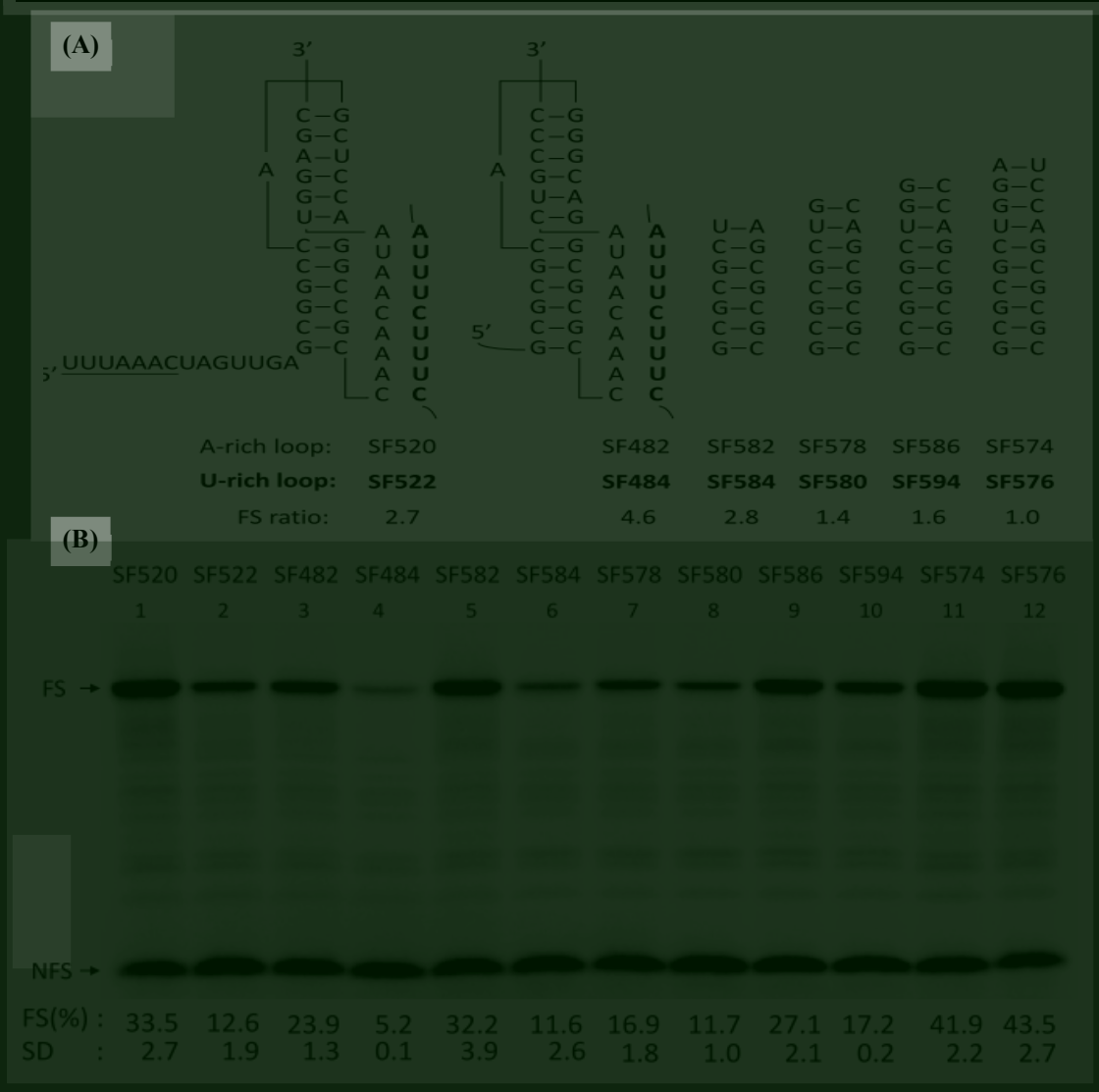


**Figure 3. The correlation between S1 length and S1-L1 interactions in frameshifter pseudoknots. (A) SF520 represents the SRV-1 frameshifter pseudoknot shown in Figure 1A. SF522 is a mutant of SF520 with a U-rich L2 sequence (in bold). SF574 is the in cis frameshifter pseudoknot that is equivalent to the one formed in trans by RNA R31b, shown in Figure 2A. SF576 is a mutant of SF574 with a U-rich L2 like SF520. The length of stem 1 of SF574 and SF576 is reduced sequentially one base-pair from top of the S1 producing constructs with 9, 8, 7, and 6 bp, respectively, with either A-rich L2 or U-rich L2. The FS (frameshifting) ratio is calculated by dividing the averaged frameshifting efficiency of A-rich loop by the averaged frameshifting efficiency of U-rich loop of constructs with the same S1 length from Figure 3B. (B) SDS-PAGE analysis of 35S-methionine labeled translation products in rabbit reticulocyte lysate. See legend to Figure 1C and Materials and Methods for more details**

demonstrate that the contribution of triple interactions between S1 and L2 is inversely correlated with the length of S1.

## Discussion

In the present study, we have demonstrated how structured ONs mimicking pseudoknots can enhance antisense-induced –1 PRF efficiency through stem stacking and tertiary loop-stem interactions. The dissection of the pseudoknot into two parts also allowed us to investigate the effect of base or sugar modifications on ribosomal frameshifting. Moreover, construction of the pseudoknot-like structures in sense supports the observation in antisense, and further demonstrates that there exists an inverse correlation between the S1 length and the contribution of S1-L2 triple interactions to frameshifting. Our findings provide a way to enhance antisense ON-induced ribosomal frameshifting and lend further support for the notion that "longer S1" frameshifting pseudoknots are not sensitive to L2 sequences while ones with a "shorter S1" are.

A pioneering study on the formation of "pseudo-half-knots" by binding of ONs to the HIV-1 TAR RNA loop opened the way to reconstruct pseudoknot structures *in trans* by ONs (25). There are three reports in which a similar idea was applied to study ribosomal frameshifting. Plant *et al.* (26) created pseudo-pseudoknots by hybridizing linear DNA ONs to the loop of a hairpin to restrict loop rotation in order to test their torsional restraint model for frameshifting. Fayet's group (27) restored a novel "kissing loop" frameshifting signal of bacterial insertional sequence (IS) *3411* by expressing part of the required structure *in trans* as a fusion with tRNA. In another study Chou *et al.* (28) designed linear RNA ONs mimicking human telomerase hTPK-Du177 pseudoknot to investigate the importance of triplex structures spanning the helical junction and triple interactions between the major groove of S2 and L1. Here, we demonstrate that a distinct type of antisense ON, namely structured ones, can also mimic pseudoknots and enhance antisense-induced frameshifting through triple interactions between the minor groove of S1 and L2. The results are in agreement with our previous data in that building up the stability in the proximal end of an mRNA-ON duplex can enhance ribosomal frameshifting (21). Note that in our pseudo-pseudoknots, in contrast to the work of Plant *et al.* (26), there is no torsional strain built-up since the antisense ON can freely rotate around the mRNA during ribosomal encounter. Yet, they are highly efficient stimulators of frameshifting.

Our data show that frameshifting induced by structured ONs is sensitive to the sequence identity of L2 when they form a 6 bp stem 1 but less so when they form a 10 bp S1 (Fig. 1C and Fig. 2B). A similar effect was observed with the corresponding *in cis* pseudoknots (Fig. 3B). One explanation for this observation is that a longer stem obviates the need for triple interactions, in other words they may be forming but they are not contributing to the stability of the structure. Unfortunately, there is not (yet) a high-resolution structure of a frameshifter pseudoknot possessing an S1 larger than 6

bp available. Therefore, it is hard to know the specific interactions, if any, between L2 and S1 in a large pseudoknot.

In the present study we addressed another important question about the impact of triple helix formation in pseudoknots with various S1 sizes. Our data show that there exists a good inverse correlation between S1 size and the effect of triplex formation. Upon reviewing viral frameshift-inducing pseudoknots (5), we can categorize them into two major groups based on S1 length: one group has an S1 length between 4 and 6 bp and the other has an S1 length of 11 to 14 bp. Interestingly, those long S1 pseudoknots have a relatively long L2 with more than 30 nts except for two frameshifting signals in *S. cerevisiae* viruses (ScV) whose L2 length is 11 nts. Pseudoknots with short S1 feature an L2 of less than 12 nts. Moreover, the long L2s are either have no apparent secondary structures (29) or a structure that is not important for frameshifting (30, 31). This may imply that the less stable short S1 pseudoknots have "evolved" specific triples to induce significant levels of frameshifting, while for pseudoknots with longer S1 the extra stabilization, contributed by base triples, may be dispensable. Here the highly flexible L2 is probably used to store genetic (protein-coding) information or perform other unknown functions rather than to stabilize the pseudoknot conformation.

Our *in cis* pseudoknot data are actually in conflict with previous findings from Brierley's lab who showed that variants of the IBV pseudoknot with less than 11 bp in S1 were largely inactive in frameshifting (32). Their pKA13 pseudoknot with a 10 bp S1 induced merely 7% of frameshifting while our SF574 and SF576 pseudoknots which have 6 out of 10 bp in common with pKA13's S1 showed 41.9% and 43.5% frameshifting, respectively (Fig. 3A and 3B). Moreover, their other pseudoknots showed background levels of frameshifting when S1 became shorter than 9 bp whereas we still detect significant levels of frameshifting with our constructs possessing an S1 of 6 to 8 bp (Fig. 3A and 3B). To elucidate why a pseudoknot whose global structure is indistinguishable from pKA13 but is just 1 bp shorter showed almost 7-fold drop in frameshifting, they separately modified the spacer length, L2 length, and S1 sequence. These changes in the context of pKA13 led to a 1.7-fold, 1.6-fold, and 2.4-fold increase in frameshifting, respectively. Yet, a construct combining all these changes was not tested. It would be interesting to know the activity of this "evolved" pseudoknot to further understand the role of S1 length in promoting frameshifting.

The linear R10 and R12 ONs with ACE modification are surprisingly efficient in inducing frameshifting (Fig. 2C) taking into account that their duplex stability is lower than the standard RNA-RNA duplex. This suggests that the 2'ACE modification may be a poor substrate for the ribosomal helicase or interferes with the

translocation step. Although the specific reason needs further investigation, the 2'ACE-modified RNAs were shown, for the first time, to be functional in inducing frameshifting and may be applied in other antisense applications such as exon skipping or microRNA inhibition.

In conclusion, our data demonstrate that pseudoknot-mimicking ONs stabilized by loop-stem | interactions are better frameshifters than hairpin-mimicking ONs. Moreover, these tertiary interactions were shown to be dependent on the length of stem S1. Finally, the use of small ONs that are amenable to chemical modification opens a new way to study ribosomal frameshifting and may ultimately lead to applications of ONs in curing defects caused by frameshift mutations.

## References

1. Gesteland,R.F., Weiss,R.B. and Atkins,J.F. (1992) Recoding: reprogrammed genetic decoding. *Science*, **257**, 1640-1641.

2. Baranov,P.V., Gesteland,R.F. and Atkins,J.F. (2002) Recoding: translational bifurcations in gene expression. *Gene*, **286**, 187-201.

3. Namy,O., Rousset,J.P., Napthine,S. and Brierley,I. (2004) Reprogrammed genetic decoding in cellular gene expression. *Mol. Cell*, **13**, 157-168.

4. Giedroc,D.P., Theimer,C.A. and Nixon,P.L. (2000) Structure, stability and function of RNA pseudoknots involved in stimulating ribosomal frameshifting1. *J. Mol. Biol.*, **298**, 167-185.

5. Brierley,I. (1995) Ribosomal frameshifting viral RNAs. *J. Gen. Virol.*, **76**, 1885-1892.

6. Baranov,P.V., Fayet,O., Hendrix,R.W. and Atkins,J.F. (2006) Recoding in bacteriophages and bacterial IS elements. *Trends in Genetics*, **22**, 174-181.

7. Larsen,B., Gesteland,R.F. and Atkins,J.F. (1997) Structural probing and mutagenic analysis of the stem-loop required for Escherichia coli dnaX ribosomal frameshifting: programmed efficiency of 50%. *J. Mol. Biol.*, **271**, 47-60.

8. Wills,N.M. (2006) A Functional -1 Ribosomal Frameshift Signal in the Human

Paraneoplastic Ma3 Gene. *J. Biol. Chem.*, **281**, 7082-7088.

9. Manktelow,E., Shigemoto,K. and Brierley,I. (2005) Characterization of the frameshift signal of Edr, a mammalian example of programmed- 1 ribosomal frameshifting. *Nucleic Acids Res.*, **33**, 1553-1563.

10. Clark,M.B., Janicke,M., Gottesbuhren,U., Kleffmann,T., Legge,M., Poole,E.S. and Tate,W.P. (2007) Mammalian Gene PEG10 Expresses Two Reading Frames by High Efficiency -1 Frameshifting in Embryonic-associated Tissues. *J. Biol. Chem.*, **282**, 37359-37369.

11. Namy,O., Moran,S.J., Stuart,D.I., Gilbert,R.J.C. and Brierley,I. (2006) A mechanical explanation of RNA pseudoknot function in programmed ribosomal frameshifting. *Nature*, **441**, 244-247.

12. Takyar,S., Hickerson,R.P. and Noller,H.F. (2005) mRNA helicase activity of the ribosome. *Cell*, **120**, 49-58.

13. Hansen,T.M., Reihani,S.N.S., Oddershede,L.B. and Sørensen,M.A. (2007) Correlation between mechanical strength of messenger RNA pseudoknots and ribosomal frameshifting. *Proc. Natl. Acad. Sci. U.S.A.*, **104**, 5830-5835.

14. Chen,G., Chang,K.-Y., Chou,M.-Y., Bustamante,C. and Tinoco,I.,Jr (2009) Triplex structures in an RNA pseudoknot enhance mechanical stability and increase efficiency of -1 ribosomal frameshifting. *Proc. Natl. Acad. Sci. U.S.A.*, **106**, 12706-12711.

15. Olsthoorn,R.C.L., Laurs,M., Sohet,F., Hilbers,C.W., Heus,H.A. and Pleij,C.W.A. (2004) Novel application of sRNA: stimulation of ribosomal frameshifting. *RNA*, **10**, 1702-1703.

16. Howard,M.T., Gesteland,R.F. and Atkins,J.F. (2004) Efficient stimulation of site-specific ribosome frameshifting by antisense oligonucleotides. *RNA*, **10**, 1653-1661.

17. Michiels,P.J., Versleijen,A.A., Verlaan,P.W., Pleij,C.W., Hilbers,C.W. and Heus,H.A. (2001) Solution structure of the pseudoknot of SRV-1 RNA, involved in ribosomal frameshifting1. *J. Mol. Biol.*, **310**, 1109-1123.

18. Olsthoorn,R.C.L., Reumerman,R., Hilbers,C.W., Pleij,C.W.A. and Heus,H.A. (2010) Functional analysis of the SRV-1 RNA frameshifting pseudoknot. *Nucleic Acids Res.*, **38**, 7665-7672.

19. Yu,C.-H., Noteborn,M.H., Pleij,C.W.A. and Olsthoorn,R.C.L. (2011) Stem-loop structures can effectively substitute for an RNA pseudoknot in -1 ribosomal frameshifting. *Nucleic Acids Res.,* **39**, 8952-8959.

20. Napthine,S., Vidakovic,M., Girnary,R., Namy,O. and Brierley,I. (2003) Prokaryotic-style frameshifting in a plant translation system: conservation of an unusual single-tRNA slippage event. *EMBO J.*, **22**, 3941-3950.

21. Yu,C.H., Noteborn,M.H.M. and Olsthoorn,R.C.L. (2010) Stimulation of ribosomal frameshifting by antisense LNA. *Nucleic Acids Res.*, **38**, 8277-8283.

22. Pleij,C.W., Rietveld,K. and Bosch,L. (1985) A new principle of RNA folding based on pseudoknotting. *Nucleic Acids Res.*, **13**, 1717-1731.

23. Scaringe,S.A. (2001) RNA oligonucleotide synthesis via 5'-silyl-2'-orthoester chemistry. *Methods*, **23**, 206-217.

24. Giedroc,D.P. and Cornish,P.V. (2009) Frameshifting RNA pseudoknots: structure and mechanism. *Virus Res.*, **139**, 193-208.

25. Ecker,D.J., Vickers,T.A., Bruice,T.W., Freier,S.M., Jenison,R.D., Manoharan,M. and Zounes,M. (1992) Pseudo--half-knot formation with RNA. *Science*, **257**, 958-961.

26. Plant,E.P. and Dinman,J.D. (2005) Torsional restraint: a new twist on frameshifting pseudoknots. *Nucleic Acids Res.*, **33**, 1825-1833.

27. Mazauric,M.-H., Licznar,P., Prère,M.-F., Canal,I. and Fayet,O. (2008) Apical loop-internal loop RNA pseudoknots: a new type of stimulator of -1 translational frameshifting in bacteria. *J. Biol. Chem.*, **283**, 20421-20432.

28. Chou,M.-Y. and Chang,K.-Y. (2010) An intermolecular RNA triplex provides insight into structural determinants for the pseudoknot stimulator of -1 ribosomal frameshifting. *Nucleic Acids Res.*, **38**, 1676-1685.

29. Brierley,I., Rolley,N.J., Jenner,A.J. and Inglis,S.C. (1991) Mutational analysis of the RNA pseudoknot component of a coronavirus ribosomal frameshifting signal. *J. Mol. Biol.*, **220**, 889-902.

30. Su,M.-C., Chang,C.-T., Chu,C.-H., Tsai,C.-H. and Chang,K.-Y. (2005) An atypical RNA pseudoknot stimulator and an upstream attenuation signal for -1

ribosomal frameshifting of SARS coronavirus. *Nucleic Acids Res*, **33**, 4265-4275.

31. Plant,E.P., Pérez-Alvarado,G.C., Jacobs,J.L., Mukhopadhyay,B., Hennig,M. and Dinman,J.D. (2005) A Three-Stemmed mRNA Pseudoknot in the SARS Coronavirus Frameshift Signal. *Plos Biol*, **3**, e172, 10.

32. Napthine,S., Liphardt,J., Bloys,A., Routledge,S. and Brierley,I. (1999) The role of RNA pseudoknot stem 1 length in the promotion of efficient -1 ribosomal frameshifting. *J. Mol. Biol.*, **288**, 305-320.

# Chapter VI

## Comparison of $preQ_1$ riboswitches by molecular dynamics simulations and ribosomal frameshifting: identification of a novel RNA-ligand interaction

Chien-Hung Yu[1]*, Jinghui Luo[2]*, Shina C. L. Kamerlin[3], Jan Pieter Abrahams[2], René C.L. Olsthoorn[1]

*contributed equally

[1]Department of Molecular Genetics and [2]Biophysical Structural Chemistry, Leiden Institute of Chemistry, Leiden University, PO Box 9502, Leiden, The Netherlands.
[3]Department of Cell and Molecular Biology (ICM), Uppsala University, BMC, Box 596, S-751 24 Uppsala, Sweden.

Manuscript in preparation

### Abstract

$PreQ_1$ riboswitches are the smallest riboswitch found to date that function as genetic control elements upon binding the metabolite molecule 7-aminomethyl-7-deazaguanine ($preQ_1$), an intermediate in queuosine (Q) biosynthesis. With only 34 nucleotides (nts), $preQ_1$ riboswitch aptamers display high affinities for their cognate ligand, binding of which stabilizes the formation of a compact RNA pseudoknot. Here we have developed a novel ligand-dependent *in vitro* assay, based on ribosomal frameshifting, to investigate the molecular basis of the $preQ_1$ affinity of two distinct $preQ_1$ aptamers uncoupled from their expression platforms. Our data show that *Bacillus subtilis* (*B. subtilis*) and *Fusobacterium nucleatum* (*F. nucleatum*) $preQ_1$ aptamers differ in their ability to act as frameshifter pseudoknots due to differences in

preQ$_1$ affinity. Molecular dynamics (MD) simulations, using the published coordinates of the *B. subtilis* aptamer, revealed the possibility of additional contacts between preQ$_1$ and residue G7 in the *F. nucleatum* aptamer. These contacts are absent in the *B. subtilis* aptamer where the corresponding residue is a U. Swapping the identity of the 7$^{th}$ nucleotide between both preQ$_1$ aptamers decreased the ligand-dependent frameshifting of the *F. nucleatum* pseudoknot more than 5-fold but increased the sensitivity of the *B. subtilis* one more than 5-fold. These data show that MD simulation is a valuable tool to investigate molecular details of RNA-ligand interactions. Combined with the high sensitivity of the *in vitro* ribosomal frameshifting assay, this study forms the basis for developing high-throughput assays of riboswitch-metabolite interactions.

## Introduction

Riboswitches are non-coding structured RNAs typically located in the 5'-untranslated regions (UTRs) that bind metabolites, such as nucleobases, coenzymes, and amino acids with high specificity and affinity to regulate gene expression (1). Although majorly found in eubacteria, some representatives exist in archaea (2) and eukaryotes (3). Riboswitches typically consist of a metabolite-binding aptamer to sense cellular metabolites to regulate an adjoining expression platform through transcriptional or translational control without assistance of proteins (4). Transcriptional control can be mediated upon metabolite binding either through the formation of a transcription terminator hairpin that stops further elongation by RNA polymerase or through disruption of an existing terminator so that transcription can be resumed. Translational control is thought to occur by metabolite induced structural changes that may expose or sequester the Shine-Dalgarno sequence thereby enabling or inhibiting translation initiation (5).

Metabolite-binding aptamers are formed from highly conserved sequences and/or structural elements. Through genome-wide bioinformatics analysis, several novel riboswitch candidates have been identified, including one that responds to preQ$_1$, a precursor of Q (6). Q is a post-transcriptional modification of the wobble base of GUN anticodons of bacterial and eukaryotic tRNAs and is important in translational fidelity (7). The aptamer domain of the preQ$_1$ riboswitch upstream of the Q biosynthesis operon consists of a minimal sequence of 34 nts and is the smallest riboswitch aptamer known to date. The preQ$_1$ aptamer generally consists of a 5 base pair (bp) stem and a loop of 10-13 nts, followed by a single-stranded region of about 11-14 nts (8) (Fig. 1). In the presence of nanomolar concentrations of preQ$_1$, the

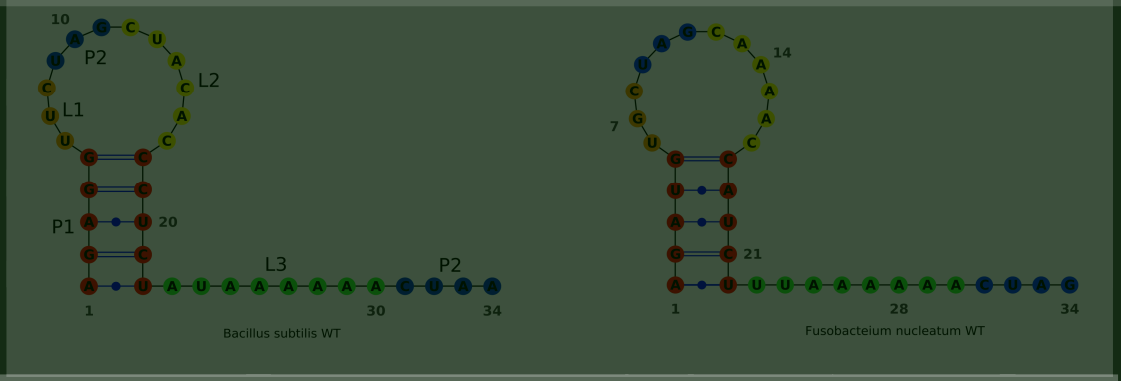


**Figure 1. The sequences and secondary structures of preQ$_1$ riboswitch aptamers from *Bacillus subtilis* (left) and *Fusobaterium nucleatem* (right). The colors of red, orange, blue, yellow and green represent stem 1 (P1), loop 1 (L1), stem 2 (P2), loop 2 (L2 ) and loop 3 (L3), respectively.**

aptamers from *B. subtilis* (9,10) *F. nucleatum* (11) and *Thermoanaerobacter tengcongensis* (12) have been shown to fold into a compact pseudoknot by pairing of 3-4 nucleotides from the loop to 3-4 nts from the downstream region.

Programmed ribosomal frameshifting (PRF) is a translational recoding process in which ribosomes can shift 1 nt forward (+1 PRF) or 1 or 2 nts backward (-1 PRF or -2 PRF) on a mRNA and resume translation in a different reading frame [see (13) for a review]. There are two critical *cis*-acting RNA elements responsible for PRF: a slippery sequence and a downstream structural element. This structural element can be either a hairpin or a pseudoknot, and the stability of which is positively correlated with frameshifting efficiency (14). Since the pseudoknot structure, which is formed upon binding of preQ$_1$ to its aptamer, is reminiscent of several frameshift inducing pseudoknots (15), it is of interest to investigate whether the ligand-induced pseudoknot can stimulate PRF as well.

In this report, we explored the ability of *F. nucleatum* and *B. subtilis* preQ$_1$ riboswitch aptamers to function as ligand-dependent pseudoknots in –1 PRF. The stability of both riboswitch aptamers was also investigated by MD simulations. Based on MD observations a novel interaction with preQ$_1$ was predicted and subsequently validated by our frameshift assay. Therefore, our combined MD simulation and frameshift assay provide a platform to understand the structural basis of ligand binding to preQ1 riboswitch aptamers and possibly others as well.

## Materials and Methods

### Frameshift reporter construction and assays

Minus 1 frameshifting was monitored by the SF reporter construct described earlier

(16). Briefly, complementary oligonucleotides (Eurogentec, Liege, Belgium) were annealed followed by ligation into SpeI/NcoI digested SF vector to obtain experimental constructs (sequences are available upon request). All the constructs were verified by DNA sequencing (LGTC, Leiden, The Netherlands).

Frameshift assays were carried out in rabbit reticulocyte lysates (RRL) (Promega, Benelux, The Netherlands) as reported (17). In short, the target plasmids were linearized by BamHI (Fermentas, The Netherlands) followed by successive phenol/chloroform extraction and ethanol precipitation. The linearized templates were transcribed by SP6 RNA polymerase. The resulting transcripts were electrophoresed in agarose gels to determine their quantity and quality. 5 nM of mRNA were then mixed with 4 µl of RRL, 0.15 µl of $^{35}$S methionine [>1000Ci (37.0TBq)/mmol, Easy Tag, PerkinElmer], 0.15 µl 1mM amino acid mix without methionine, and various concentration of preq1 (0~200 µM) in a final volume of 10 µl, and incubated at 30ºC for 1 hour. Note that the $preQ_1$ compound, a generous gift of Dr. Iwata-Reuyl, was first dissolved at a concentration of 200 mM in DMSO, and then diluted to 2mM in RNase free water as our working solution of which 1 µl was added to the translation mixture. We kept the final concentration of DMSO in the translation mixture at 0.1% to prevent adverse effects on translation. After translation, samples were boiled with 2X Laemmli buffer for 3 min and loaded onto 13% SDS-PAGE. Gels were then dried and exposed to phosphoimager screen. The intensity of shifted and non-shifted protein products were quantified by Quantity One (Biorad, The Netherlands). After subtracting the background, the frameshifting efficiency of each construct at each concentration of $preQ_1$ was calculated as: the amount of -1 frameshifted product divided by the sum of the amount of in-frame product and -1 frameshifted product after correction for the number of methionines in each fragment, and then multiplied by 100.

**Construction of $preQ_1$ riboswitch aptamer of *F. nucleatum* from known coordinates of *B. subtilis***

The NMR solution structure of $preQ_1$ in complex with the 34 nts long aptamer domain of the $preQ_1$ riboswitch (PDB ID: 2L1V) from *B. subtilis* served as the homology structure for building the $preQ_1$ aptamer of *F. nucleatum* by RNABuilder 2.3 package (18). To predict the structure of $preQ_1$ aptamer of *F. nucleatum*, we first aligned the secondary structure between aptamers from different species, established by comparative sequence analysis based on the NMR structure. Subsequently, the threading force was used to build initial models of the $preQ_1$ aptamer of *F. nucleatum*. Energy minimizations were carried out to remove bad contacts in the initial model of the *F. nucleatum* aptamer with 3000 steps using the steepest descent algorithm followed by 3000 steps with a conjugate gradient algorithm of energy minimization. In addition,

the apo-preQ$_1$ aptamer systems were obtained by removing the preQ$_1$ molecule from the preQ$_1$ aptamer of *B. subtilis* and *F. nucleatum*.

**Molecular dynamics simulations**

The structures of preQ$_1$ aptamers of *B. subtilis* from NMR and *F. nucleatum* from RNA Builder were used as starting structures for MD simulations. The force field of the preQ$_1$ system was calculated with ANTCHAMBER using the AM1-bcc model and the Leap module in AMBER Tools. Both simulation systems were neutralized with $Mg2^+$ and $Cl^-$ in order to reach 2 mM $Mg2^+$ in solution and solved with TIP3P water molecules in a cubic box, allowing for 12 Å of water around the nucleic acid systems. All simulations were performed in GROMACS 4.5.1 package with the AMBER99 force field. The steepest descent algorithm and conjugate gradient algorithm were implemented for energy minimization of the structures as above, and then each system was equilibrated for 30 ps at 300K by diffusing water around the structures. Simulations were carried out at a constant temperature of 300K and at 1 bar pressure using the Berendsen algorithm and a periodic boundary system. The particle mesh Ewald (PME) method was used to treat long-range interactions. The bond distances and bond angles of the solvent water were constrained via the SETTLE algorithm. Other bond distances were handled via the LINCS algorithm. The resulting trajectories were analyzed with the GROMACS analyze package. The figures were made by Pymol.

## Results

**PreQ$_1$ riboswitch aptamers from *F. nucleatum* and *B. subtilis* induce -1 PRF to different extents**

The characterized preQ$_1$ riboswitch aptamers (9–12) show resemblance to a subset of frameshifting pseudoknot structures (15). Therefore we examined if this kind of ligand-responsive pseudoknot structures can induce -1 PRF using our frameshift reporter system (16). Interestingly, the preQ$_1$ riboswitch aptamer (Fn1) of *F. nucleatum* showed a preQ$_1$ concentration-dependent -1 PRF and reached a significant 20% of frameshifting at 200 µM of preQ$_1$ (Fig. 2b and 2d). Note that a cytidine was inserted into L3 in these constructs to prevent the creation of a premature stop codon. Removal of the 3' part of stem 2 (P2) abolished frameshifting (data not shown), indicating that ligand itself is not responsible for frameshifting but the formation of the pseudoknot is.

With the *B. subtilis* aptamer (Bs1), the induced frameshift efficiency was almost??? 3-fold lower than that of the Fn1 of *F. nucleatum* (Fig. 2a, and 2c), likely as a result of

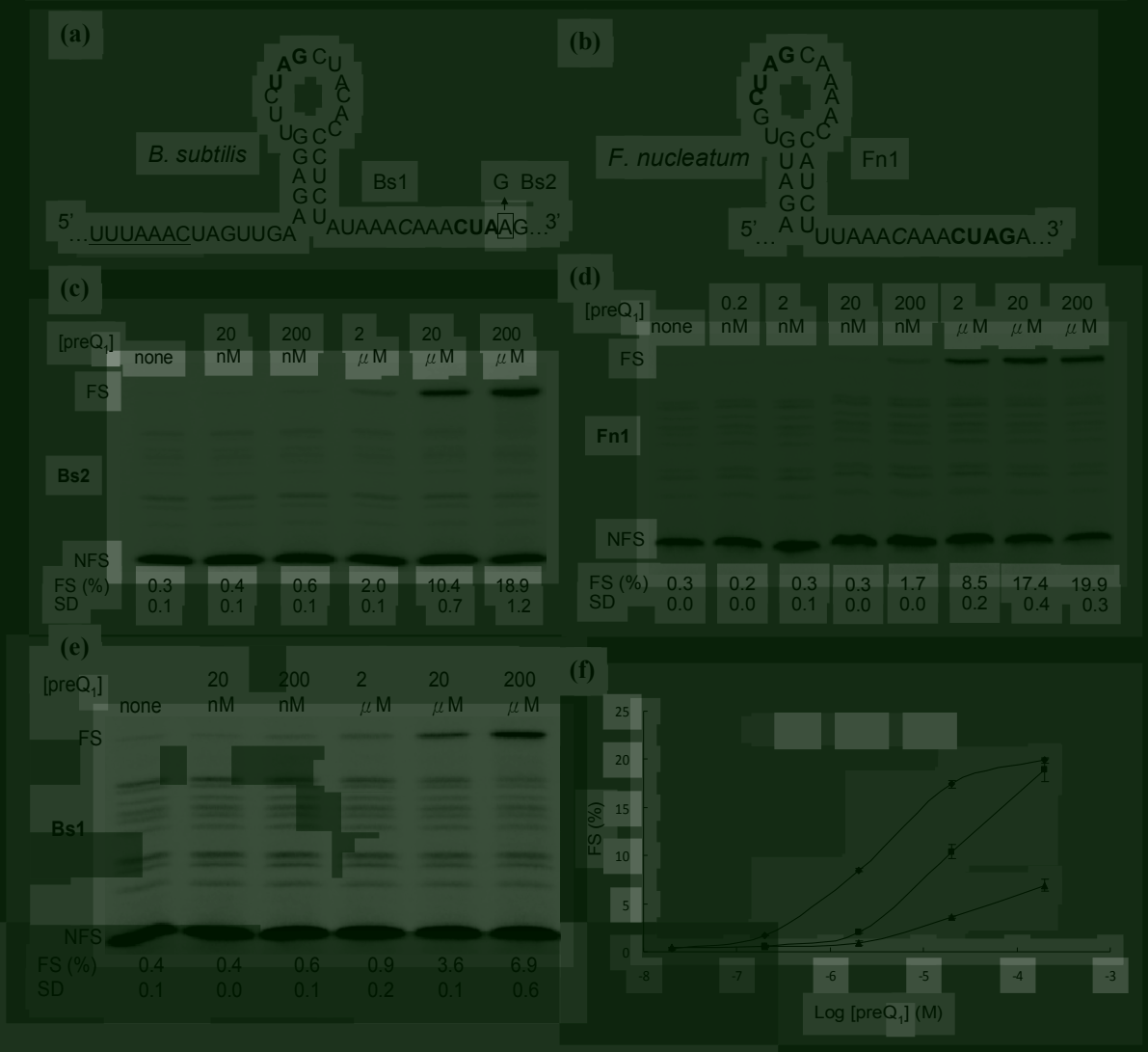


**Figure 2. Minus 1 PRF induced by preQ$_1$ riboswitch aptamers. The relevant sequences of the frameshift reporter constructs contained preQ$_1$ aptamers from *B. subtilis* (a) or *F. nucleatum* (b) are shown. The sequences in bold indicate base pairs formed upon ligand binding. The cytidines in italic are the insertions to prevent pre-mature stop codon in frameshift assays. Slippery sequence is underscored. (c-e) SDS-PAGE analysis of $^{35}$S-methionine labeled translation products of each frameshift construct in RRL in different preQ$_1$ concentrations of each frameshift construct. The appearance of 65-kD FS product indicates the occurrence of -1 ribosomal frameshifting while the NSF indicates zero-frame product without frameshifting. (f) Graph showing the frameshift efficiency (at the y-axis) induced by each preQ$_1$ riboswitch aptamer construct (Diamond, square, and triangle represent Fn1, Bs2, and Bs1, respectively) at various concentrations of preQ$_1$ compound (at the x-axis). The error bars represent the standard deviation of at least two independent assays. See Materials and Methods for details.**

weaker P2 (3 bp vs. v.s 4 bp in *F. nucleatum*). Introduction of a fourth bp in P2 of the *B. subtilis* aptamer (Bs2) to create the same P2 stem as in Fn1, did increase frameshifting to a level similar as of Fn1 at 200μM preQ1 (Fig. 2a and 2e). However,

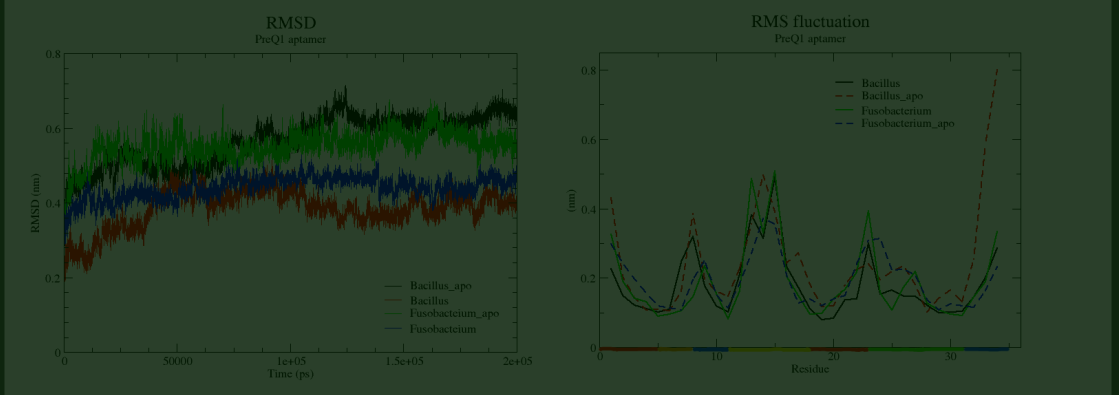


**Figure 3. Root mean square deviation (RMSD) (A) (black and red lines indicate apo and bound *B. subtilis* aptamers, respectively; green and blue lines represent apo and bound *F. nucleatum* aptamers, respectively) and root mean square fluctuations (RMSF) (B) (black and green lines indicate bound aptamers of *B. subtilis* and *F.nucleatum,* respectively; red and blue dash lines represent apo aptamers of *B. subtilis* and *F.nucleatum,* respectively) of the preQ$_1$ aptamer system and the Apo-preQ$_1$ aptamer system during 200 ns of molecular dynamics simulation. Loops and stems of aptamers are colored according to the scheme of Figure 1.**

the Bs2 aptamer responded more slowly than Fn1 to changes in the preQ1 concentrations (Fig. 2f). The results suggest that, although the overall stability of Fn1 and Bs2 aptamers are similar, they are different in their ligand affinity. To investigate the structural details behind the varied ligand sensitivities of these aptamers, we decided to use computer-assisted MD simulations.

**Structure and dynamics comparison of preQ$_1$ aptamers from *B. subtilis* and *F. nucleatum***

Since a high-resolution structure of the *F. nucleatum* preQ$_1$ riboswitch aptamer is not available, we utilized the RNABuilder 2.3 package and the NMR coordinates of the *B. subtilis* preQ1 aptamer solution structure (9, 19) to build a 3D model of the *F. nucleatum* aptamer. Subsequently, a relatively long MD simulation (200 ns) was implemented on the known *B. subtilis* aptamer and the homology structure of the *F. nucleatum* aptamer. Another 200 ns of simulations were carried out on both aptamer structures after removal of preQ$_1$ from the coordinate file. The starting structure and average structure of MD simulations of preQ$_1$-aptamers and apo-preQ$_1$ aptamers from the two species were monitored carefully in order to detect signs of instabilities from coordinates that may result from the modeled structure or simulation parameters.

The root mean square deviations (RMSD) of both aptamers in their ligand-bound or ligand-free state over 200 ns simulation are shown in Figure 3A. The data show that

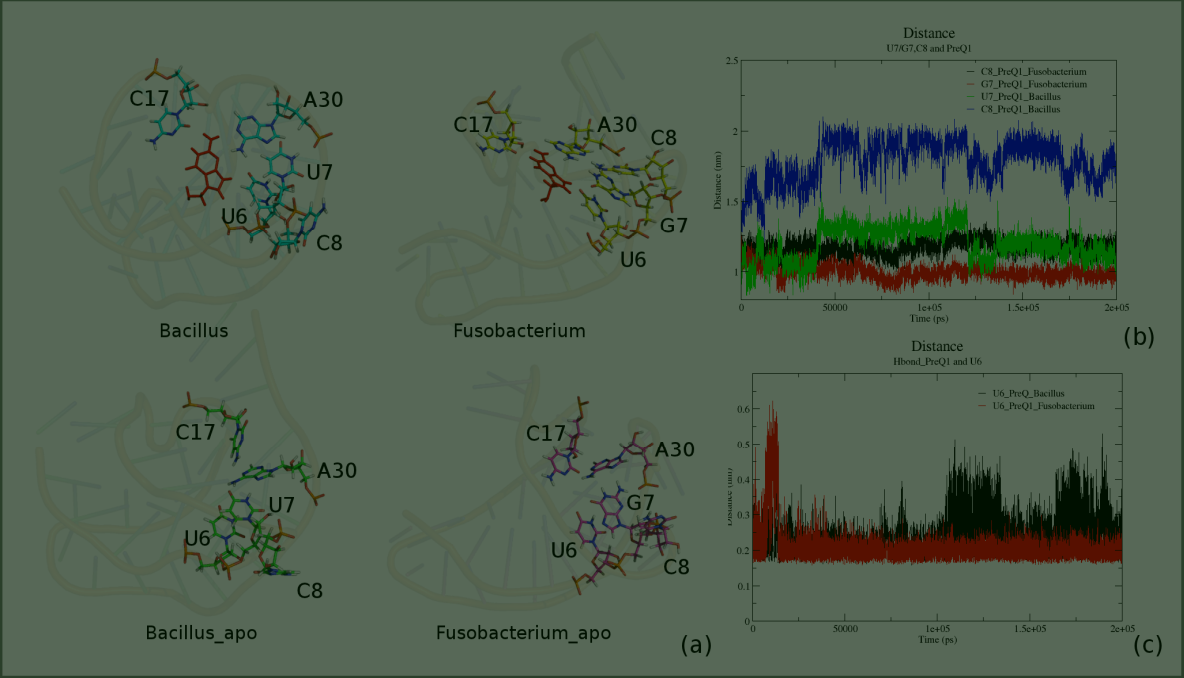


**Figure 4. Comparison of the binding pocket of *B. subtilis* and *F. nucleatum* aptamers in bound and apo forms. (a) The final snapshots of bound nucleotides and preQ$_1$ in the different states. (b) The distances between nucleotides from L1 and preQ$_1$ (green and blue lines indicate U7 and C8 of *B. subtilis* aptamer, respectively; red and black lines represent G7 and C8 of *F. nucleatum* aptamer, respectively). (c) The distances of dynamics hydrogen bonds between U6 and preQ$_1$ from *B. subtilis* (black) and *F. nucleatum* (red) over the simulations.**

ligand-bound aptamers of *B. subtilis* and *F. nucleatum* with averaged RMSDs around 0.4 nm are relatively stable compared to their ligand-free state with averaged RMSDs around 0.6 nm. The resemblance of the *B. subtilis* and *F. nuclaatum* RMSD data further show that the computer built structure of the *F. nucleatum* preQ$_1$ aptamer is reliable.

Root mean square fluctuation (RMSF) analysis of the 200 ns trajectory compared to starting structures was applied to obtain information on the flexibility of each nucleotide (Fig. 3B). Consistent with a previous simulation study (20) both apo and bound aptamers are very flexible. However, in contrast to the previous simulation study, we found that the L2 regions of apo and bound aptamers are highly flexible, which is consistent with crystallization (10) and NMR studies (9).

Figure 3B also shows that stem P2 is very unstable in the apo form of the *B. subtilis* aptamer but was stabilized in the presence of preQ$_1$ whereas both apo and bound forms were stable, during the 200ns simulation, in the case of *F. nucleatum*. This difference could be due to the different P2 stability of each aptamer. Interestingly, a relatively small but significant difference in fluctuation in the L1 region of both aptamers was observed. Since L1 is involved in preQ$_1$ binding, we decided to focus on interactions

between nts in the binding pocket and $preQ_1$.

**Contacts between $preQ_1$ and nucleotides from the binding pocket**

To identify which nucleotides interact with the ligand, we analyzed the final structures obtained after 200 ns of MD simulations of apo-preQ1 and preQ1 aptamers of *B. subtilis* and *F. nucleatum*. From comparisons of the binding pocket nucleotides between bound and unbound state (Figure 4A), we conclude that the pairing pattern in the binding pocket is similar to the one determined by NMR spectroscopy of the *B. subtilis* aptamer (9): preQ1 interacts with C17 via its Watson-Crick edge and with U6 and A30 via its sugar side. However, the nucleotides of the binding pocket of *F. nucleatum* aptamer are significantly different (Fig. 4A).

Under NMR conditions the *B. subtilis* U7 and C8 were observed to undergo fast conformational exchange (9). In simulation, we found C8 is far away from $preQ_1$ (Fig. 4A and 4B, blue line) while the distance between U7 and $preQ_1$ was observed that fluctuate between two values (Fig. 4B, green line), in good agreement with NMR study. However, in *F. nucleatum* aptamer, the distances between G7, C8 and preQ1 stay relatively constant and fluctuate less during the course of the MD simulation (Fig. 4B, G7 in red and C8 in black). As shown in Figure 4A, preQ1-U6:G7 tend to form a triplet interaction in the aptamer of *F. nucleatum* that was not observed in the case of *B. subtilis*. This novel interaction may contribute to the higher ligand binding affinity (Fig. 1C) and relatively high stability of G7 (Fig. 4B, red) of the *F. nucleatum* aptamer.

This idea is supported by inspection of the distance of the H-bond between U6, another nucleotide of L1, and $preQ_1$. The hydrogen bond in *F. nucleatum* aptamer was stabilized after 30 ns of MD simulation with averaged distance between 2-3Å (Fig. 4C). However, in the case of *B. subtilis*, the preQ1-U6 distance undergoes fluctuations from 2-5Å in the course of 200 ns of MD simulations (Fig. 4C, black lines). This result further indicates that the preQ1-U6:G7 triple in the *F. nucleatum* aptamer stabilizes the binding pocket and brings U6 close to $preQ_1$.

***In vitro* evidence for the role of the $7^{th}$ nucleotide in pseudoknot stability**

To support the observation from the MD simulation that the $7^{th}$ nucleotide may be involved in ligand binding and thereby may affect the stability of pseudoknot structure of the aptamer, we constructed two mutants in which the identity of the $7^{th}$ nucleotide in both $preQ_1$ aptamers was swapped (Fig. 5) and analyzed these in the frameshift assay. As shown in Figure 5, when G7 of the *F. nucleatum* aptamer was changed to U as in *B. subtilis*, its frameshift efficiency (Fn2) decreased about 5-fold compared to Fn1 (Fig. 1). However, when U7 of the preQ1 aptamer of *B. subtilis* was

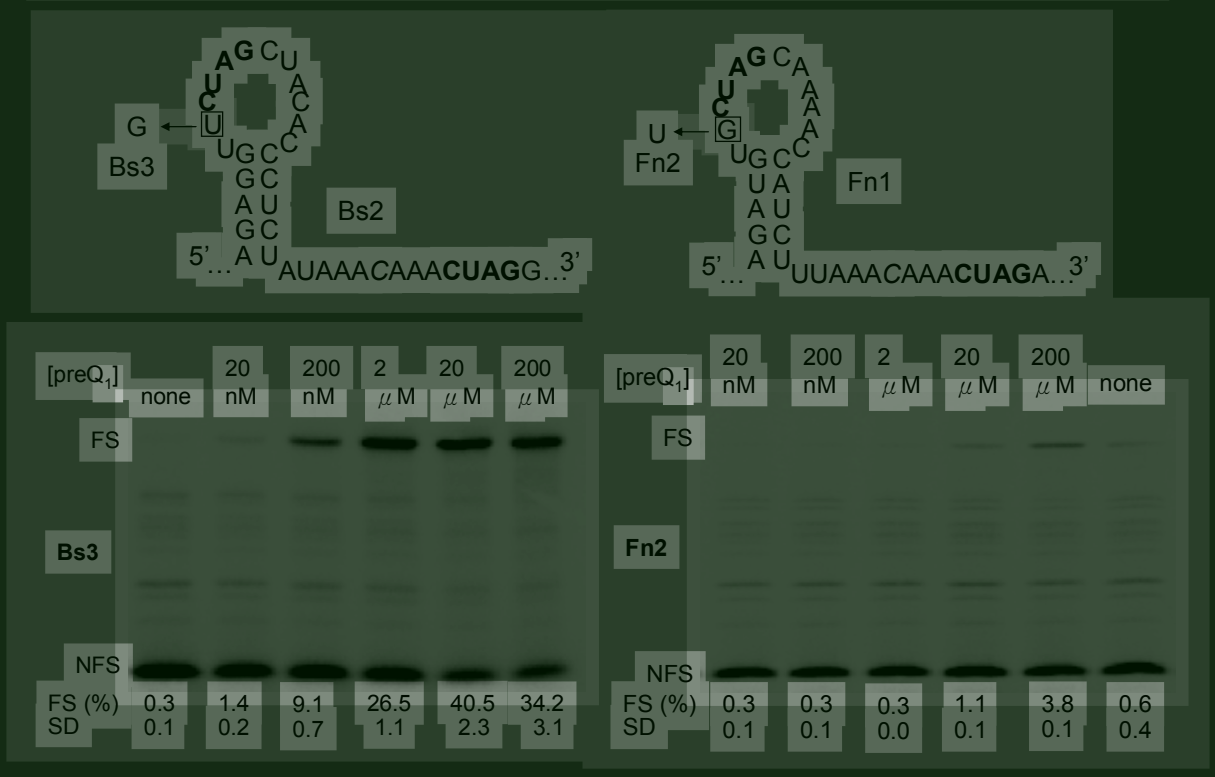


**Figure 5. The 7th nucleotide in preQ$_1$ aptamers plays a role in stabilizing ligand-bound pseudoknot structures. The sequence of two mutants at 7th nucleotide position is shown. The bottom pictures show representative $^{35}$S-methionine labeled SDS-PAGE. The concentration of added preQ$_1$ and frameshifting efficiency are indicated. See legend to Figure 2 for more details.**

mutated to G (Bs3), both the sensitivity and frameshift efficiency were raised about 5-fold with respect to Bs2 (Figure 1). Therefore, our experimental analysis validated the observation from the MD simulation that the 7$^{th}$ nucleotide in preQ1 aptamers of two different species does indeed affect the stability of their ligand-bound pseudoknot structures.

## Discussion

We have shown here that preQ$_1$ riboswitch aptamers from *B. subtilis* and *F. nucleatum* can induce significant -1 PRF upon ligand binding. This is quite striking given: i) the presence of an extra 6-nt loop between stems P1 and P2, and ii) the low number of G-C base pairs and low number of total base pairs that are present in the ligand-stabilized pseudoknot. It has been suggested that the first few bps should be G-C to prevent "breathing" of the first stem and efficiently stall ribosomes (15). Moreover, in known natural frameshifter pseudoknots, only the *Sugarcane yellow leaf virus* (ScYLV) frameshift signal has a similarly low GC content (2 AU bps out of 5

bps) in the first stem (21). Resemblance of the preQ1-aptamer to these small luteovirus frameshifter pseudoknots has been noticed by Micura and co-workers (11). In *ScYLV* and *Beet western yellows virus* (BWYV) (22) pseudoknots, the structure is stabilized by interactions between nucleotides in L1 with stem P2 and L3 and P1 (preQ1 aptamer nomenclature). In the solution (9) and crystal (10) structures of preQ1 aptamers in the ligand-bound state, minor groove triples involving adenines of L3 and base pairs of P1 have been observed. These so-called "A-minor" motifs (23) are critical in stabilizing P1(11) and therefore may help P1 to resist unwinding by ribosomal helicase (24) and thus promote frameshifting as discovered in typical frameshifting pseudoknots (25,26). Major groove triples, on the other hand, are even more crucial for luteovirus (27) and telomerase pseudoknots (28). In $preQ_1$ aptamers, interaction of nucleotides from L1 with the C17:$preQ_1$ base pair may be analogous to the luteovirus C-G:C triple (27).

Despite all analogies to luteovirus pseudoknots the presence of a 6-nt loop between stems P1 and P2 in preQ1 aptamers is rarely seen in a frameshifter pseudoknot (see below) as such a loop would have a large destabilizing effect. Apparently in the ligand-bound form, re-organisation of L2 compensates for the destabilizing effect.

The only known frameshifter pseudoknot with a large L2 is found in the ovine Visna-Maedi lentivirus (29) Here 7nts (5'CGUCCGC3') are located between two stems of 7 bps each. Changes in length and composition of L2 appeared detrimental for frameshifting. Possibly, L2, which is invariable in all related small ruminant lentiviruses (Yu & Olsthoorn, unpublished data), is binding some metabolite as well.

It is interesting that these functionally distinct RNA elements have evolved similar motifs to regulate gene expression in a protein-independent manner (4,30). Besides, it has been suggested that the relatively small size of the $preQ_1$ aptamer is generally less likely to be detected using automated searching methods and may comprise a substantial fraction of yet to be discovered riboswitches (6). Taken together, it may suggest that there is an undiscovered frameshift mechanism exploiting riboswitch-like ligand-induced conformational changes to regulate gene expression.

Recently, another riboswitch aptamer was reported to induce -1 PRF in response to its ligand S-adenosylhomocysteine (SAH) (31). However, this study was hampered by the low frameshift efficiency and the lack of an atomic model to correlate mutations in the aptamer to frameshift data.

In our frameshift reporter constructs, the $preQ_1$ aptamers are flanked by long strands of RNA but are nonetheless fully responsive to ligand addition. This may explain that we need higher concentration of preQ1 [reported Kd ~20nM (6)] to induce frameshifting since alternative structures may form under this situation.

However, these constructs may better resemble the natural situation as compared to small synthetic RNAs used in structural studies and binding assays. Moreover, using frameshifting assays to detect ligand-aptamer interactions, although not quantitative, shows not only ligand-dependent but reasonable sensitivity (between 20 nM to 200 nM) and broad dynamic range (20 nM to 200 μM). Since the preQ1 riboswitch is responsible in regulating genes expression of Q synthesis, which is essential for survival, it is probable that we can utilize frameshift assays to select compounds that can bind to preQ1 aptamer to inhibit the growth of pathogens. Furthermore, using a eukaryotic cell-free translation system to monitor prokaryotic RNA-ligand interaction is an advantage to anti-bacterial drug discovery since we can simultaneously monitor potential adverse effects on eukaryotic translation. Thus, using frameshift assays in analyzing preQ1 aptamers may have great potential in high throughout selection of compounds with anti-bacterial activity.

Through computer-assisted simulation, we can build the unresolved *F. nucleatum* $preQ_1$ aptamer structure by the known coordinate of *B. subtilis* $preQ_1$ aptamer with high accuracy (Fig. 3). In agreement with chemical probing and NMR spectroscopy (11), the simulated aptamer does represent a pseudoknot structure in ligand-bound state. A further comparison between the two aptamers shows that the identity of 7th nucleotide affects ligand binding, and this was subsequently confirmed by the frameshift assay. This novel interaction could not have been found without applying this type of research since the atomic-level structure of F. nucleatum aptamer is not available yet. Therefore, this analysis pipeline shows the promising ability to study the structural details of cognate riboswitch aptamers and provides a relatively fast and economical way for designing aptamers with superior ligand binding affinity.

## Acknowledgements

We thank Prof. Dr. Dirk Iwata-Reuyl (Portland State University, Portland, United States) for providing us with preQ1 and Uppsala University for running simulation times in Uppmax.

## References

1. Wakeman,C.A., Winkler,W.C. and Dann,C.E.,3rd (2007) Structural features of metabolite-sensing riboswitches. *Trends Biochem. Sci.*, **32**, 415-424.

2. Weinberg,Z., Wang,J.X., Bogue,J., Yang,J., Corbino,K., Moy,R.H. and Breaker,R.R. (2010) Comparative genomics reveals 104 candidate structured RNAs from bacteria, archaea, and their metagenomes. *Genome Biol.*, **11**, R31.

3. Thore,S., Leibundgut,M. and Ban,N. (2006) Structure of the eukaryotic thiamine pyrophosphate riboswitch with its regulatory ligand. *Science*, **312**, 1208-1211.

4. Serganov,A. and Patel,D.J. (2007) Ribozymes, riboswitches and beyond: regulation of gene expression without proteins. *Nat. Rev. Genet.*, **8**, 776-790.

5. Bastet,L., Dubé,A., Massé,E. and Lafontaine,D.A. (2011) New insights into riboswitch regulation mechanisms. *Mol. Microbiol.*, **80**, 1148-1154.

6. Roth,A., Winkler,W.C., Regulski,E.E., Lee,B.W.K., Lim,J., Jona,I., Barrick,J.E., Ritwik,A., Kim,J.N., Welz,R., et al. (2007) A riboswitch selective for the queuosine precursor preQ1 contains an unusually small aptamer domain. *Nat. Struct. Mol. Biol.*, **14**, 308-317.

7. Meier,F., Suter,B., Grosjean,H., Keith,G. and Kubli,E. (1985) Queuosine modification of the wobble base in tRNAHis influences “in vivo” decoding properties. *EMBO J.*, **4**, 823-827.

8. Meyer,M.M., Roth,A., Chervin,S.M., Garcia,G.A. and Breaker,R.R. (2008) Confirmation of a second natural preQ1 aptamer class in Streptococcaceae bacteria. *RNA*, **14**, 685-695.

9. Kang,M., Peterson,R. and Feigon,J. (2009) Structural Insights into riboswitch control of the biosynthesis of queuosine, a modified nucleotide found in the anticodon of tRNA. *Mol. Cell*, **33**, 784-790.

10. Klein,D.J., Edwards,T.E. and Ferré-D’Amaré,A.R. (2009) Cocrystal structure of a class I preQ1 riboswitch reveals a pseudoknot recognizing an essential hypermodified nucleobase. *Nat. Struct. Mol. Biol.*, **16**, 343-344.

11. Rieder,U., Lang,K., Kreutz,C., Polacek, N., and Micura, R. (2009) Evidece for pseudoknot formation of class I preQ1 riboswitch aptamers. *Chembiochem*, **4**,

1141-1144.

12. Spitale,R.C., Torelli,A.T., Krucinska,J., Bandarian,V. and Wedekind,J.E. (2009) The structural basis for recognition of the PreQ0 metabolite by an unusually small riboswitch aptamer domain. *J. Biol. Chem.*, **284**, 11012-11016.

13. Farabaugh,P.J. (1996) Programmed translational frameshifting. *Microbiol. Rev.*, **60**, 103-134.

14. Chen,G., Chang,K.-Y., Chou,M.-Y., Bustamante,C. and Tinoco,I.,Jr (2009) Triplex structures in an RNA pseudoknot enhance mechanical stability and increase efficiency of -1 ribosomal frameshifting. *Proc. Natl. Acad. Sci. U.S.A.*, **106**, 12706-12711.

15. Giedroc,D.P., Theimer,C.A. and Nixon,P.L. (2000) Structure, stability and function of RNA pseudoknots involved in stimulating ribosomal frameshifting1. *J. Mol. Biol.*, **298**, 167-185.

16. Olsthoorn,R.C.L., Laurs,M., Sohet,F., Hilbers,C.W., Heus,H.A. and Pleij,C.W.A. (2004) Novel application of sRNA: stimulation of ribosomal frameshifting. *RNA*, **10**, 1702-1703.

17. Yu,C.-H., Noteborn,M.H., Pleij,C.W.A. and Olsthoorn,R.C.L. (2011) Stem-loop structures can effectively substitute for an RNA pseudoknot in -1 ribosomal frameshifting. *Nucleic Acids Res.*, **39**, 8952-8959.

18. Flores,S.C., Wan,Y., Russell,R. and Altman,R.B. (2010) Predicting RNA structure by multiple template homology modeling. *Pac. Symp. Biocompu.t*, 216-227.

19. Zhang,Q., Kang,M., Peterson,R.D. and Feigon,J. (2011) Comparison of solution and crystal structures of preQ1 riboswitch reveals calcium-induced changes in conformation and dynamics. *J. Am. Chem. Soc.*, **133**, 5190-5193.

20. Petrone,P.M., Dewhurst,J., Tommasi,R., Whitehead, L., and Pomerantz, A.K. (2011) Atomic-scale characterization of conformational changes in the preQ1 riboswitch aptamer upon ligand binding. *J. Mol. Graph. Model*, **30**, 179-185.

21. Cornish,P.V., Hennig,M., and Giedroc, D.P. (2005) A loop 2 cytidine-stem 1 minor groove interaction as a positive determinant for pseudoknot-stimulated -1 ribosomal frameshifting. *Proc. Natl. Acad. Sci. U. S. A.*, 102, 12694-12699.

22. Pallan,P.S., Marshall,W.S., Harp,J., Jewett,F.C.3rd, Wawrzak,Z., Brown, B.A.2nd, Rich,A., and Egli,M. (2005) Crystal structure of a luteoviral RNA pseudoknot and

model for a minimal ribosomal frameshifting motif. *Biochemistry*, **44**, 11315-11322.

23. Nissen,P., Ippolito,J.A, Ban,N., Moore,P.B., and Steitz, T.A. (2001) RNA tertiary interactions in the large ribosomal subunit: the A-minor motif. *Proc. Natl. Acad. Sci. U. S. A.*, **98**, 4899-4903.

24. Takyar,S., Hickerson,R.P., and Noller, H.F. (2005) mRNA helicase activity of the ribosome. *Cell*, **120**, 49-58.

25. Su,L., Chen,L., Egli,M., Berger,J.M., and Rich,A. (1999) Minor groove RNA triplex in the crystal structure of a ribosomal frameshifting viral pseudoknot. *Nat. Struct. Biol.*, **6**, 285-292.

26. Olsthoorn,R.C., Reumerman,R., Hilbers,C.W., Pleij,C.W., and Heus,H.A. (2010) Functional analysis of the SRV-1 RNA frameshifting pseudoknot. *Nucleic Acids Res.*, **38**, 7665-7672.

27. Giedroc,D.P., and Cornish,P.V. (2009) Frameshifting RNA pseudoknots: structure and mechanism.*Virus Res.*, **139**, 193-208.

28. Theimer,C.A., Blois,C.A., and Feigon,J. (2005) Structure of the human telomerase RNA pseudoknot reveals conserved tertiary interactions essential for function. *Mol. Cell*, **17**, 671-682.

29. Pennell,S., Manktelow,E., Flatt,A., Kelly,G., Smerdon,S.J., and Brierley, I. (2008) The stimulatory RNA of the Visna-Maedi retrovirus ribosomal frameshifting signal is an unusual pseudoknot with an interstem element. *RNA*, **14**, 1366-1377.

30. ten Dam,E., Brierley,I., Inglis,S., and Pleij,C. (1994) Identification and analysis of the pseudoknot-containing gag-pro ribosomal frameshift signal of simian retrovirus-1. *Nucleic Acids Res.*, **22**, 2304-2310.

31 Chou,M.-Y., Lin,S.-C. and Chang,K.-Y. (2010) Stimulation of -1 programmed ribosomal frameshifting by a metabolite-responsive RNA pseudoknot. *RNA*, **16**, 1236-1244.

# Chapter Ⅶ

## General discussion

## 1. Frameshifting pseudoknot-derived hairpins are still efficient frameshifters

It has long been believed that simple stem-loops are not efficient in inducing -1 PRF. This assumption was mainly based on experiments with the hairpin derivatives of the wild-type (wt) and minimal IBV frameshifting pseudoknot which were almost inactive (1) and 5-10 fold less efficient (2), respectively, in frameshifting compared to their respective pseudoknots (in these derivatives the stem of the hairpin has the same composition as the stems of the pseudoknot). In the latter case, although a specific value was never shown, it can be inferred from published data that the absolute frame shifting efficiency is 4-8% (2). However, several frameshifting hairpins either in the genome of prokaryotes or eukaryotic RNA viruses have been discovered to date. Combined with the notion that no cellular factors are known to bind to frameshift structures (3), it is logical to assume that simple hairpins are merely serving as physical barriers to stall translating ribosomes over the slippery sequence and thereby enhance opportunity of a reading frameshift. To support this assumption, we first made hairpin mutants based on IBV frameshifting pseudoknots (Fig. 1) to test their frameshifting ability in our assay system [Note that the spacer between slippery sequence and the hairpins is 7 nt in our system but 6 nt in the published one (1)]. Strikingly, the wt IBV derived-hairpin (two A-U bps were swapped to prevent the creation of a premature stop codon) induced 8.2% of frameshifting rather than the previously reported inactive in frameshifting. A variant with a C • C instead of G • A mismatch yielded 14.1% of frameshifting. Interestingly, with the minimal IBV-derived hairpin (which has a G-U wobble basepair instead of the wt G • A mismatch) a very significant 25.7% of frameshifting was obtained. Stabilizing the stem further increased its frameshifting capacity to ~ 30%.

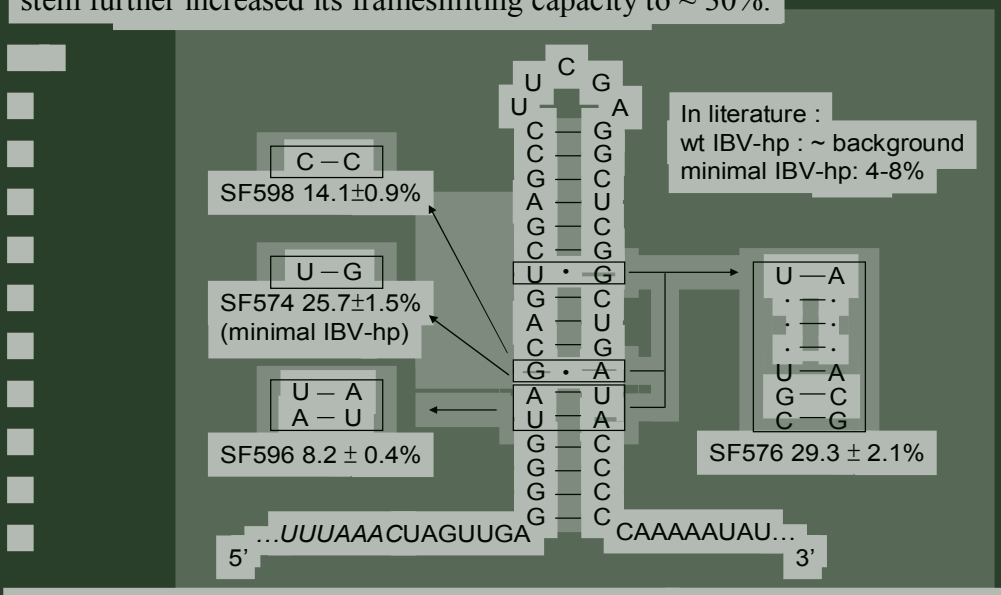


**Figure 1. Mutations in the IBV frameshifting pseudoknot-derived hairpins and their effects on -1 frameshifting efficiency.**

In accordance with above findings we have demonstrated in chapter 3 that the SRV-1 frameshifting pseudoknot-derived hairpin can also stimulate efficient frameshifting and is merely 1.5-fold less than active than its pseudoknotted counterpart. Our results seem to be in conflict with previous findings mentioned above, but may be explained by different applied experimental settings such as length of spacer, source of the reticulocyte lysate, capped or non-capped mRNAs, etc. The fact that we see the same trend in vivo using HeLa cells validates our *in vitro* conditions.

So, why does nature favor pseudoknots over hairpins to stimulate -1 PRF? Several possibilities can be envisaged to answer this important issue. One is that the stability of pseudoknots may be easier to fine tune to stimulate a broader range of frameshifting to meet different functional demands: (i) our reporter assays *in vivo* showed the highest frameshifting efficiency induced by SRV-1 pseudoknot was 1.5-fold higher than the maximum capacity of its derived hairpins (chapter 3), implying broader range of pseudoknot structures to stimulate -1 PRF; (ii) pseudoknot structures have possibilities to get "bonus" stability from stem-loop interactions namely triple interactions without sacrificing the functional peptide sequences while simple hairpin structures can only increase their GC content to increase stability i.e. limiting diversity of peptide sequences. But we have to note that nature seems not to pursue the highest frameshifting all the time. For example, maintaining a level of 5-10% of frameshifting is critical to the life cycle and infectivity of HIV-1 (4).

The relatively fast folding of hairpin structures compared to pseudoknot structures may be another factor for organisms to choose their frameshifting signals. Since the folding rate of a hairpin that is in a millisecond level is much faster than a pseudoknot that may take seconds to refold, we can reasonably assume that the structure of the encountered frameshifting signal will be different for the first and the following translating ribosomes depending on whether the frameshifting signal is a hairpin or a pseudoknot. In specific, the hairpin structure may stay the same while the pseudoknot may not have enough time to refold to its productive conformation after being melted by the first "shifted" ribosome, assuming that decoding is faster than refolding. Besides, the rate of decoding a designated gene may be regulated by the context of the translation initiation region, the relative aboundance of tRNAs to decode its gene, up or down regulation by RNA binding proteins or the embedded RNA structures; these cis or trans-acting signals may have evolved regarding the functional aspects of the gene (5, 6). A lot of information has to be unearthed to get a clear picture. Nevertheless, the first step will be testing the assumption that a fast-refolding hairpin can lead to a higher frameshifting efficiency than a slow-refolding pseudoknot when increasing the ribosome loading rate. In distinct to a previous report using antibiotics

to globally affect translation initiation of ribosomes (5), we attempt to use the well-defined system that fine tuning translation initiation through modulation of the stability of hairpin structure in the initiation region of MS2 coat-protein gene (7). By modulation of the initiation rate, the "distance" between translating ribosomes can be adjusted. Therefore, we may have chance to monitor the effect of structural folding in related to frameshifting efficiency.

## 2. The novel application of antisense oligonucleotides (AONs)- as a roadblock to stimulate -1 PRF

AONs have already been widely used in gene regulation, such as induction of RNaseH activity to degrade target RNA, loading onto RNA-induced silencing complexes (RISCs) to post-transcriptionally regulate gene expression (8), blocking splice sites to redirect splicing (9), or blocking translation initiation by hybridizing to 5'-UTR (10). Recently, AONs have been shown to induce efficient -1 PRF or +1 PRF expanding their application potential in antisense technology (11–13). Backed-up by our data on the artificial frameshifting hairpins we suggest that a physical barrier to stall ribosomes to initiate frameshifting should be one of the, if not the sole, mechanisms of -1 PRF.

Although antisense RNA itself is efficient in inducing -1 PRF, its relatively unstable nature limits its application *in vivo*. Several kinds of modification either in the 2' hydroxyl or in the internucleotide linkage aimed at protecting from nuclease-mediated degradation have been created. For example, phosphorothioated RNA can resist RNase, however off-target effects make it a less ideal candidate for AON applications (14). Morpholinos and peptide nucleic acids (PNA) can duplex to RNA with increased thermodynamic stability and are also resistant to nuclease degradation but the neutral property of these molecules is a hindrance for cellular uptake (14). On the other hand, locked nucleic acid (LNA), where linkage of the 2' oxygen and 4' carbon atoms "locks" the ribose in the 3' endo conformation, may be a promising candidate for further application because of its RNA-mimicking conformation and superior stability (15).

We have demonstrated that LNA-modified AONs can induce efficient -1 PRF (chapter 4), indicating that the ribosomal helicase cannot distinguish between RNA-RNA and RNA-LNA duplexes. This observation is in agreement with a previous publication using AONs to investigate the ribosomal helicase activity showing that that ribosomes can unwind duplexes independent of the 2'OH (16). An advantage of LNA modification is that we can change the duplex stability without changing the sequence; in this way we could further show that the stability of the proximal end of the duplex, i.e. the end facing the ribosome, is important for

frameshifting (chapter 4). It is noteworthy that recently it was shown that LNA modified AONs, at concentrations in the low micromolar range, can enter cultured cells without any additive to serum or tansfection reagent by a process termed gymnosis. In light of our data of LNA-induced -1 PRF, it may provide a way to treat frameshift-related diseases by LNA modified AONs.

Since AONs can mimic the stem region of hairpin structures, it is reasonable to assume the pseudoknot-mimicking structures can also be constructed by AONs. Based on the knowledge of solution structure (17) and extensive genetic analysis of SRV-1 frameshifting pseudoknot (18), we have designed AONs that simulate a pseudoknot to induce efficient -1 PRF (chapter 5). These "pseudo" pseudoknot structures can freely rotate along the mRNA like linear AONs can, suggesting that the torsional restraint of the second stem, S2, is dispensable in our experimental setup (19). Therefore, we can deduce that the stability of the structured AONs to stall translating ribosomes is contributed by the loop-stem interactions and/or stacking of the two stems. The stacking of the two stems did play a role in stabilizing the overall structure since replacing the RNA S2 duplex by a DNA duplex, while keeping all other nucleotides in the RNA form, resulted in a more than 2-fold decrease in frameshifting efficiency (data not shown).

However, we have found the highest level that was reached by linear AONs of 12-18 nts is only 13% frameshifting (chapter 4), indicating that the loop-stem interactions must contribute to the profound 25% frameshifting efficiency induced by the structured AON R31 (chapter 5). The loop-stem interactions in "real" frameshifting pseudoknots can be characterized by L2 lying in the shallow groove of S1 or L1 aligning in the deep groove of S2. In our structured AONs, the S1-L2 can be the other source of stability to induce -1 PRF. The possibility of an interaction between the mRNA and S2 of the AON cannot be ruled out but was not tested. It is worthwhile to investigate if unexpected interactions are involved in stabilizing AON-mRNA since there is a poly adenosine tract in close proximity to S2 of AON (Chapter 5, fig. 2). Nevertheless, the *in trans* pseudoknot-mimicking AONs may be beneficial to investigate the hard-to-predict S1-L2 interactions pseudoknots as well as improving pseudoknot structure prediction algorithms.

Apart from modification of nucleotide or internucleotide linker, expressing the AONs within a tRNA scaffold could be an alternative way to protect these AONs *in vivo* to do their job (20). A recent publication has demonstrated that expressing a hairpin with a 6 nt bulge, embedded within a $tRNA^{lys}$ scaffold, which can bind to the loop region of a stem-loop structure in mRNA can induce -1 PRF in *E. coli* (21). We have repeated this experiment with similar results; however, we could not induce frameshifting with our own constructs using the same $tRNA^{lys}$-scaffold (data not

shown in this thesis).

A lot of efforts were made by us to test if AONs can induce -1 PRF in cultured cells. The types of AONs that were tested include RNA, 2'O-methylated RNA, PNA, and LNA-DNA hybrids. Either co-transfections with reporter plasmid or transcribed mRNA with AON failed to show significant -1 PRF (about 2-fold above background). By using inverted and confocal fluorescent microscopy to trace a fluorescein isothiocyanate (FITC)-labeled 2'O-methylated AON we could observe that most AONs stayed in the nucleus instead of the cytoplasm. To induce frameshifting AONs should stay in the right compartment. Therefore, the reason why we could not induce efficient -1 PRF by AONs in cultured cells in contrast to our *in vitro* experiments may be due to unproductive compartmentalization of AONs. In considering the proposed mechanism of cation lipid transfection, the nucleic acid-cation lipid complexes are internalized through endocytosis followed by their release from endosomal vesicles possibly through swelling and rupture of endosomes. After being released from endosomes, the complexes should be kept intact in order to cross the nuclear membrane with negative charge. The hypothesis that follows this mechanism is that the pH of cytoplasm should be acidic to keep cation lipid vectors fully or partially protonated, and the AON-cation lipid complexes can be internalized rapidly into the nucleus due to the small size of AONs. It could be the reason why AONs accumulated in the nucleus as reported in literature and observed in our experiments. To overcome this problem, we either have to slow down the efficiency of nuclear-entry probably by lowering temperature to increase the time-scale of cytoplamic AONs since it has been suggested that the cation lipid transfection is thermal dependent (22), or we have to use non-charged AONs through other ways of delivery. Furthermore, it may be interesting to follow the migration of synthetic siRNA or microRNA during transfection since both of them are functional in the cytoplasmic compartment.

## 3. Ligand-induced pseudoknot conformation of preQ$_1$ aptamer can stimulate efficient -1 PRF

It has been suggested by Pleij and colleagues that there is no trans-acting factor involved in regulating -1 PRF since adding increasing amounts of a frameshifting pseudoknot did not affect -1 PRF efficiency (3). Recently, however, either endogenous proteins or screened small chemicals were reported to interact with frameshifting signals to affect frameshifting efficiency (23–25). These results expand the complexity of PRF and imply undiscovered roles of cellular factors, such as proteins or metabolites in PRF.

A recently defined preQ$_1$ riboswitch is found to change its conformation upon ligand binding thereby regulating its expression platform through transcriptional

termination or hindering access to the Shine-Dalgano sequence (26, 27). Interestingly, the resolved structure of the ligand-bound aptamer (28) is similar to a frameshifting pseudoknot and indeed we could demonstrate that the 34-nts aptamers from two different bacterial species can both induce -1 PRF in a ligand concentration-dependent manner (chapter 6). Using computer-assisted methods we first reconstructed the unresolved $preQ_1$ aptamer from *Fusobacterium nucleatum* based on the known *Bacillus subtilis* preQ1 aptamer coordinates (28) followed by monitoring the unfolding process using molecular dynamics (MD) simulations. A hitherto undiscovered interaction by a nucleotide in the L1 region which affect ligand-binding was proposed and proven by frameshifting assays. Further studies using simulation and energy landscape calculation to investigate the interaction between ligand and nucleotides in the binding pocket may help to solve the question of how these aptamers attain high specificity in ligand selection.

From frameshifting point of view, this kind of ligand-induced -1 PRF may offer information about how to describe the stability of frameshifting structures since the free energy of the RNA structure is not correlated with frameshifting efficiency. By probing the enthalpy changes of unbound (unproductive in frameshifting) and bound (productive in frameshifting) with various levels of frameshifting constructs may delineate the energy requirements profile for ribosomes to unfold frameshifting structures under physiological condition. In combination with data of the requiring work (mechanical force) to pull mRNAs detected by optical tweezers (29) may provide better parameters to describe the stability of a given frameshifting signal.

Another advantage of this riboswitch-to-frameshifting is the potential to select antimicrobial chemicals. PreQ1 is an essential compound for bacteria and shutting off its synthesis e.g. premature transcription termination by activating the riboswitch is probably lethal. A candidate that efficiently and specifically fits into the binding pocket of $preQ_1$ aptamers should therefore also be able to induce -1 PRF. Furthermore, since we use rabbit reticulocyte lysates, an eukaryotic translation system, for our frameshifting assays, we can concurrently monitor if there is any inhibitory effect for translational machinery. Therefore, a biological relevant high throughput system can be applied to select promising candidates.

## 4. Conclusions

In this thesis, we have shown that hairpin structures can act as efficient frameshifting signals thereby challenging the general concept that hairpin structures cannot replace pseudoknots in frameshifting. Furthermore, we have demonstrated that not only nucleotide modifications at critical positions but also structures that mimic pseudoknots can improve AONs-induced -1 PRF efficiency. A novel ligand-induced

pseudoknot based on the preQ1 riboswitch was shown to stimulate -1 PRF in a ligand-concentration dependent manner by stabilizing the pseudoknot structure. Altogether, these presented data may not only help to interpret fundamental questions of PRF but also provide possibilities in treating disease by means of PRF.

## References


1. Brierley,I., Rolley,N.J., Jenner,A.J. and Inglis,S.C. (1991) Mutational analysis of the RNA pseudoknot component of a coronavirus ribosomal frameshifting signal. *J. Mol. Biol.*, **220**, 889-902.

2. Somogyi,P., Jenner,A.J., Brierley,I. and Inglis,S.C. (1993) Ribosomal pausing during translation of an RNA pseudoknot. *Mol. Cell. Biol.*, **13**, 6931-6940.

3. ten Dam,E., Brierley,I., Inglis,S. and Pleij,C. (1994) Identification and analysis of the pseudoknot-containing gag-pro ribosomal frameshift signal of simian retrovirus-1. *Nucleic Acids Res.*, **22**, 2304-2310.

4. Shehu-Xhilaga,M., Crowe,S.M. and Mak,J. (2001) Maintenance of the Gag/Gag-Pol ratio is important for human immunodeficiency virus type 1 RNA dimerization and viral infectivity. *J. Virol.*, **75**, 1834-1841.

5. Lopinski,J.D., Dinman,J.D. and Bruenn,J.A. (2000) Kinetics of ribosomal pausing during programmed -1 translational frameshifting. *Mol. Cell Biol.*, **20**, 1095-1103.

6. Gendron,K., Charbonneau,J., Dulude,D., Heveker,N., Ferbeyre,G. and Brakier-Gingras,L. (2008) The presence of the TAR RNA structure alters the programmed -1 ribosomal frameshift efficiency of the human immunodeficiency virus type 1 (HIV-1) by modifying the rate of translation initiation. *Nucleic Acids Res.*, **36**, 30-40.

7. de Smit,M.H. and van Duin,J. (1990) Secondary structure of the ribosome binding site determines translational efficiency: a quantitative analysis. *Proc. Natl. Acad. Sci. U.S.A.*, **87**, 7668-7672.

8. Nesterova,M. and Cho-Chung,Y.S. (2004) Killing the messenger: antisense DNA and siRNA. *Curr. Drug Targets*, **5**, 683-689.

9. Aartsma-Rus,A. (2010) Antisense-mediated modulation of splicing: therapeutic implications for Duchenne muscular dystrophy. *RNA Biol.*, **7**, 453-461.

10. Nasevicius,A. and Ekker,S.C. (2000) Effective targeted gene /`knockdown/' in zebrafish. *Nat. Genet.*, **26**, 216-220.

11. Olsthoorn,R.C.L., Laurs,M., Sohet,F., Hilbers,C.W., Heus,H.A. and Pleij,C.W.A. (2004) Novel application of sRNA: stimulation of ribosomal frameshifting. *RNA*, **10**, 1702-1703.

12. Howard,M.T., Gesteland,R.F. and Atkins,J.F. (2004) Efficient stimulation of site-specific ribosome frameshifting by antisense oligonucleotides. *RNA*, **10**, 1653-1661.

13. Henderson,C.M., Anderson,C.B. and Howard,M.T. (2006) Antisense-induced ribosomal frameshifting. *Nucleic Acids Res.*, **34**, 4302-4310.

14. Dias,N. and Stein,C.A. (2002) Antisense Oligonucleotides: Basic Concepts and Mechanisms. *Mol. Cancer Ther.*, **1**, 347 -355.

15. Petersen,M. and Wengel,J. (2003) LNA: a versatile tool for therapeutics and genomics. *Trends Biotechnol.*, **21**, 74-81.

16. Takyar,S., Hickerson,R.P. and Noller,H.F. (2005) mRNA helicase activity of the ribosome. *Cell*, **120**, 49-58.

17. Michiels,P.J., Versleijen,A.A., Verlaan,P.W., Pleij,C.W., Hilbers,C.W. and Heus,H.A. (2001) Solution structure of the pseudoknot of SRV-1 RNA, involved in ribosomal frameshifting. *J. Mol. Biol.*, **310**, 1109-1123.

18. Olsthoorn,R.C.L., Reumerman,R., Hilbers,C.W., Pleij,C.W.A. and Heus,H.A. (2010) Functional analysis of the SRV-1 RNA frameshifting pseudoknot. *Nucleic Acids Res.*, **38**, 7665-7672.

19. Plant,E.P. and Dinman,J.D. (2005) Torsional restraint: a new twist on frameshifting pseudoknots. *Nucleic Acids Res.*, **33**, 1825 -1833.

20. Ponchon,L. and Dardel,F. (2007) Recombinant RNA technology: the tRNA scaffold. *Nat. Methods*, **4**, 571-576.

21. Mazauric,M.-H., Licznar,P., Prère,M.-F., Canal,I. and Fayet,O. (2008) Apical loop-internal loop RNA pseudoknots: a new type of stimulator of -1 translational frameshifting in bacteria. *J. Biol. Chem.*, **283**, 20421-20432.

22. Ishii,T., Okahata,Y. and Sato,T. (2001) Mechanism of cell transfection with

plasmid/chitosan complexes. *Biochim. Biophys. Acta*, **1514**, 51-64.

23. Marcheschi,R.J., Tonelli,M., Kumar,A. and Butcher,S.E. (2011) Structure of the HIV-1 Frameshift Site RNA Bound to a Small Molecule Inhibitor of Viral Replication. *ACS Chem. Biol.*, **6**, 857-864.

24. Kobayashi,Y., Zhuang,J., Peltz,S. and Dougherty,J. (2010) Identification of a cellular factor that modulates HIV-1 programmed ribosomal frameshifting. *J. Biol. Chem.*, **285**, 19776-19784.

25. Kwak,H., Park,M.W. and Jeong,S. (2011) Annexin A2 binds RNA and reduces the frameshifting efficiency of infectious bronchitis virus. *PLoS ONE*, **6**, e24067.

26. Roth,A., Winkler,W.C., Regulski,E.E., Lee,B.W.K., Lim,J., Jona,I., Barrick,J.E., Ritwik,A., Kim,J.N., Welz,R., et al. (2007) A riboswitch selective for the queuosine precursor preQ1 contains an unusually small aptamer domain. *Nat. Struct. Mol. Biol.*, **14**, 308-317.

27. Jenkins,J.L., Krucinska,J., McCarty,R.M., Bandarian,V. and Wedekind,J.E. (2011) Comparison of a preQ1 riboswitch aptamer in metabolite-bound and free states with implications for gene regulation. *J. Biol. Chem.*, **286**, 24626-24637.

28. Kang,M., Peterson,R. and Feigon,J. (2009) Structural Insights into riboswitch control of the biosynthesis of queuosine, a modified nucleotide found in the anticodon of tRNA. *Mol. Cell*, **33**, 784-790.

29. Green,L., Kim,C.-H., Bustamante,C. and Tinoco,I.,Jr (2008) Characterization of the mechanical unfolding of RNA pseudoknots. *J. Mol. Biol.*, **375**, 511-528.

## Samenvatting

Boodschapper RNA (mRNA), het medium dat de overdracht van erfelijke informatie van DNA naar eiwit verzorgt, wordt gedecodeerd in tripletten door ribosomen. Tijdens dit proces (translatie) is het van cruciaal belang dat het juiste leesraam gehandhaafd blijft. In sommige gevallen kunnen ribosomen gedwongen worden om hun vertaalwerk in een ander leesraam voort te zetten (ribosomal frameshifting of RF) doordat ze een stap terug of vooruit geduwd worden (–1 of +1RF) door signalen die in het mRNA verborgen liggen. In dit proefschrift is gekeken naar signalen die verantwoordelijk zijn voor –1 RF.

RF is vrij zeldzaam tijdens de translatie van cellulaire mRNAs maar gebeurt regelmatig tijdens vertaling van virus mRNAs, zoals die van het SARS coronavirus of van HIV-1. Deze virus mRNAs bevatten een tweetal signalen die nodig zijn om een op de tien of zelfs tot een op de twee ribosomen naar het –1 leesraam te dirigeren. Het eerste signaal is een zogenaamde "slippery sequence" waar het ribosoom zijn uitglijer maakt, het tweede is een bepaalde structuur in het RNA die zich hier 5 tot 8 nucleotiden stroomafwaarts van bevindt. De "slippery sequence" heeft de samenstelling X.XXY.YYZ waarin X= G, A of U is en Y=A of U en Z iedere nucleotide zolang Y≠Z en de punten het oorspronkelijke leesraam aanduiden. Bijzonder efficiënte combinaties zijn bijv. UUUUUUA en AAAAAAG of UUUAAAC waarop de bijbehorende tRNAs na de shift nog steeds 3 van de 3 of 2 van de drie base paren met het codon in het –1 leesraam kunnen maken. Hoewel deze combinaties van nature al enige frameshifting opleveren ~1% kan de stroomafwaarts gelegen structuur deze frequentie tot wel 50 keer verhogen.

Wat is er nu zo speciaal aan die structuren? In de meeste gevallen vormt deze structuur een pseudoknoop of in enkele gevallen een reguliere haarspeld. In een pseudoknoop vormt de lus van de haarspeld ook weer een haarspeld. Deze dubbele haarspeld vouwt zich op tot een soort krakeling en vormt een uitzonderlijk lastige barrière doordat een pseudoknoop moeilijk te ontwarren is voor ribosomen. Met als gevolg dat tijdens de translocatiestap het translatieproces zodanig geblokkeerd wordt dat het tRNA op de P-site wordt verbogen en uiteindelijk onder de mechanische stress terugschuift in het –1 leesraam. Het ribosoom kan nu wel de translocatiestap uitvoeren en ondervindt nu geen last meer van de pseudoknoop. Markant gegeven is dat tijdens dit soort proeven een haarspeld met dezelfde samenstelling als de pseudoknoop van IBV niet in staat bleek om tRNA te verbuigen. Hoewel dat in overeenstemming bleek te zijn met functionele assays gedaan door datzelfde laboratorium leek dat niet te staven met het feit dat voor sommige virussen zoals HIV-1 een haarspeld voldoende is om RF te stimuleren. Lange tijd werd gedacht dat

artificiële haarspelden niet in staat waren om RF te stimuleren en werden ook verwoede pogingen gedaan om de HIV-1 haarspeld toch tot een pseudoknoop te kneden, ons inziens tevergeefs. In 2004 werd namelijk onafhankelijk van elkaar door ons en een ander lab aangetoond dat een antisense RNA oligonucleotide gebonden op 5-8 nucleotiden vanaf de "slippery site" in staat was om RF te stimuleren. Niks geen pseudoknoop nodig. Het was dan ook te voorspellen dat een artificiële haarspeld ook zou werken. In **hoofdstuk 3** van dit proefschrift laten we zien dat haarspeldvarianten van de SRV-1 gag-pro frameshifter pseudoknoop inderdaad goede stimulators van RF zijn en slechts 1.5 keer slechter dan de SRV-1 pseudoknoop. Deze proeven werden zowel *in vitro* met rabbit reticulocyte lysate (RRL) als in HeLa cellen uitgevoerd met gelijkwaardige resultaten, en tonen aan dat de haarspeld een bona fide frameshift stimulator is.

Als een haarspeld slechts 1.5 keer slechter is dan een pseudoknoop waarom vinden we in de natuur dan zo vaak pseudoknopen als frameshift stimulators en nauwelijks haarspelden? En wat is de reden dat pseudoknopen 1.5 keer beter zijn dan haarspelden in frameshifting? Het antwoord op deze laatste vraag komt uit eerdere experimenten die lieten zien dat de nucleotiden in de tweede lus van een frameshifter pseudoknoop betrokken zijn bij de vorming van een "triple helix" door middel van interacties met de basen uit de eerste stam van de pseudoknoop. Mutaties in deze "triples" kunnen de efficiëntie van een frameshifter pseudoknoop met een factor 5 tot 10 verlagen. Een voorbeeld hiervan is ook te zien in Figuur 1 van **hoofdstuk 4**. Haarspelden kunnen in theorie ook triples vormen met de nucleotiden die erna in het mRNA liggen. In de praktijk bleek dat niet het geval te zijn of in ieder geval, mochten ze wel vormen, geen bijdrage te leveren aan de RF efficiëntie. Waarschijnlijk omdat deze nucleotiden niet gefixeerd worden, zoals bij een pseudoknoop, maar te flexibel zijn. Als vuistregel kunnen we stellen dat een triple helix, zoals die van een pseudoknoop, anderhalf keer (triple:double=1.5) beter is dan een dubbele helix, zoals die van een haarspeld of duplex gevormd door binding van een antisense oligonucleotide.

Een andere reden voor de voorkeur voor pseudoknopen heeft wellicht te maken met verschillende vouwingsnelheden van haarspelden en pseudoknopen. Dit zou er toe kunnen leiden dat na passage van het eerste "shifted" ribosoom en voor aankomst van het volgende ribosoom, de haarspeld al wel volledig hervouwen is maar een pseudoknoop nog niet. Afhankelijk van de translatie-snelheid zou het percentage frameshifting gereguleerd kunnen worden, wat misschien een evolutionair voordeel oplevert. Op dit vlak valt er nog een hoop uit te zoeken.

Zoals gezegd, kunnen antisense RNA oligo's ook RF stimuleren, maar zijn ze voor eventuele toepassingen *in vivo* minder geschikt vanwege hun instabiele aard. Verschillende modificaties van de 2'OH of van de internucleotide band die

beschermen tegen afbraak door RNAses zijn bekend, maar vele daarvan zijn niet ideaal vanwege toxiciteit, neveneffecten ("off-target effects"), of slechte cel-opname. Een recente modificatie genaamd LNA ("locked nucleic acid"), waarbij een brug tussen de 2' zuurstof en de 4' koolstof de ribose in een gunstige 3' endo conformatie fixeert, lijkt geen van genoemde nadelen te hebben. In **hoofdstuk 4** laten we zien dat de introductie van twee LNA-modificaties in een DNA oligonucleotide voldoende is om dezelfde hoeveelheid RF te induceren als een RNA oligonucleotide. Een bijkomend voordeel van LNA is dat we de stabiliteit van de duplex kunnen variëren zonder dat we de sequentie hoeven te veranderen. Op die manier hebben we aangetoond dat de stabiliteit aan de kant waar het ribosoom de duplex nadert belangrijk is voor RF.

Hoewel de beschreven antisense oligonucleotiden in staat waren om circa 15% RF te induceren wilden we proberen om dit nivo te verhogen met het oog op eventuele toekomstige medische toepassingen. Door gebruik te maken van de kennis opgedaan bij het bestuderen van de efficiëntere pseudoknopen, hebben we oligonucleotiden ontworpen die na binding aan het mRNA een pseudoknoop nabootsen (**hoofdstuk 5**). Deze "pseudo-pseudoknopen" waren betere RF stimulators dan de lineaire antisense oligonucleotiden uit **hoofdstuk 4**. In feite bieden we een haarspeld aan waarvan een gedeelte van de lus kan hybridizeren met het mRNA en de overblijvende nucleotiden uit de lus triple interacties met de duplex kunnen vormen, zoals in een "echte" pseudoknoop. Op die manier levert een complementariteit van 6 basenparen met het mRNA al bijna 2%, en 10-11 basenparen maar liefst 25% RF op. Dit in tegenstelling tot de normale 12-18 basenparen duplexen die "slechts" 13% RF opleveren. Deze toename is gedeeltelijk toe te schrijven aan de vorming van triple interacties van de lus van de haarspeld met de eerste stam (S1).

Een bijkomend voordeel van de antisense RF assay is de mogelijkheid om modificaties te testen bijvoorbeeld zoals de LNA modificatie. Zo konden we het effect van nucleotiden in de lus bestuderen door ze geheel te vervangen door een poly-ethyleenglycol (PEG)-linker wat leidde tot een circa 1.5-voudige verlaging van RF. Een dergelijke modificatie was in een normale RF assay met alle signalen in één lang mRNA onmogelijk geweest.

Er werden ook vele pogingen gedaan om de werking van antisense oligonucleotiden in cellijnen te testen (deze staan niet beschreven in dit proefschrift). Verschillende types oligonucleotiden zoals RNA, 2'O-methyl RNA, PNA (peptide nucleic acid) en LNA-DNA hybriden werden getest in combinatie met een RF reporterconstruct of het mRNA transcript daarvan. Helaas, zonder succes. In het meest gunstige geval zagen we slechts een tweevoudige toename ten opzichte van het achtergrondsignaal. Als belangrijkste reden voor het falen van dergelijke

experimenten kunnen we aanvoeren dat het oligonucleotide niet op de juiste plek in de cel terechtkwam, met name omdat met confocale fluorescentiemicroscopie bleek dat een fluoresceine-gemerkte oligonucleotide in de nucleus terechtkwam en niet in het cytoplasma waar de translatie plaatsvindt. In de toekomst zullen andere transfectiemethoden moeten worden gebruikt of ontwikkeld om deze oligonucleotiden wel in het cytoplasma te krijgen en te houden.

Het was al langer bekend dat de RF efficiëntie beïnvloed kan worden door tRNA en spermidine concentraties, bepaalde antibiotica of eiwitten. Deze factoren moduleren in het algemeen de werking van het ribosoom of de translatie an sich. In **hoofdstuk 6** toonden we aan dat een klein molecuul in staat is om RF te moduleren door de vorming van een pseudoknoop te stabiliseren. Dit molecuul is een bacteriële metaboliet, 7-aminomethyl-7-deazaguanine of kortweg preQ1, die normaliter betrokken is bij de biosynthese van de base queosine. PreQ1 synthese in bacteriën wordt gereguleerd door een "riboswitch", een RNA sequentie die preQ1 kan binden en transcriptie of translatie van genen betrokken bij preQ1 synthese aan of uit kan zetten. De structuur van het preQ1-bindende gedeelte van de riboswitch, ook wel de preQ1 aptameer genoemd, is een pseudoknoop die overeenkomsten vertoond met sommige kleine frameshifter pseudoknopen. We vonden dat preQ1 aptameren van *Fusobacterium nucleatum* en *Bacillus subtilis* beide in staat waren om RF te stimuleren op een concentratie-afhankelijke manier, maar met verschillende efficiënties. Met behulp van computer-gestuurde methodes hebben we eerst de structuur van de *Fusobacterium nucleatum* aptameer gereconstrueerd op basis van *Bacillus subtilis* aptameer coördinaten. Vervolgens werd ontvouwing van de aptameren met en zonder PreQ1 nagebootst door middel van Molecular Dynamics simulaties. Tot onze verrassing ontdekten we dat in *F. nucleatum* een extra nucleotide betrokken zou kunnen zijn bij de binding van preQ1. Mutatie van dit nucleotide in de Fusobacterium aptameer leidde tot een drastische afname van de preQ1-afhankelijke RF. Interessant genoeg, leidde de introductie van dit nucleotide in de Bacillus aptameer tot een enorme toename in RF. Dit is waarschijnlijk een van de weinige succesvolle voorbeelden van de ontdekking van nieuwe interacties m.b.v. computer gestuurde simulaties van een RNA-ligand complex. Daarnaast biedt dit ligand-afhankelijke RF systeem de mogelijkheid om analoga van preQ1 te testen die wellicht kunnen competeren met preQ1 binding en op die manier potentiële antibacteriële middelen kunnen worden.

Samenvattend kunnen we stellen dat we hebben aangetoond dat artificiële haarspelden wel degelijk goede RF stimulatoren zijn, suggererend dat de rol van de RNA structuur voornamelijk ligt in het opwerpen van een barrière voor het ribosoom. Dit werd nogmaals ondersteund door het feit dat antisense oligonucleotiden ook in

staat zijn om RF te stimuleren. De superioriteit van pseudoknopen als RF stimulators is vooral te danken aan de vorming van een triple helix. Door zogenaamde "pseudo-pseudoknopen" te maken met gestructureerde antisense RNA oligonucleotiden konden we het effect van deze triple helix inderdaad aantonen. We hebben ook laten zien dat RF in principe gereguleerd kan worden door een metaboliet op een manier die mogelijk ook in de natuur voorkomt.

Tot slot kunnen we concluderen dat het in dit proefschrift beschreven onderzoek heeft bijgedragen aan een beter begrip van de rol van RNA structuren in de stimulatie van ribosomale frameshifting. Deze kennis kan van toepassing zijn op het behandelen van ziektes die veroorzaakt worden door frameshift mutaties.

## Curriculum Vitae

Chien-Hung Yu was born on 10th August 1980 in Nantou County, Taiwan. In 1998, he graduated from the Taipei Municipal Chien Kuo High School. During this period, he got interested in chemistry and biology subjects. Thereafter, he followed a BSc-study in the Department of Agriculture Chemistry, National Taiwan University and obtained his bachelor degree in 2002. In the same year, he started his first research project, which was dedicated to the role of the C-terminal domain of ClpQ (*hslU*), which is responsible for the subunit oligomerization of ClpQ. His research project was carried out under the supervision of Dr. Whi-Fin Wu, Institute of Microbiology, Department of Agriculture Chemistry, National Taiwan University and he obtained his master degree in September 2004. After one year and three months mandatory military service, from February 2006 till July 2007 he joined the group of Prof. Dr. Bor-Ching Sheu, Department of Obstetrics and Gynecology, College of Medicine, National Taiwan University Hospital to investigate the role of $CD4^+CD25^+$ regulatory T cells (Treg) in inhibiting tumor-infiltrating lymphocytes in cervical and endometrial cancer. He started in September 2007 as a PhD student in the group of Molecular Genetics, Leiden Institute of Chemistry, under supervision of Dr. R.C.L. Olsthoorn and Prof. Dr. M.H.M. Noteborn. The results of the latter period are described in this thesis.

## List of publications


1. Lee, Y.Y., Chang, C.F., Kuo, C.L., Chen, M.C., Yu, C.H., Lin, P.I., and Wu, W.F. (2003) Subunit oligomerization and substrate recognition of the Escherichia coli ClpYQ (HslUV) protease implicated by in vivo protein-protein interactions in the yeast two-hybrid system. *J. Bacteriol.*, **185**, 2393-2401.

2. Lien, H.Y., Yu, C.H., Liou, C.M., and Wu, W.F. (2009) Regulation of clpQY (hslVU) Gene Expression in Escherichia coli. *Open Microbiol. J.*, **3**, 29-39.

3. Yu, C.H., Noteborn, M.H., and Olsthoorn, R.C. (2010) Stimulation of ribosomal frameshifting by antisense LNA. *Nucleic Acids Res.*, **38**, 8277-8283.

4. Yu, C.H., Noteborn, M.H., Pleij, C.W., and Olsthoorn, R.C. (2011) Stem-loop structures can effectively substitute for an RNA pseudoknot in -1 ribosomal frameshifting. *Nucleic Acids Res.*, **39**, 8952-8959.

5. Yu, C.H., Noteborn, M.H., and Olsthoorn, R.C. Antisense oligonucleotides that mimic a pseudoknot are highly efficient in stimulating –1 ribosomal frameshifting. Submitted to *Nucleic Acids Res*.

6. Yu, C.H., Luo J., Kamerlin S.C.L., Abrahams J.P., and Olsthoorn, R.C. Comparison of $preQ_1$ riboswitches by molecular dynamics simulations and ribosomal frameshifting: identification of a novel RNA-ligand interaction. Manuscript in preparation.

# Acknowledgements